CLUB DIRIGENTI TECNICI

Giovedì, 15 Febbario 2018
Sala Spagna del Centro Skillab
C.so Stati Uniti, 38 – Torino

Nuovi fenomeni fisici connessi alla frattura dei materiali e ai terremoti

Alberto Carpinteri

Politecnico di Torino, Dipartimento di Ingegneria Strutturale, Edile e Geotecnica

Alberto Carpinteri · Giuseppe Lacidogna
Amedeo Manuello *Editors*

Acoustic, Electromagnetic, Neutron Emissions from Fracture and Earthquakes

Springer

BOOK AND PAPERS PUBLISHED IN PEER-REVIEWED JOURNALS

A. Carpinteri, G. Lacidogna, A. Manuello (Editors): *Acoustic, Electromagnetic, Neutron Emissions from Fracture and Earthquakes,* Springer International Publishing AG Switzerland (2015), VIII + 264.

A. Carpinteri, F. Cardone, G. Lacidogna: "Piezonuclear neutrons from brittle fracture: Early results of mechanical compression tests", *Strain*, Vol. 45 (2009), 332-339.

F. Cardone, A. Carpinteri, G. Lacidogna: "Piezonuclear neutrons from fracturing of inert solids", *Physics Letters A*, Vol. 373 (2009), 4158-4163.

A. Carpinteri, O. Borla, G. Lacidogna, A. Manuello: "Neutron emissions in brittle rocks during compression tests: Monotonic vs. cyclic loading", *Physical Mesomechanics*, Vol. 13 (2010), 268-274.

A. Carpinteri, G. Lacidogna, A. Manuello, O. Borla: "Energy emissions from brittle fracture: Neutron measurements and geological evidences of piezonuclear reactions", *Strength, Fracture and Complexity,* Vol. 7 (2011), 13-31.

A. Carpinteri, A. Manuello: "Geomechanical and geochemical evidence of piezonuclear fission reactions in the Earth's Crust", *Strain*, Vol. 47, Suppl. 2 (2011), 267-281.

A. Carpinteri, A. Chiodoni, A. Manuello, R. Sandrone: "Compositional and microchemical evidence of piezonuclear fission reactions in rock specimens subjected to compression tests", Strain, Vol. 47, Suppl. 2 (2011), 282-292.

A. Carpinteri, A. Manuello: "An indirect evidence of piezonuclear fission reactions: Geomechanical and geochemical evolution in the Earth's Crust", Physical Mesomechanics, Vol. 15 (2012), 37-46.

A. Carpinteri, G. Lacidogna, A. Manuello, O. Borla: "Piezonuclear fission reactions in rocks: Evidences from microchemical analysis, neutron emission, and geological transformation", Rock Mechanics and Rock Engineering, Vol. 45 (2012), 445-459.

A. Carpinteri, G. Lacidogna, O. Borla, A. Manuello, G. Niccolini: "Electromagnetic and neutron emissions from brittle rocks failure: Experimental evidence and geological implications", Sadhana, Vol. 37 (2012), 59-78.

A. Carpinteri, G. Lacidogna, A. Manuello, O. Borla: "Piezonuclear neutrons from earthquakes as a hypothesis for the image formation and the radiocarbon dating of the Turin Shroud", Scientific Research and Essays, Vol. 7 (2012), 2603-2612.

A. Carpinteri, G. Lacidogna, A. Manuello, O. Borla: "Piezonuclear fission reactions from earthquakes and brittle rocks failure: Evidence of neutron emission and non-radioactive product elements", Experimental Mechanics, Vol. 53 (2013), 345-365.

A. Carpinteri, A. Manuello: "Reply to comments by U. Bardi, G. Comoretto on geomechanical and geochemical evidence of piezonuclear fission reactions in the Earth's Crust", Strain, Vol. 49 (2014), 548-551.

A. Carpinteri, A. Manuello, D. Veneziano, N.D. Cook: "Piezonuclear fission reactions simulated by the lattice model", Journal of Condensed Matter Nuclear Science, Vol. 15 (2015), 149-161.

A. Carpinteri, O. Borla, A. Manuello, D. Veneziano, A. Goi: "Hydrogen embrittlement and piezonuclear reactions in electrolysis experiments", Journal of Condensed Matter Nuclear Science, Vol.15 (2015), 162-182.

U. Lucia, A. Carpinteri: "GeV plasmons and spalling neutrons from crushing of iron-rich natural rocks", Chemical Physics Letters, Vol. 640 (2015), 112-114.

F. Cardone, A. Manuello, R. Mignani, A. Petrucci, E. Santoro, M. Sepielli, A. Carpinteri: "Ultrasonic piezonuclear reactions in steel and sintered ferrite bars", Journal of Advanced Physics, Vol. 5 (2016), 69-75.

A. Carpinteri, O. Borla: "Fracto-emissions as seismic precursors", Engineering Fracture Mechanics, Vol. 177 (2017), 239-250.

MAJOR INVITED PRESENTATIONS AT INTERNATIONAL CONFERENCES

Plenary Lecture on "Energy emissions from fracture of concrete: Acoustic, electromagnetic, piezonuclear", 7th International Conference on Fracture Mechanics of Concrete and Concrete Structures", Jeju-Korea, 2010

Opening Lecture on "Evidence of piezonuclear fission reactions: Neutron emissions, microchemical analysis, geological transformations", 9th Youth Symposium on Experimental Solid Mechanics, Trieste-Italy, 2010

Closing Lecture on "Piezonuclear reactions produced by brittle fracture: From laboratory to planetary scale", 19th European Conference on Fracture, Kazan-Russia, 2012

Honorary Presidential Lecture on "Piezonuclear fission reactions due to fracture and earthquakes: From the chemical evolution of our planet to the so-called cold fusion", 13th International Conference on Fracture, Beijing-China, 2013

Invited Lecture on "Piezonuclear fission reactions from fracture and turbulence: The chemical evolution in the planets of the Solar System", European Academy of Sciences, Toulouse-France, 2013

Distinguished Lecture in Solid Mechanics on "Acoustic, electromagnetic, and neutron emissions from brittle fracture and earthquakes", California Institute of Technology, Pasadena-California, USA, 2014

Invited Lecture on "Hydrogen embrittlement, microcracking, and piezonuclear fission reactions at the Ni and Pd electrodes of electrolysis "cold fusion" experiments", 12th International Conference on Nanostructured Materials, Moscow-Russia, 2014

Invited Seminar on "Acoustic, electromagnetic, and neutron emissions from brittle fracture and earthquakes", Perm State University, Perm-Russia, 2014

Keynote Lecture on "Opto-acoustic and neutron emissions from fracture and earthquakes", Annual Conference and Exposition on Experimental and Applied Mechanics, Costa Mesa-California, USA, 2015

Invited Lecture on "LENR induced by nanomechanics instabilities and vibrations: From the geochemical evolution of the planet to cold fusion", Seminario ENEA sulle Reazioni Nucleari a Bassa Energia, Roma-Italy, 2016

Invited Lecture on "Nano-scale fracture phenomena and TeraHertz pressure waves as the fundamental reasons for geochemical evolution", 14th International Conference on Fracture, Rhodes-Greece, 2017

Honorary Professorship Lecture on "Fracto-emissions as seismic precursors", Tianjin University, Tianjin-China, 2017

NEUTRON EMISSION FROM FRACTURE AT THE LABORATORY SCALE

NEUTRON EMISSION FROM ROCK SPECIMENS

During a preliminary experimental analysis four rock specimens were used:

- **two made of Carrara marble, specimens P1 and P2;**
- **two made of Luserna granite, specimens P3 and P4;**
- **all of them measuring 6x6x10 cm^3.**

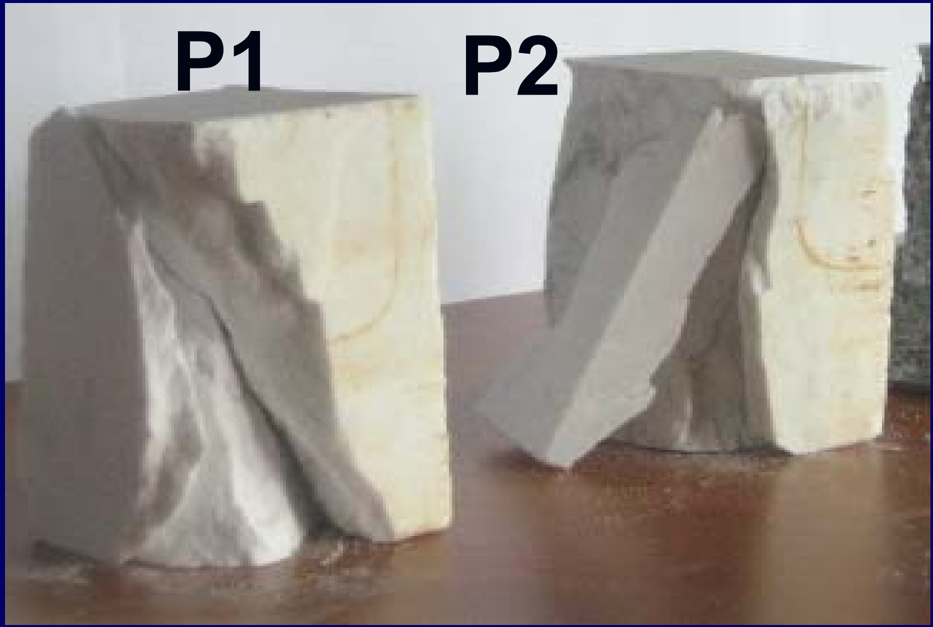

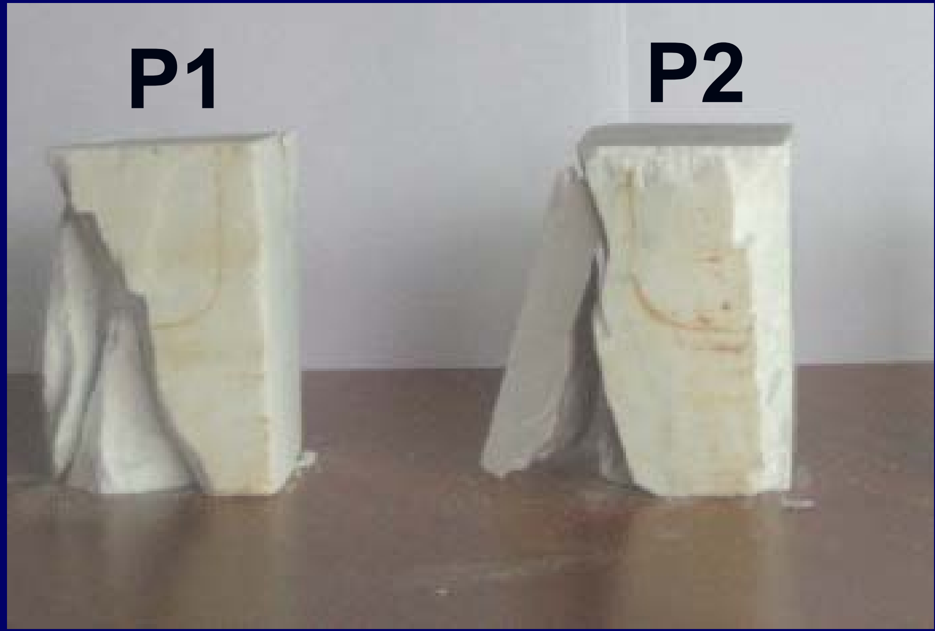

Specimens P1 and P2 in Carrara marble following compression failure.

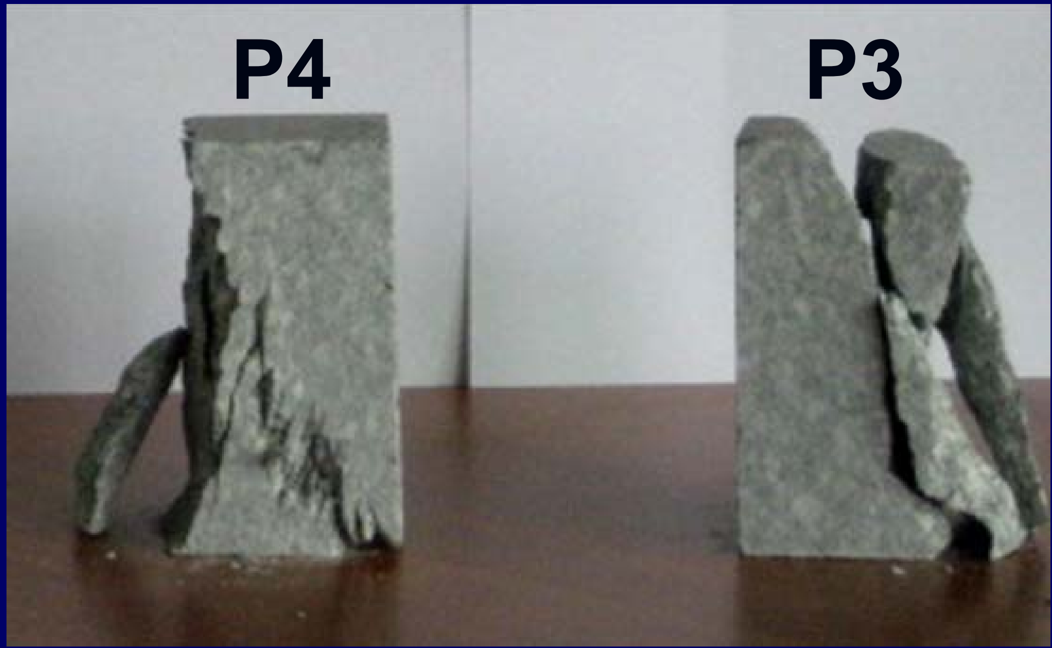

Specimens P3 and P4 in Luserna granite following compression failure.

Brittle Fracture Experiment on Carrara Marble specimen

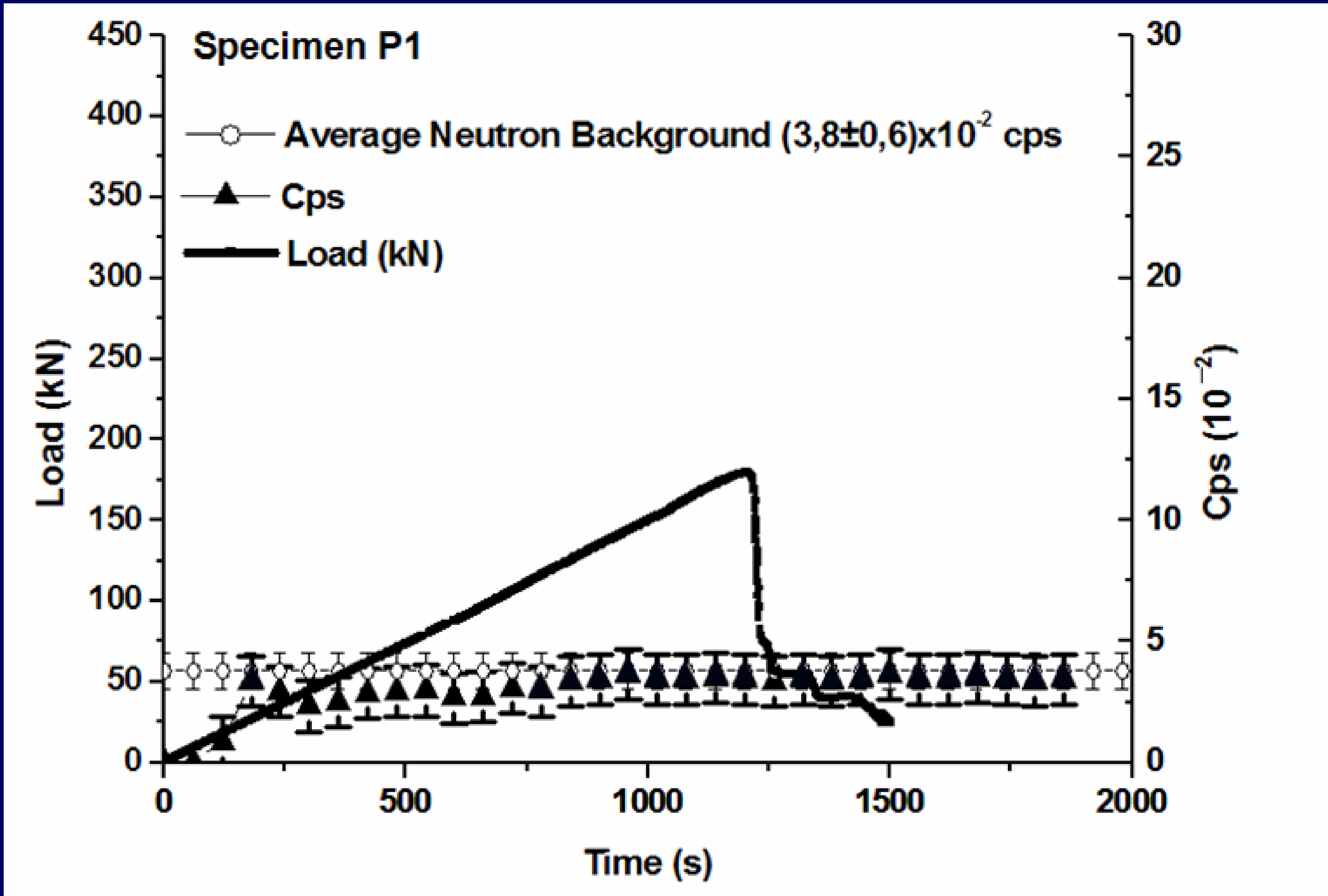

Load vs. time and cps curve for P1 test specimen of Carrara marble.

Brittle Fracture Experiment on granite specimen

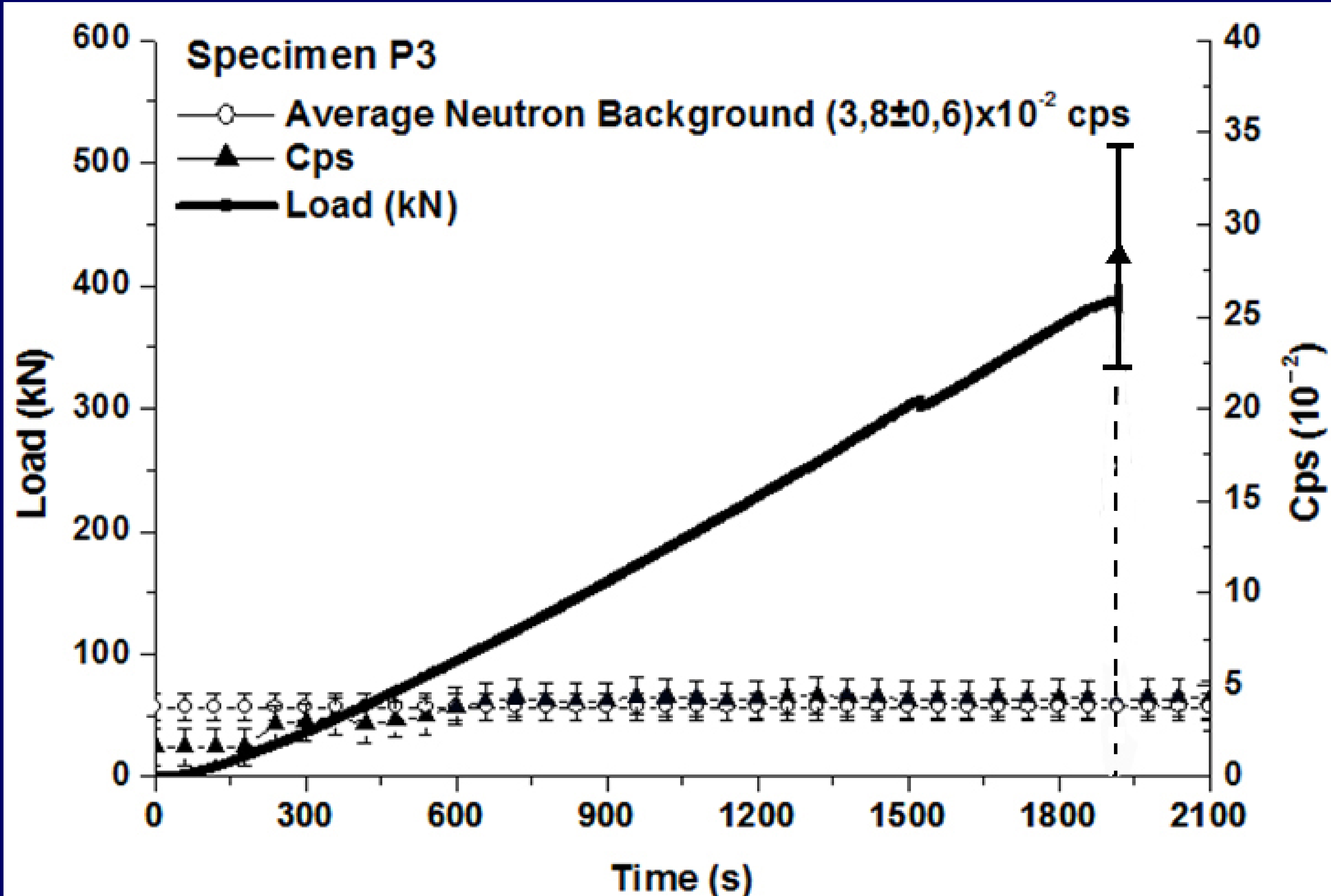

Load vs. time and cps curve for P3 test specimen of granite.

Neutron emissions were measured on nine Green Luserna stone cylindrical specimens, of different size and shape (D=28, 56, 112 mm; λ= 0.5, 1.0, 2.0)

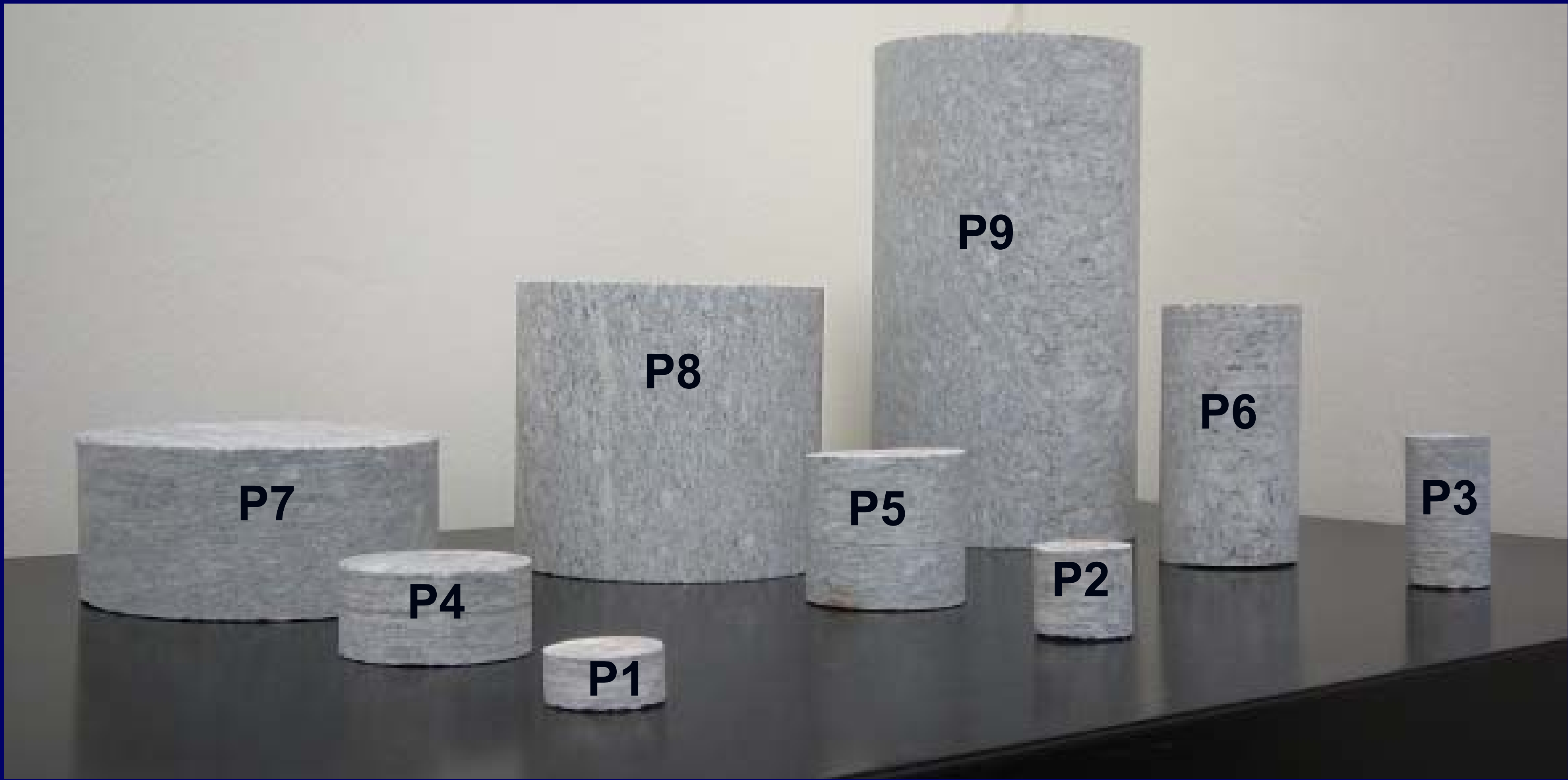

DUCTILE, BRITTLE AND CATASTROPHIC BEHAVIOUR

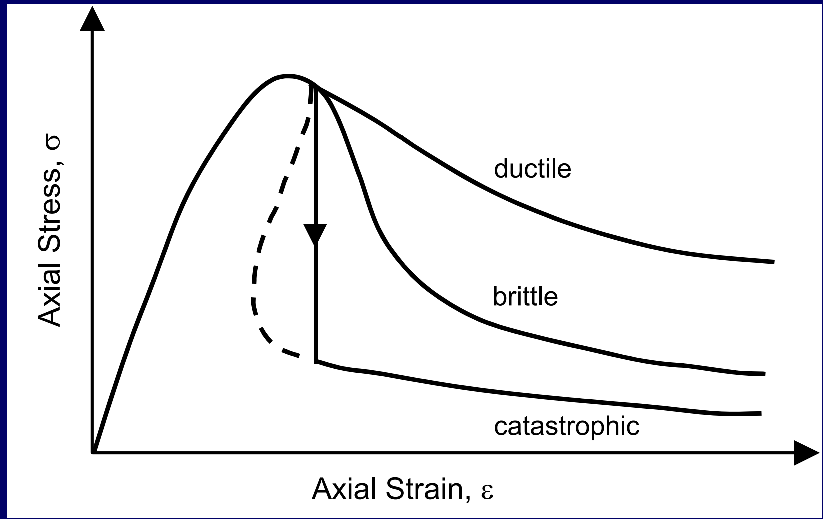

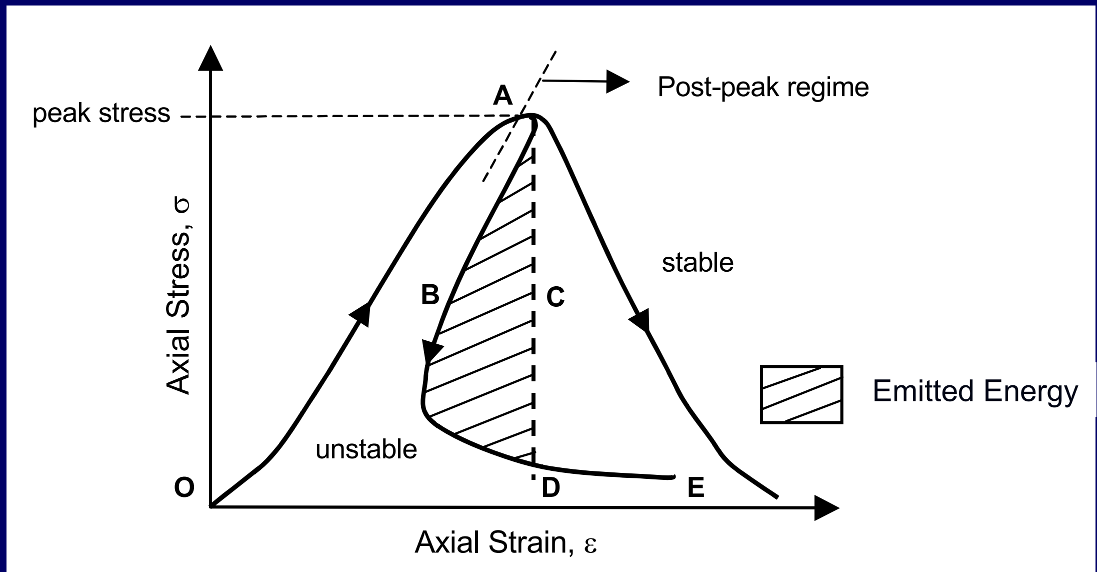

Energy emission and stable vs. unstable stress-strain behaviour

Subsequent stages in the deformation history of a specimen in compression[(I)] [(II)]

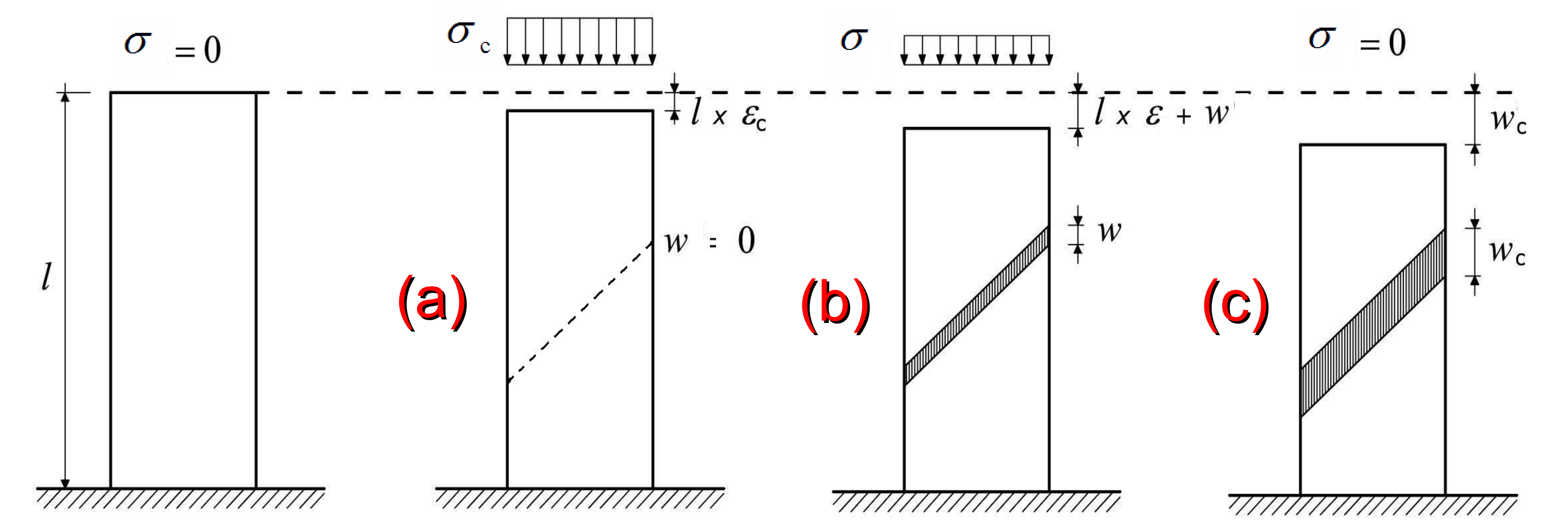

$$\delta = \varepsilon_c l = \frac{\sigma_c}{E} l; \qquad \delta = \frac{\sigma}{E} l + w; \qquad \delta \geq w_c.$$

(I) Carpinteri, A., "Cusp catastrophe interpretation of fracture instability", *J. of Mechanics and Physics of Solids*, 37, 567-582 (1989).

(II) Carpinteri, A., Corrado, M., "An extended (fractal) overlapping crack model to describe crushing size-scale effects in compression", *Eng. Failure Analysis*, 16,

Stress vs. displacement response of a specimen in compression

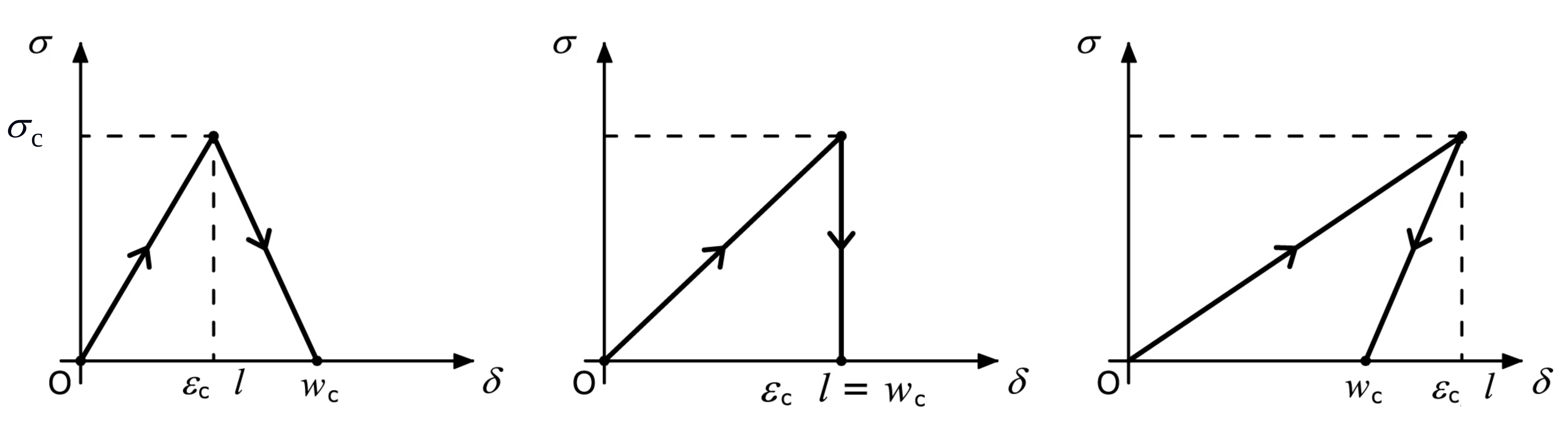

Normal softening

Vertical drop

Catastrophic behaviour

Different Materials Used in the Experimental Investigation

- Luserna stone
- Basalt
- Magnetite
- Mortar enriched with iron dioxide
- Carrara marble
- Gypsum
- Steel

Different Testing Modalities in the Experimental Investigation

Compression tests under monotonic displacement control

Cyclic loading 2 Hz

Cyclic loading 200 Hz

Ultrasonic vibration 20 kHz

Uniaxil tensile tests

NEUTRON EMISSION FROM CAVITATION IN LIQUIDS AND FRACTURE IN SOLIDS

MATERIAL		NEUTRON EMISSION
LIQUIDS – **Cavitation**		
Iron chloride	→	up to 2.5 times the Background Level
SOLIDS – **Fracture**		
Steel	→	up to 2.5 times the Background Level
Granite (Fe ~ 1.5%)	→	up to 10^1 times the Background Level
Basalt (Fe ~ 15%)	→	up to 10^2 times the Background Level
Magnetite (Fe ~ 75%)	→	up to 10^3 times the Background Level
Marble	→	Background Level

Cyclic Loading Experiments on Basaltic Rocks

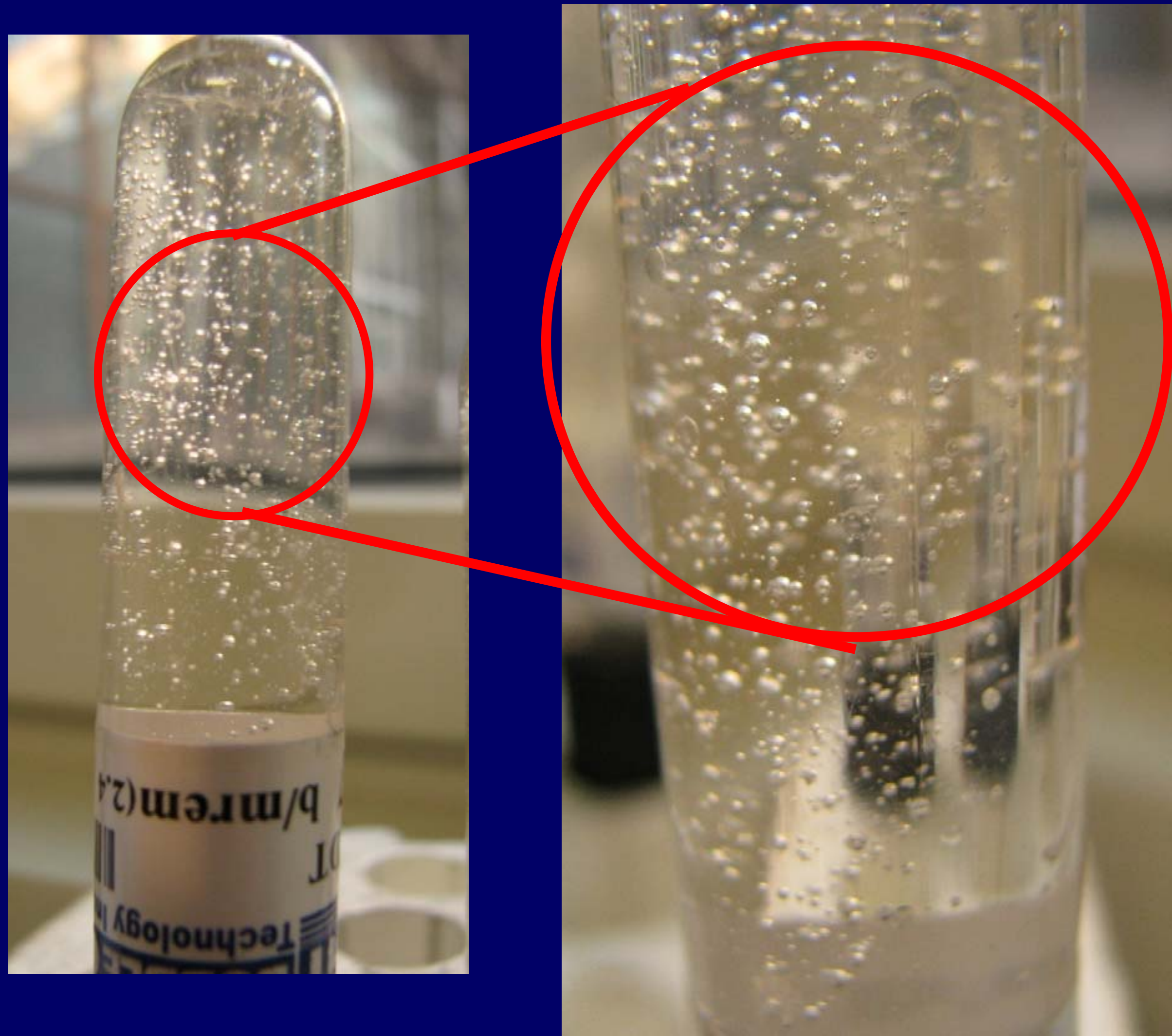

The equivalent neutron dose, at the end of the test on basaltic rock, was 2.62 ± 0.53 mSv/h (Average Background Dose = 41.95 ± 0.85 nSv/h).

$$\frac{\text{Effective Neutron Dose}}{\text{Average Background Dose}} \cong 50$$

Physics Letters A 373 (2009) 4158–4163

Contents lists available at ScienceDirect

Physics Letters A

www.elsevier.com/locate/pla

Piezonuclear neutrons from fracturing of inert solids

F. Cardone[a,b], A. Carpinteri[c,*], G. Lacidogna[c]

[a] *Istituto per lo Studio dei Materiali Nanostrutturati (ISMN-CNR), Via dei Taurini 19, 00185 Roma, Italy*
[b] *Dipartimento di Fisica "E. Amaldi", Università degli Studi "Roma Tre", Via della Vasca Navale, 84-00146 Roma, Italy*
[c] *Department of Structural Engineering and Geotechnics, Politecnico di Torino, Corso Duca degli Abruzzi 24, 10129 Turin, Italy*

ARTICLE INFO

Article history:
Received 17 March 2009
Received in revised form 2 September 2009
Accepted 10 September 2009
Available online 16 September 2009
Communicated by F. Porcelli

Keywords:
Neutron emission
Piezonuclear reactions
Rocks crushing failure
Strain localization
Material interpenetration

ABSTRACT

Neutron emission measurements by means of helium-3 neutron detectors were performed on solid test specimens during crushing failure. The materials used were marble and granite, selected in that they present a different behaviour in compression failure (i.e., a different brittleness index) and a different iron content. All the test specimens were of the same size and shape. Neutron emissions from the granite test specimens were found to be of about one order of magnitude higher than the natural background level at the time of failure. These neutron emissions should be caused by nucleolysis or piezonuclear "fissions" that occurred in the granite, but did not occur in the marble: $Fe_{26}^{30} \to 2Al_{13}^{14} + 2$ neutrons. The present natural abundance of aluminum (7–8% in the Earth crust), which is less favoured than iron from a nuclear point of view, is possibly due to the above piezonuclear fission reaction. Despite the apparently low statistical relevance of the results presented in this Letter, it is useful to present them in order to give to other teams the possibility to repeat the experiment.

CHEMICAL COMPOSITION CHANGES AT THE LABORATORY SCALE

ENERGY DISPERSIVE X-RAY SPECTROSCOPY: COMPOSITIONAL ANALYSIS OF PRODUCT ELEMENTS

Two different kinds of samples were examined: (i) polished thin sections from the external surface; (ii) small portions from the fracture surface.

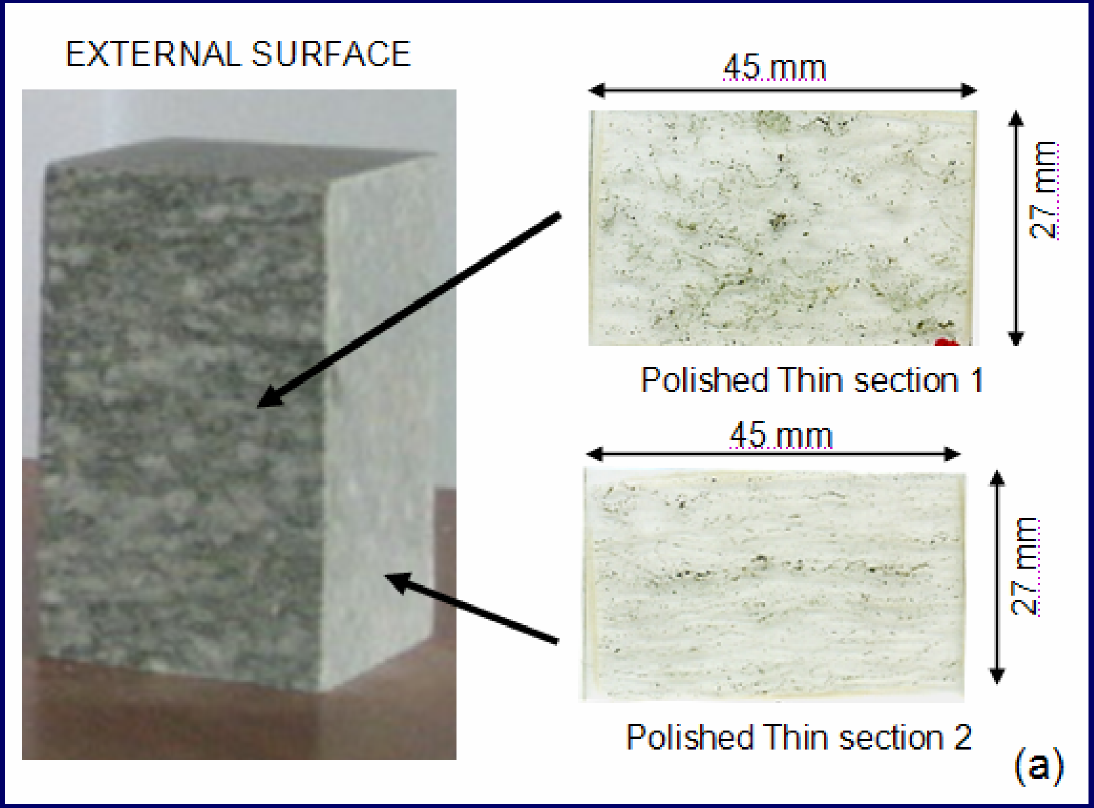

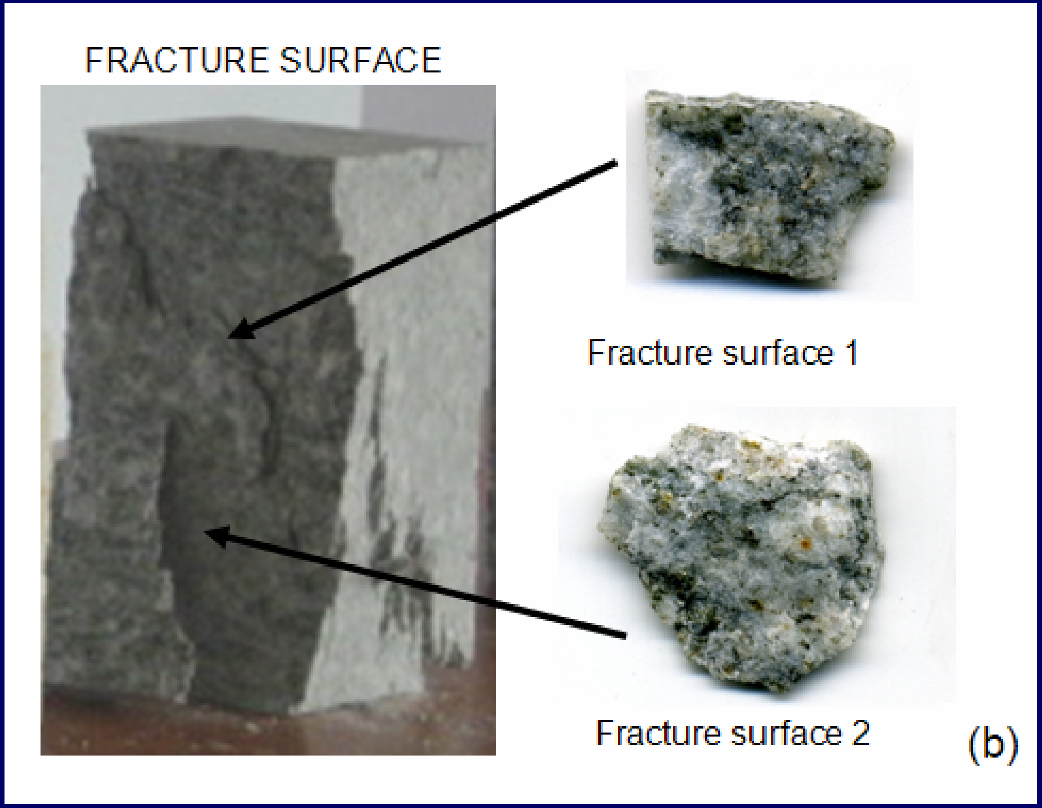

Phengite (Granite) : Fe concentrations

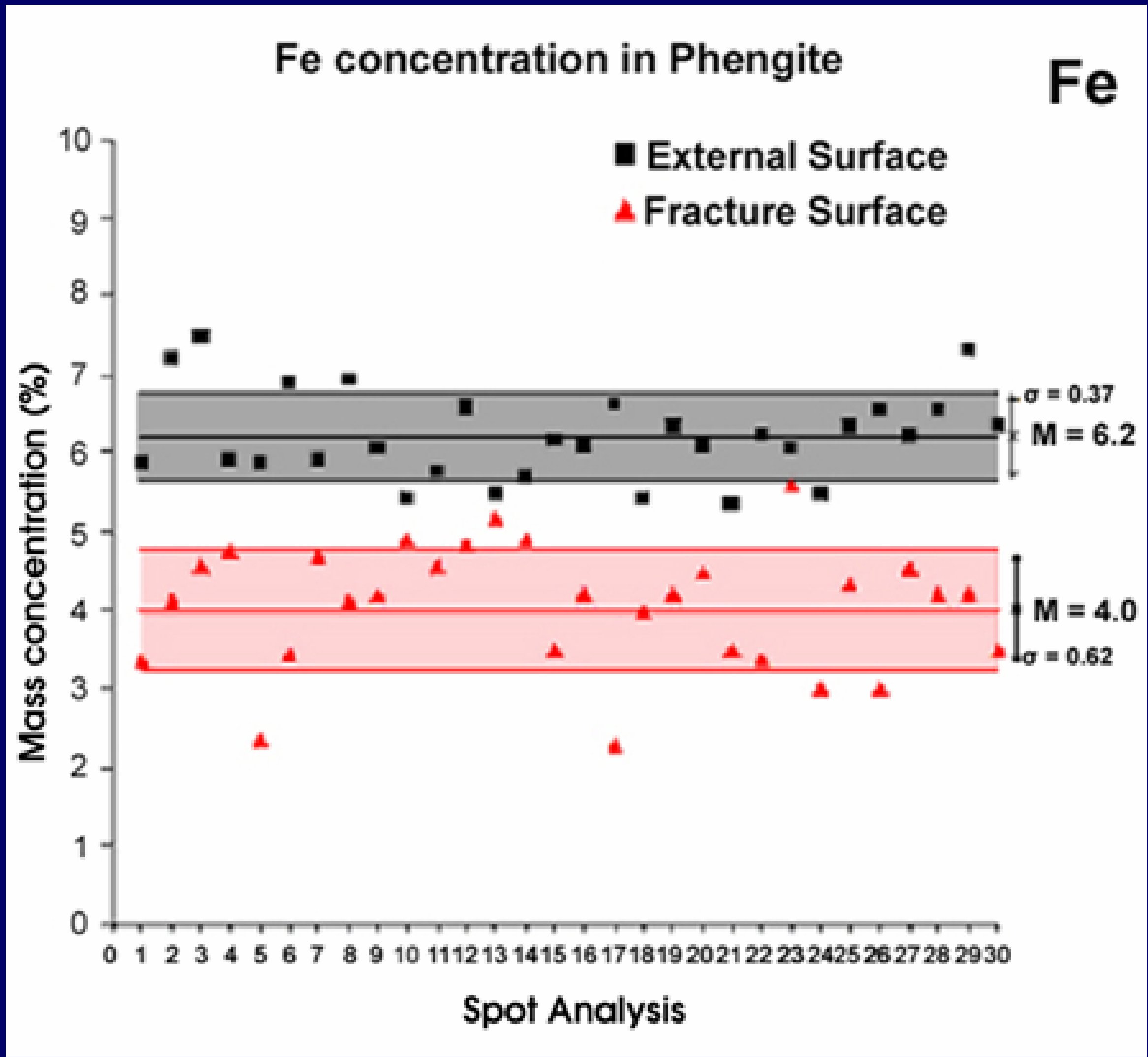

External Surf.:

Fe content = 6.2%

Fracture Surf.:

Fe content = 4.0%

Fe content decrease

–2.2%

Phengite (Granite) : Al concentrations

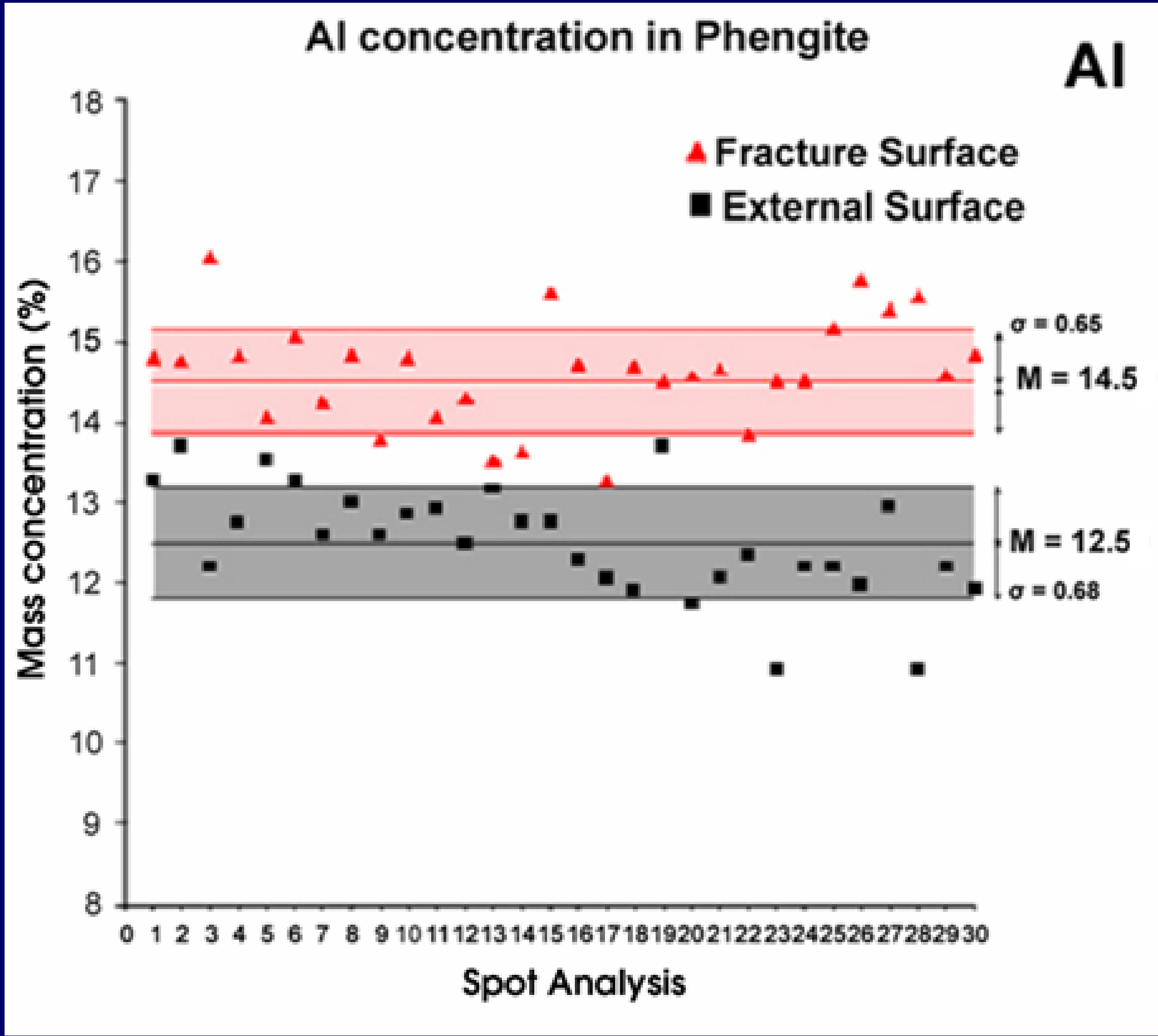

Fracture Surf.:

Al content = 14.5%

External Surf.:

Al content = 12.5%

Al content increase

+2.0%

Phengite (Granite)

	External surface mean value (wt%)	Fracture surface mean value (wt%)	Increase/ decrease with respect to Phengite	Increase/ decrease with respect to the same element
Fe	6.2	4.0	– 2.2%	– 35%
Al	12.5	14.5	+ 2.0%	+ 16%
Si	28.0	27.8	NO VARIATIONS	NO VARIATIONS
Mg	0.7	0.8	NO VARIATIONS	NO VARIATIONS
K	8.0	7.7	NO VARIATIONS	NO VARIATIONS

$$Fe^{56}_{26} \rightarrow 2\,Al^{27}_{13} + 2n$$

Biotite (Granite)

	External surface mean value (wt%)	Fracture surface mean value (wt%)	Increase/ decrease with respect to Biotite	Increase/ decrease with respect to the same element
Fe	21.2	18.2	– 3.0%	– 14%
Al	8.1	9.6	+ 1.5%	+ 18%
Si	18.4	19.6	+ 1.2%	+ 6%
Mg	1.5	2.2	+ 0.7%	+ 46%
K	6.9	7.1	NO VARIATIONS	NO VARIATIONS

$$Fe_{26}^{56} \rightarrow 2\,Al_{13}^{27} + 2n$$

$$Fe_{26}^{56} \rightarrow Mg_{12}^{24} + Si_{14}^{28} + 4n$$

Olivine (Basalt)

	External surface mean value (wt%)	Fracture surface mean value (wt%)	Increase/ decrease with respect to Olivine	Increase/ decrease with respect to the same element
Fe	18.4	14.4	– 4.0%	– 21%
Si	18.3	20.5	+ 2.2%	+ 12%
Mg	21.2	22.8	+ 1.6%	+ 7%
Ca	0.5	0.5	NO VARIATIONS	NO VARIATIONS

$$Fe^{56}_{26} \rightarrow Mg^{24}_{12} + Si^{28}_{14} + 4n$$

Magnetite

	External surface mean value (wt%)	Fracture surface mean value (wt%)	Increase/ decrease with respect to Magnetite	Increase/ decrease with respect to the same element
Fe	64.8	36.8	– 27.9%	– 43%
Al	–	10.1	+ 10.1%	BEFORE ABSENT
Mn	–	2.2	+ 2.2%	BEFORE ABSENT
Si	1.6	10.3	+ 8.7%	+ 540%
O	31.8	38.5	+ 6.7%	+ 21%

$$Fe^{56}_{26} \rightarrow 2Al^{27}_{13} + 2n$$

$$Fe^{56}_{26} \rightarrow Mn^{55}_{25} + H^{1}_{1}$$

$$Fe^{56}_{26} \rightarrow Si^{28}_{14} + O^{16}_{8} + 2He^{4}_{2} + 4n$$

Carrara Marble

	External surface mean value (wt%)	Fracture surface mean value (wt%)	Increase/ decrease with respect to Carrara Marble	Increase/ decrease with respect to the same element
Ca	13.4	9.8	– 3.6%	– 26%
Mg	0.7	0.3	– 0.4%	– 57%
O	45.8	36.8	– 9.0%	– 19%
C	40.1	53.1	+ 13.0%	+ 32%

$$Ca_{20}^{40} \rightarrow 3C_{6}^{12} + He_{2}^{4}$$

$$Mg_{12}^{24} \rightarrow 2C_{6}^{12}$$

$$O_{8}^{16} \rightarrow C_{6}^{12} + He_{2}^{4}$$

NEUTRON EMISSION FROM FRACTURE AT THE PLANETARY SCALE

WAVELENGTH vs FREQUENCY

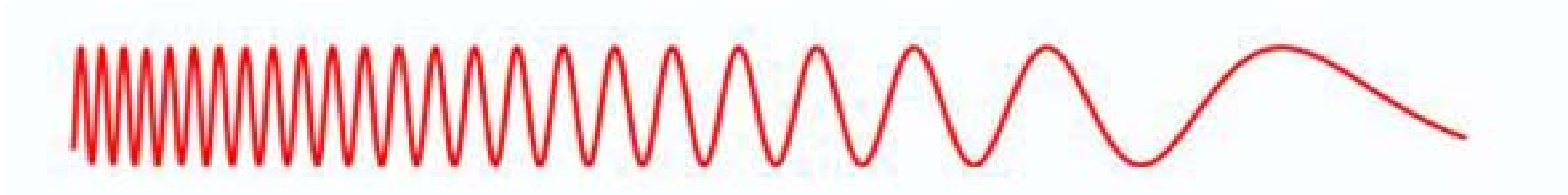

f (Hertz): 10^{12}, 10^{9}, 10^{6}, 10^{3}, 10^{0}

Proteins | Bacteria | Insects | Humans | Earthquakes

λ (Metre): 10^{-9}, 10^{-6}, 10^{-3}, 10^{0}, 10^{3}

$$\textit{wave velocity} = \lambda \times f \approx 10^3 \text{ m s}^{-1}$$

FRACTO-EMISSIONS MEASUREMENT

NEUTRON DETECTOR

Neutron Emission (THz – GHz)

TELESCOPIC ANTENNA

Electromagnetic Emission (GHz – MHz)

PZT TRANSDUCER

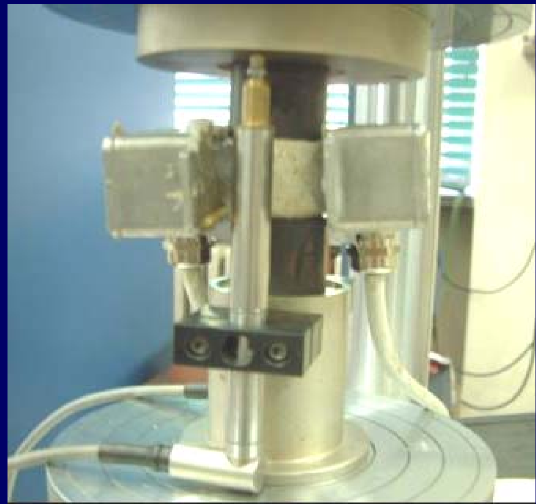

Ultrasonic Acoustic Emission (MHz – kHz)

HUMAN EAR

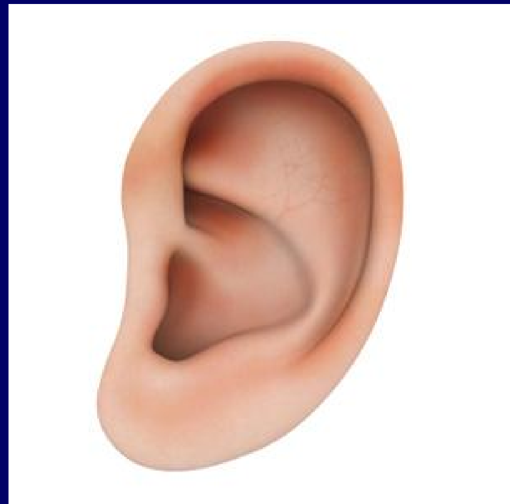

Audible Field (kHz – Hz)

PLANCK EQUATION

$$E = h \times f$$

Vibrational Energy vs Vibrational Frequency in the Atomic Lattice

$$0.025 \text{ eV} = (4.13 \times 10^{-15}) \text{ eVs} \times (6.05 \times 10^{12}) \text{ s}^{-1}$$

(1) TeraHertz phonons present an energy equivalent to that of thermal neutrons

(2) TeraHertz phonons present a frequency equivalent to the Debye frequency (atomic lattice resonance at 4.79 THz for Ca, 6.24 THz for U, and 7.77 THz for Fe)

NEUTRON EMISSION FROM EARTHQUAKES

- Sobolev, G.A., Shestopalov, I.P., Kharin, E.P. "**Implications of Solar Flares for the Seismic Activity of the Earth**". Izvestiya, *Phys. Solid Earth* **34**: 603-607 (1998).

- Volodichev, N.N., Kuzhevskij, B.M., Nechaev, O. Yu., Panasyuk M., and Podorolsky M.I., "**Lunar periodicity of the neutron radiation burst and seismic activity on the Earth**", *Proc. of the 26th International Cosmic Ray Conference,* Salt Lake City, 17-25 August, 1999.

- Sigaeva, E., Nechaev, O., Panasyuk, M., Bruns, A., Vladimirsky, B. and Kuzmin Yu., "**Thermal neutrons' observations before the Sumatra earthquake**", *Geophysical Research Abstracts,* **8**: 00435 (2006).

Neutron flux up to 10^0 cm^{-2} s^{-1} (10^3 times the background level) was detected in correspondence to earthquakes with a magnitude of the 4th degree in Richter Scale (Volodichev N.N., et al. (1999)).

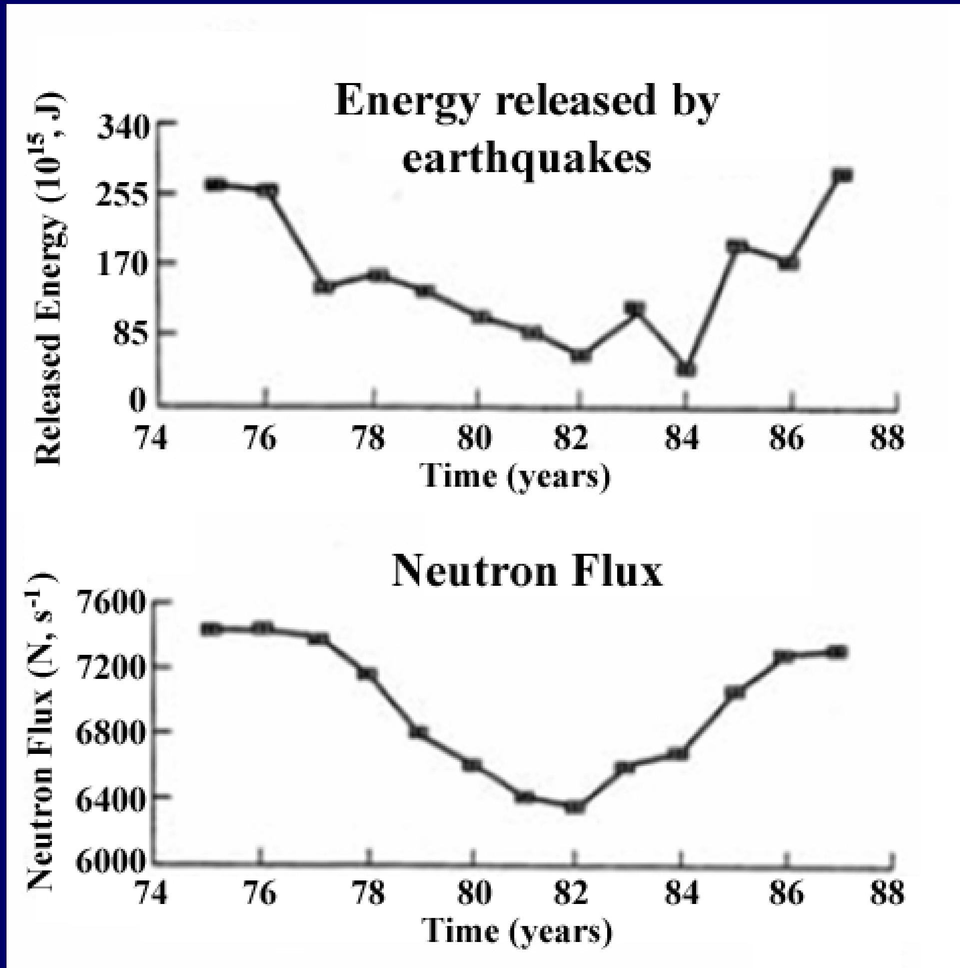

Seismic activity and neutron flux measurements in the period 1975-1987, Kola Peninsula, Russia (Sobolev et al. 1998).

EARTHQUAKE PREPARATION ZONE

$$R = 10^{0.433M+0.60}\ \text{km}\ ^{(*)}$$

- Sumatra 2004 (M = 9.2)
- Chile 2010 (M = 8.8)
- Japan 2011 (M = 9.0)

(*) Dobrovolsky I. P., Zubkov S. I., Miachkin V. I., (1979) "Estimation of the size of earthquake preparation zones" Pure and Applied Geophysics Volume 117, Issue 5, pp 1025-1044.

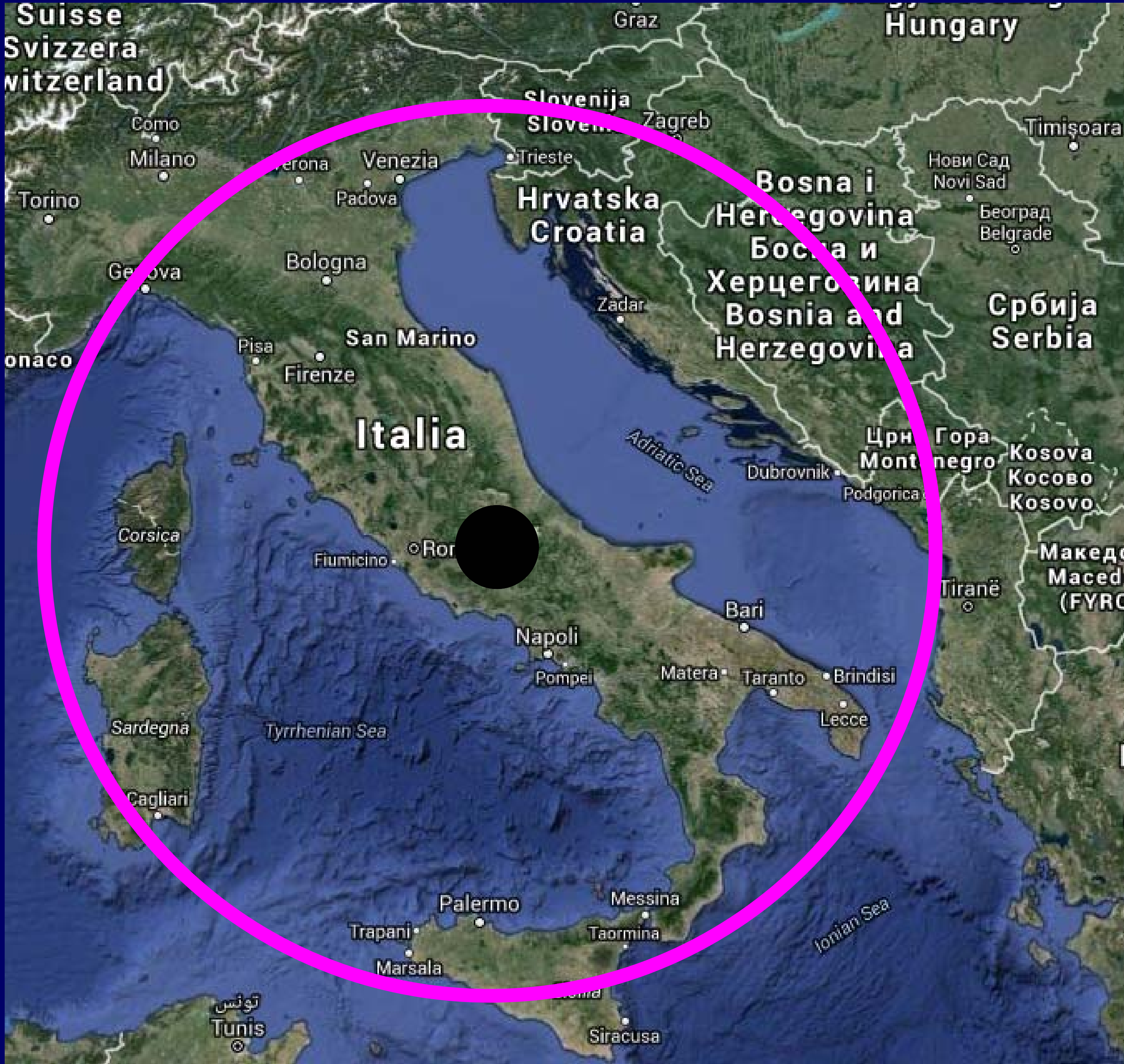

Equivalent crack size from 10^{-9} m to 10^{-6} m

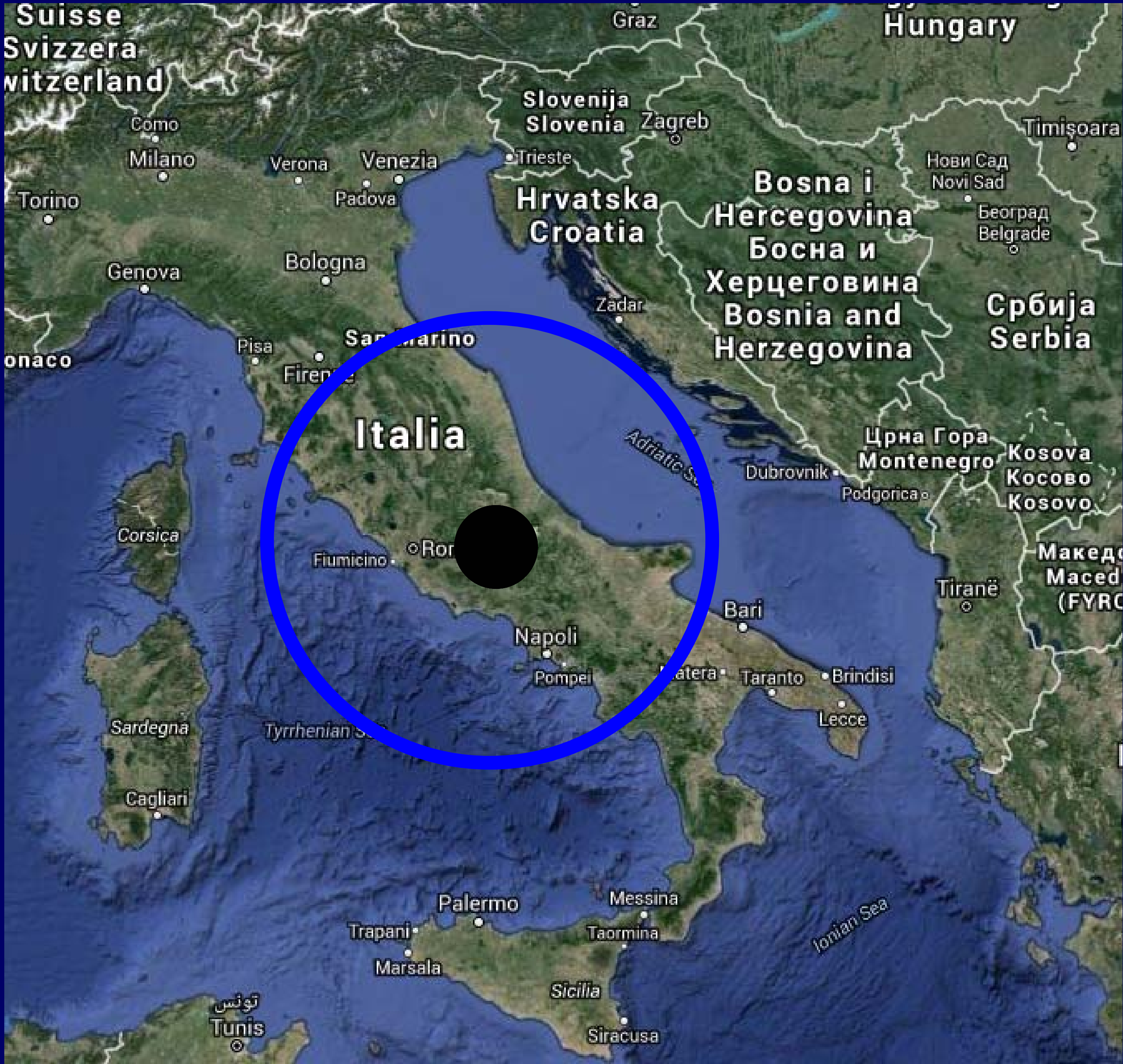

Equivalent crack size from 10^{-6} m to 10^{-3} m

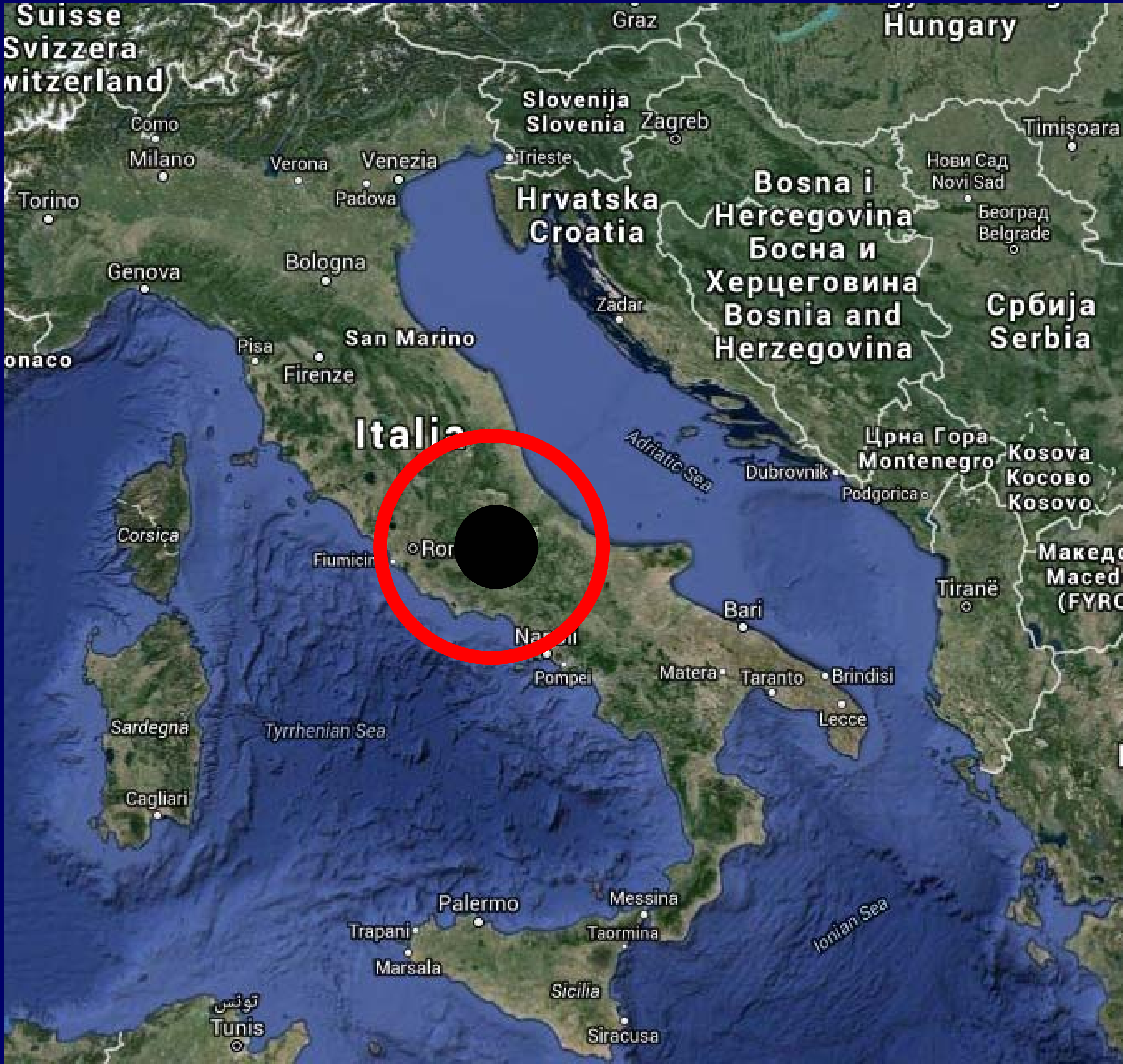

Equivalent crack size from 10^{-3} m to 10^{0} m

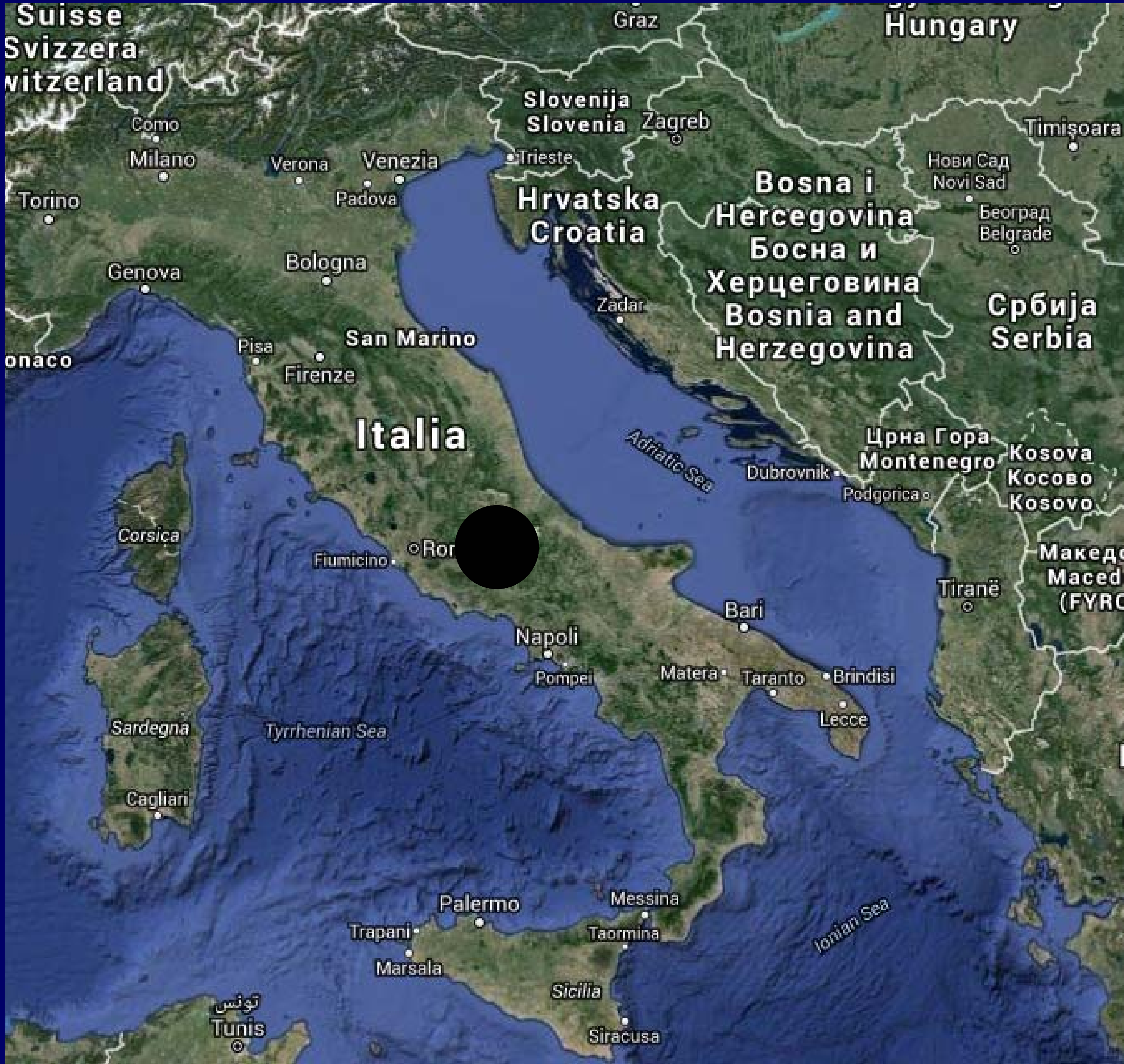

Equivalent crack size > ≈ 10^0 m

MONITORING OF A GYPSUM MINE IN MURISENGO (ITALY)

The mine is structured in five levels and a pillar located at about 100 meters below the ground level has been subjected to a multi-parameter monitoring since July 1st, 2013.

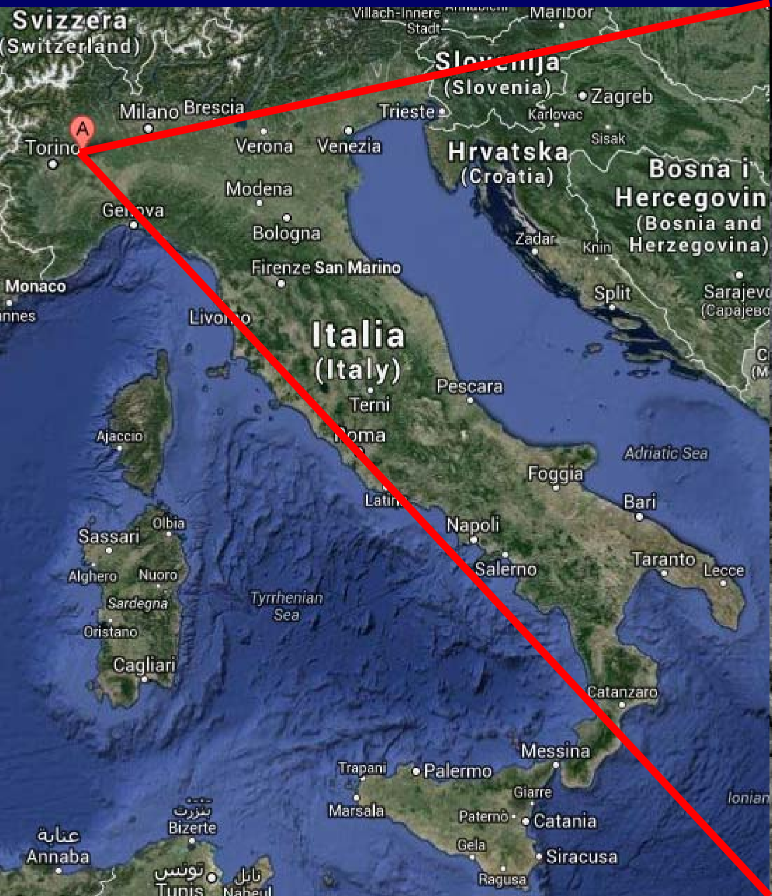

Seismic activity: July 1st, 2013 – June 30, 2017, at a distance ≤ 100 km

396 earthquakes with a local magnitude ≥ 1.8 (Richter)

48 seismic swarms (epicentre magnitude 2.5 – 4.7)

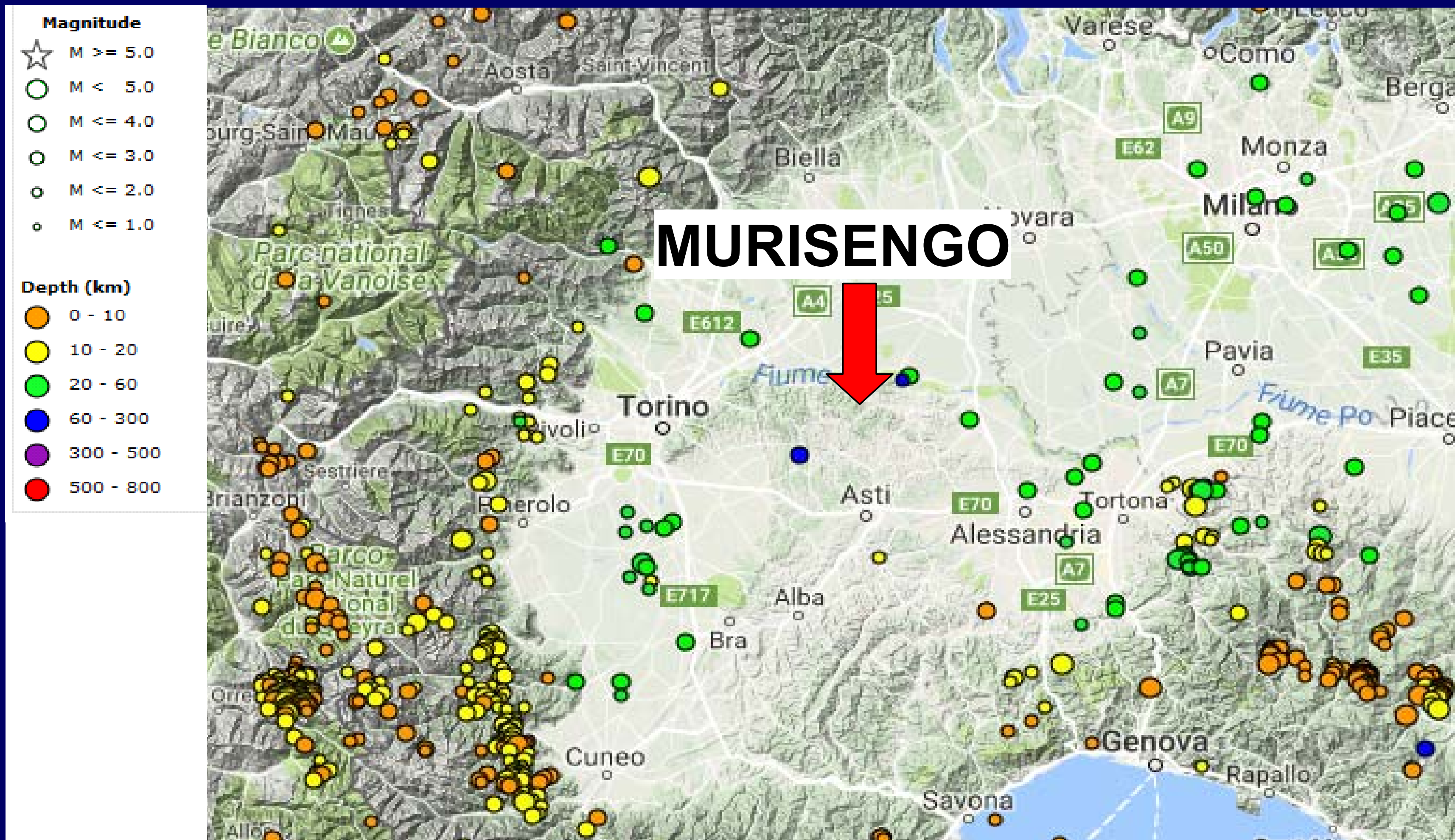

EARTHQUAKE MULTI-MODAL ANALYSIS (First Sem. 2015)

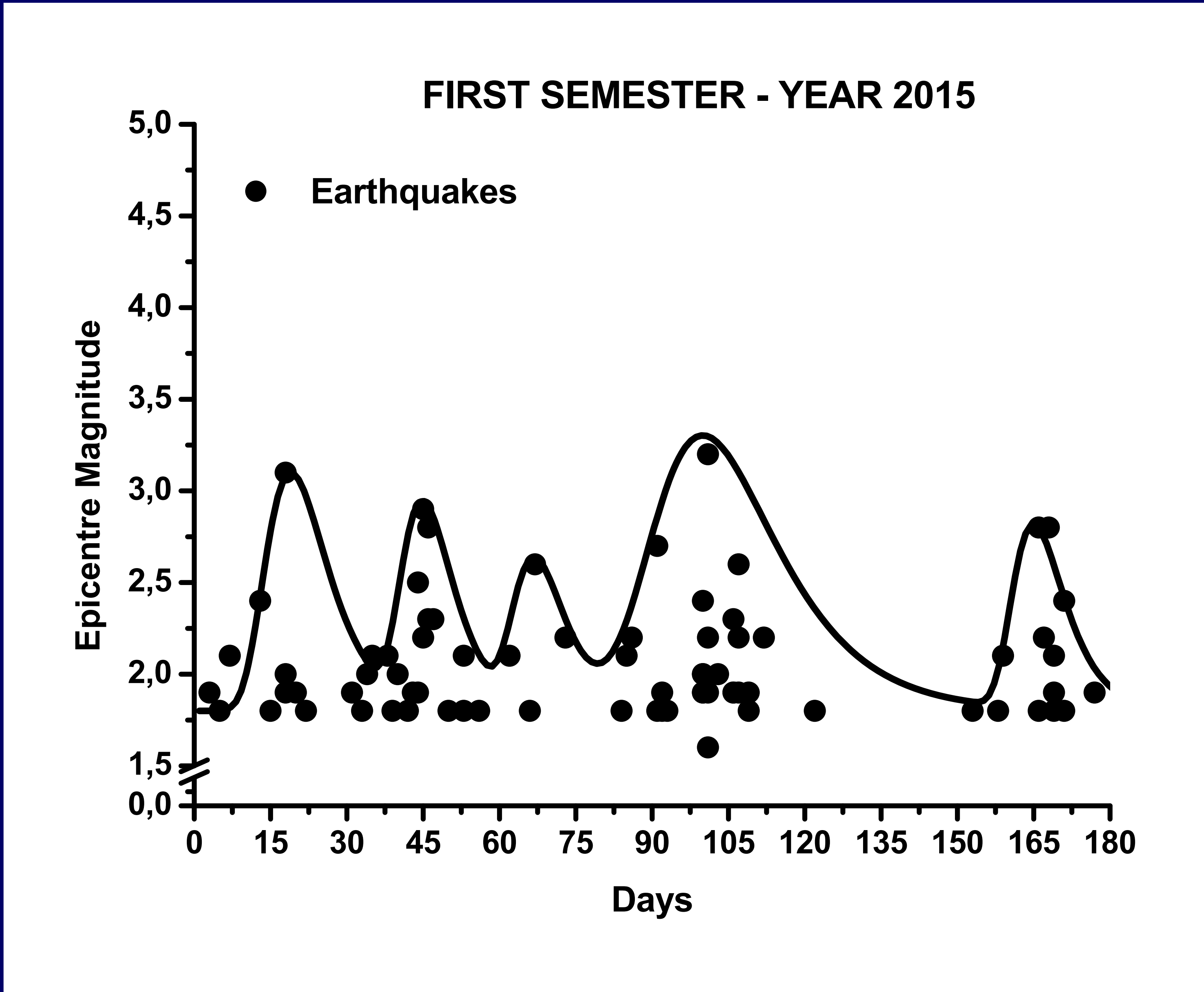

AE MULTI-MODAL ANALYSIS (First Sem. 2015)

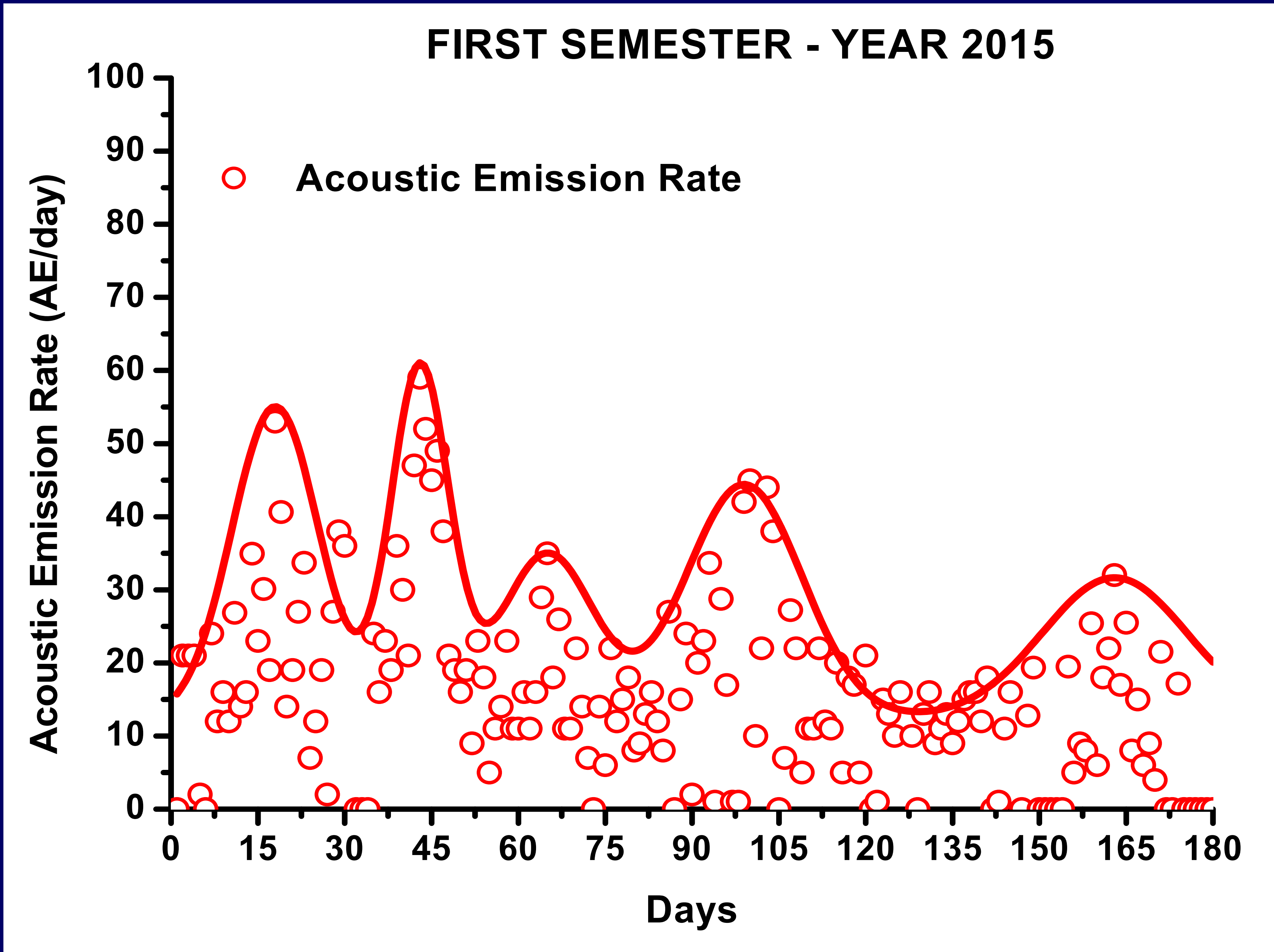

EME MULTI-MODAL ANALYSIS (First Sem. 2015)

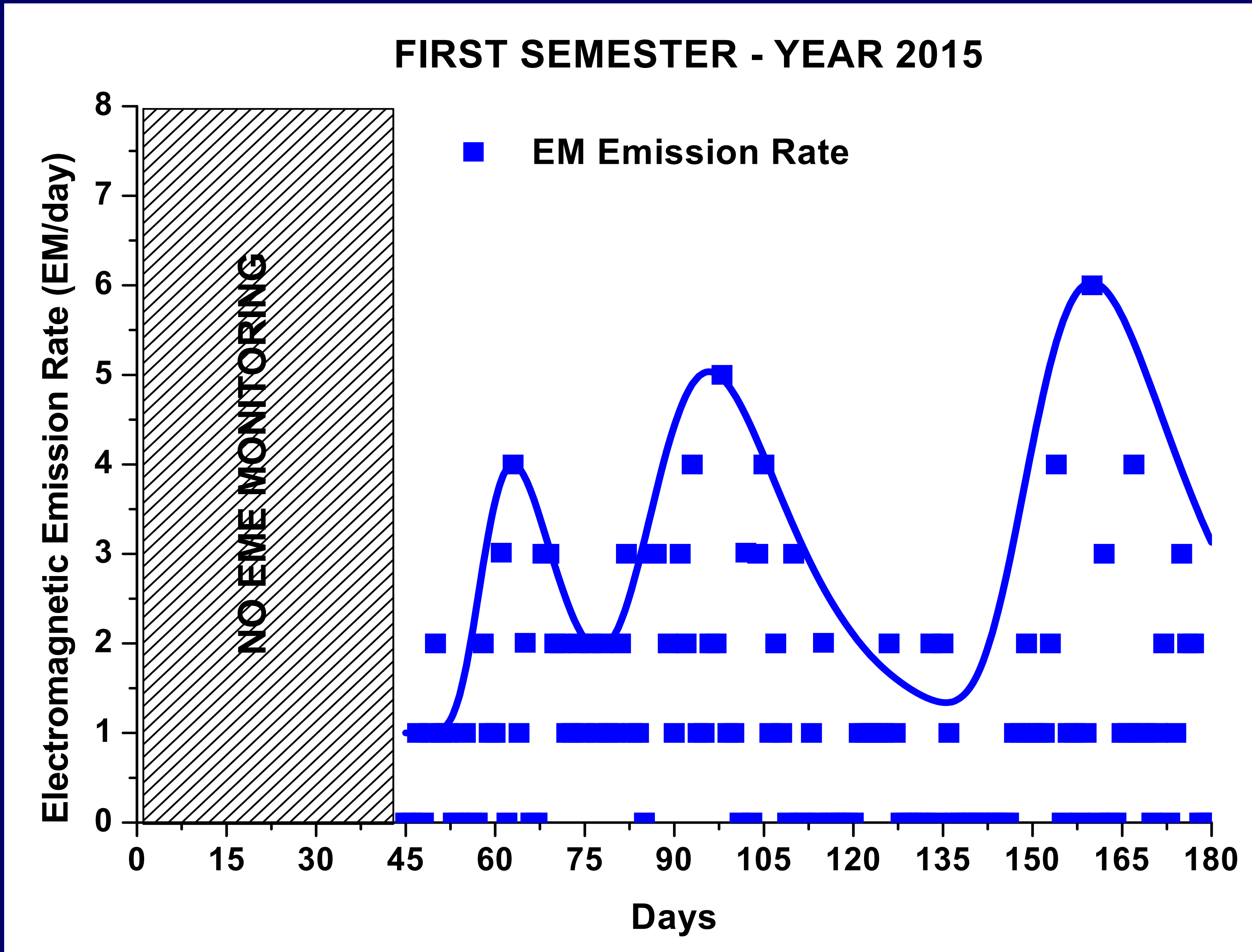

NE MULTI-MODAL ANALYSIS (First Sem. 2015)

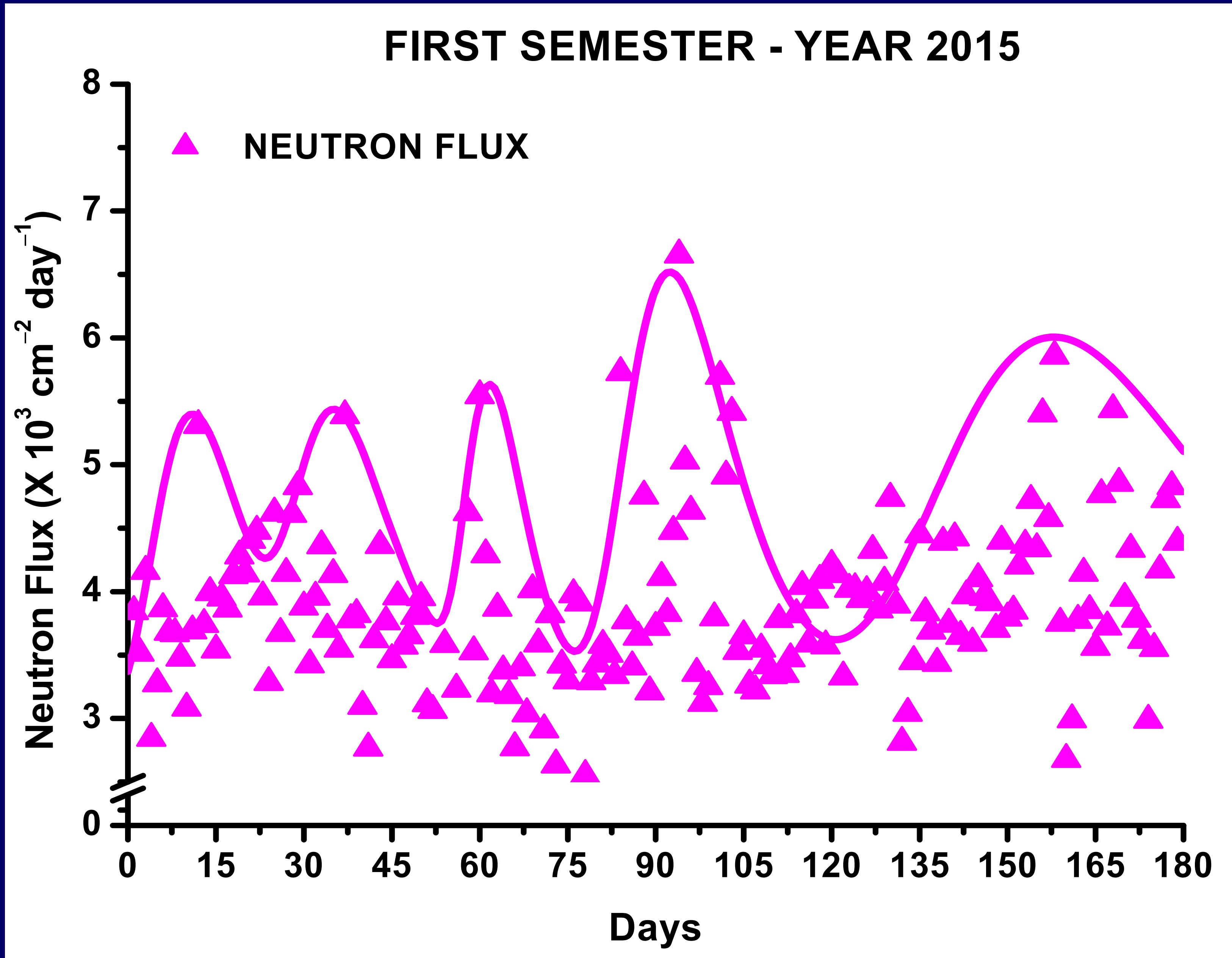

AE vs EARTHQUAKES (Second Sem. 2013)

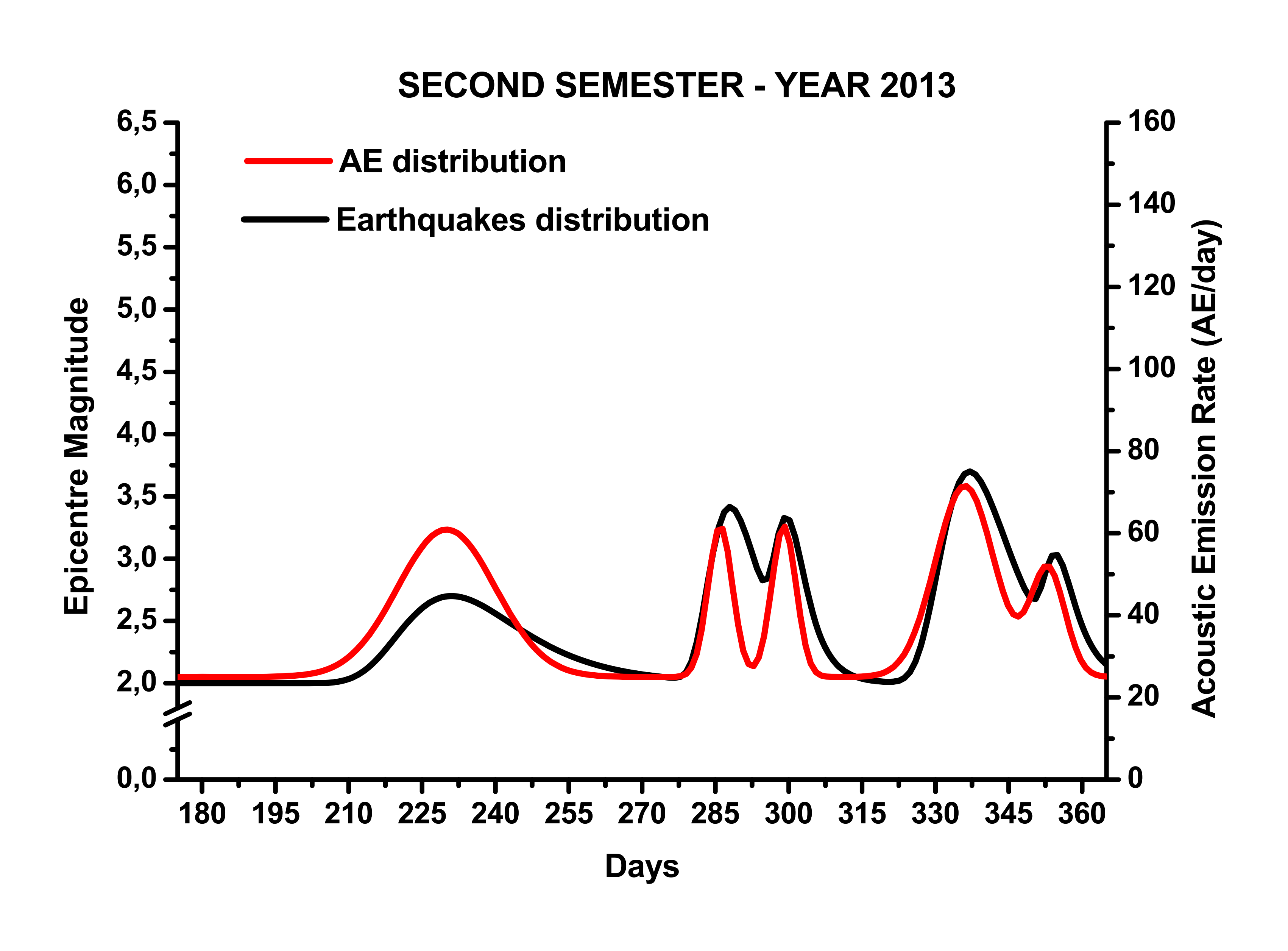

AE vs EARTHQUAKES (First Sem. 2014)

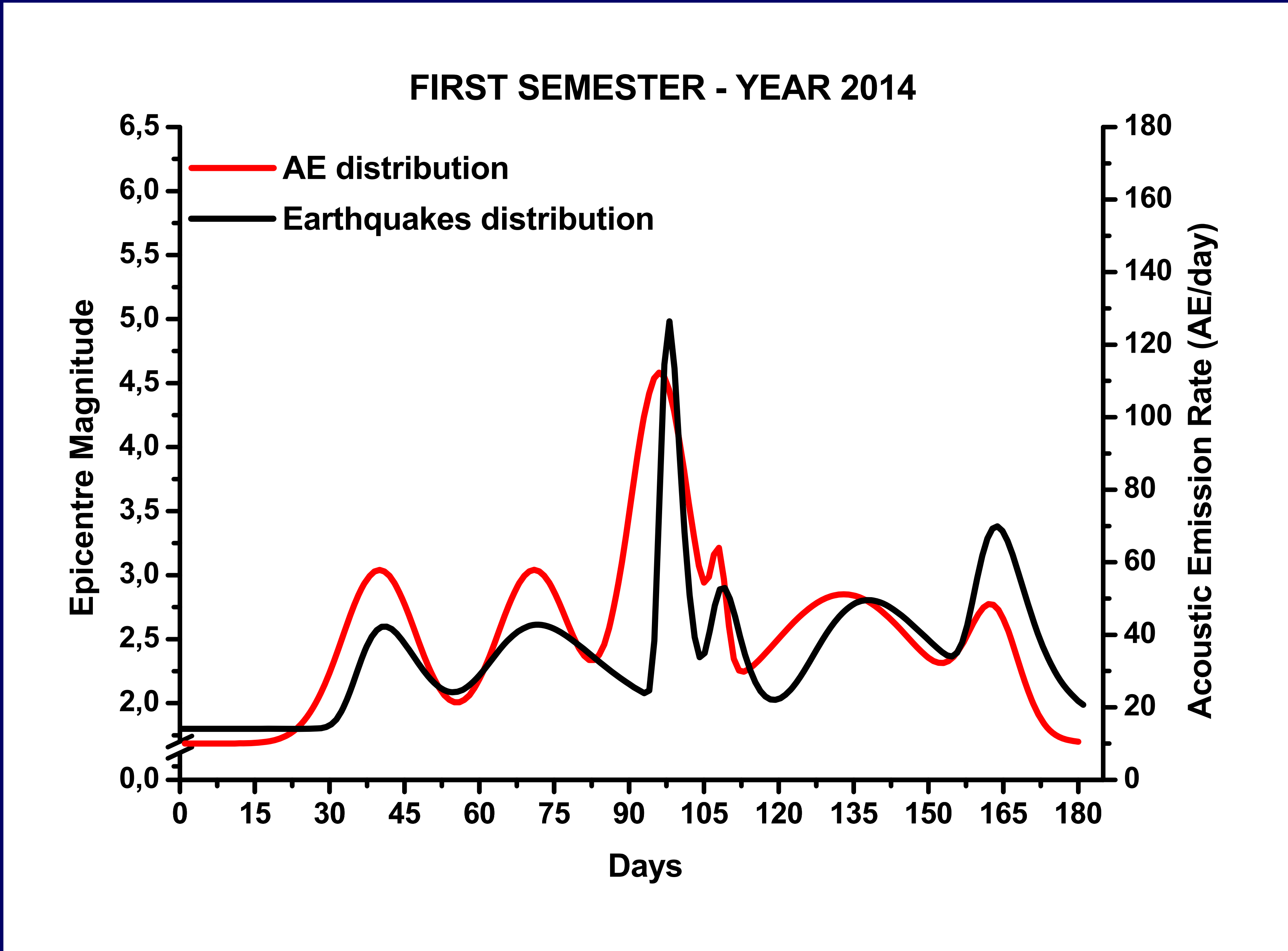

AE vs EARTHQUAKES (Second Sem. 2014)

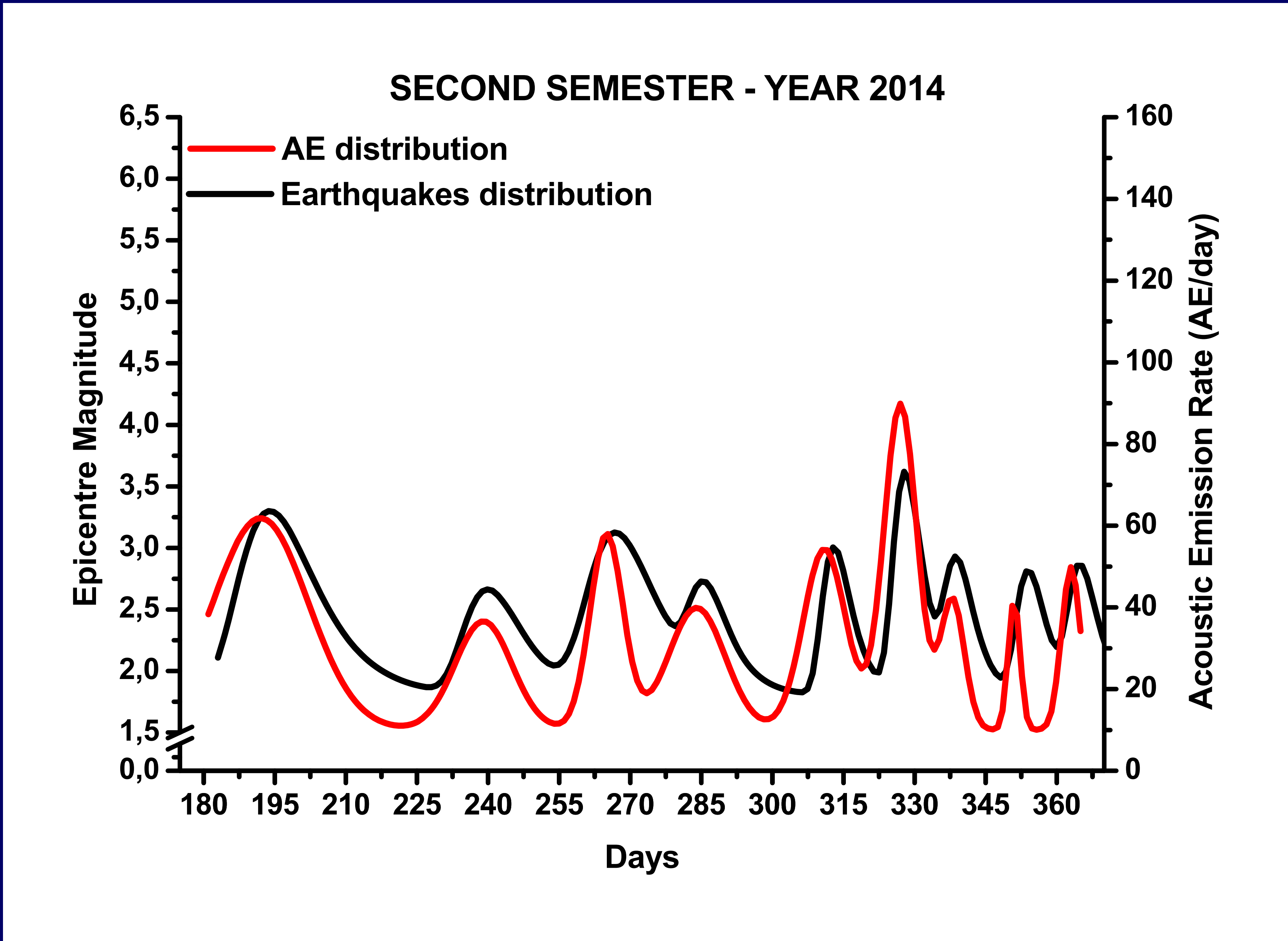

AE vs EARTHQUAKES (First Sem. 2015)

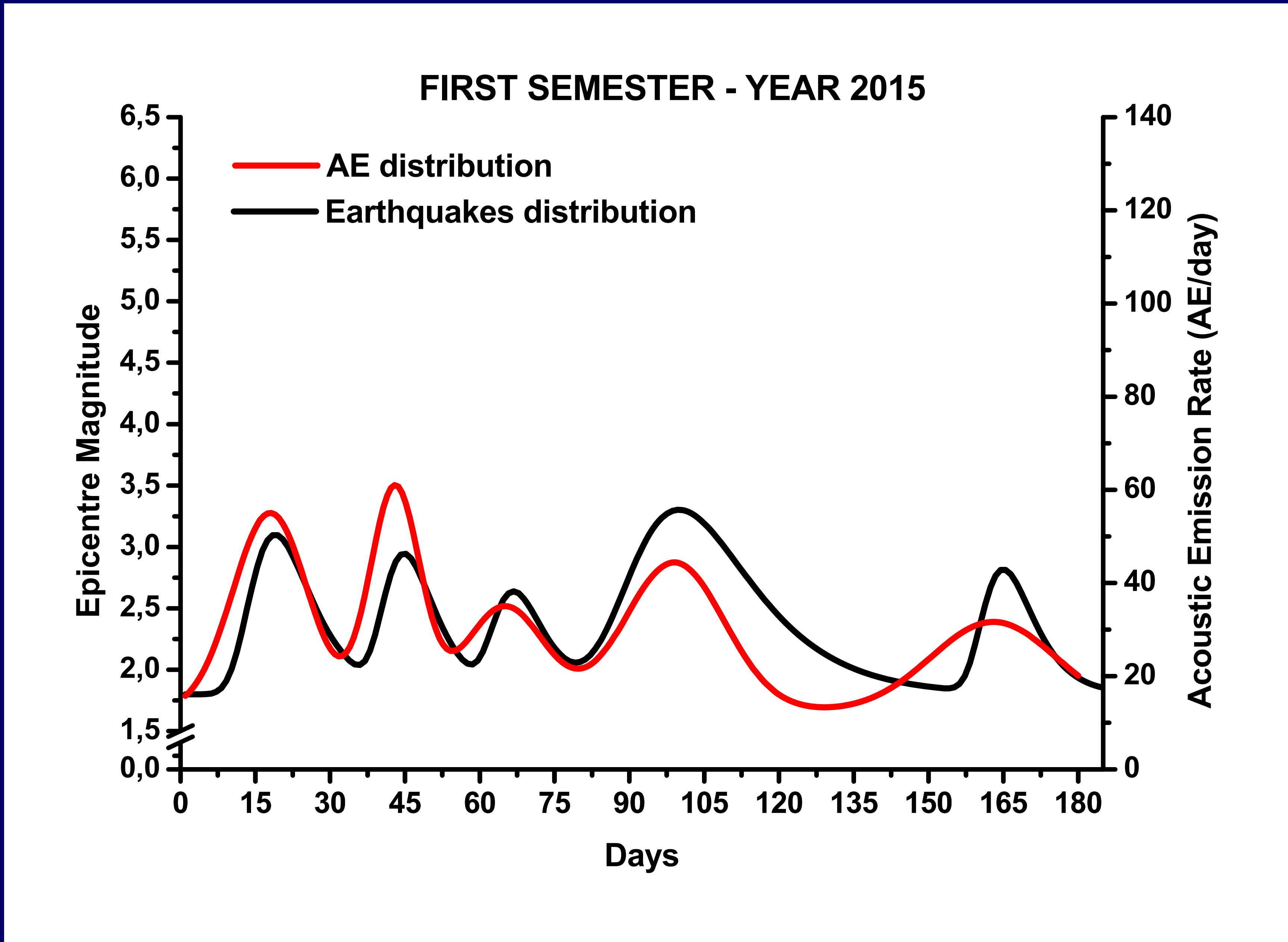

AE vs EARTHQUAKES (Second Sem. 2015)

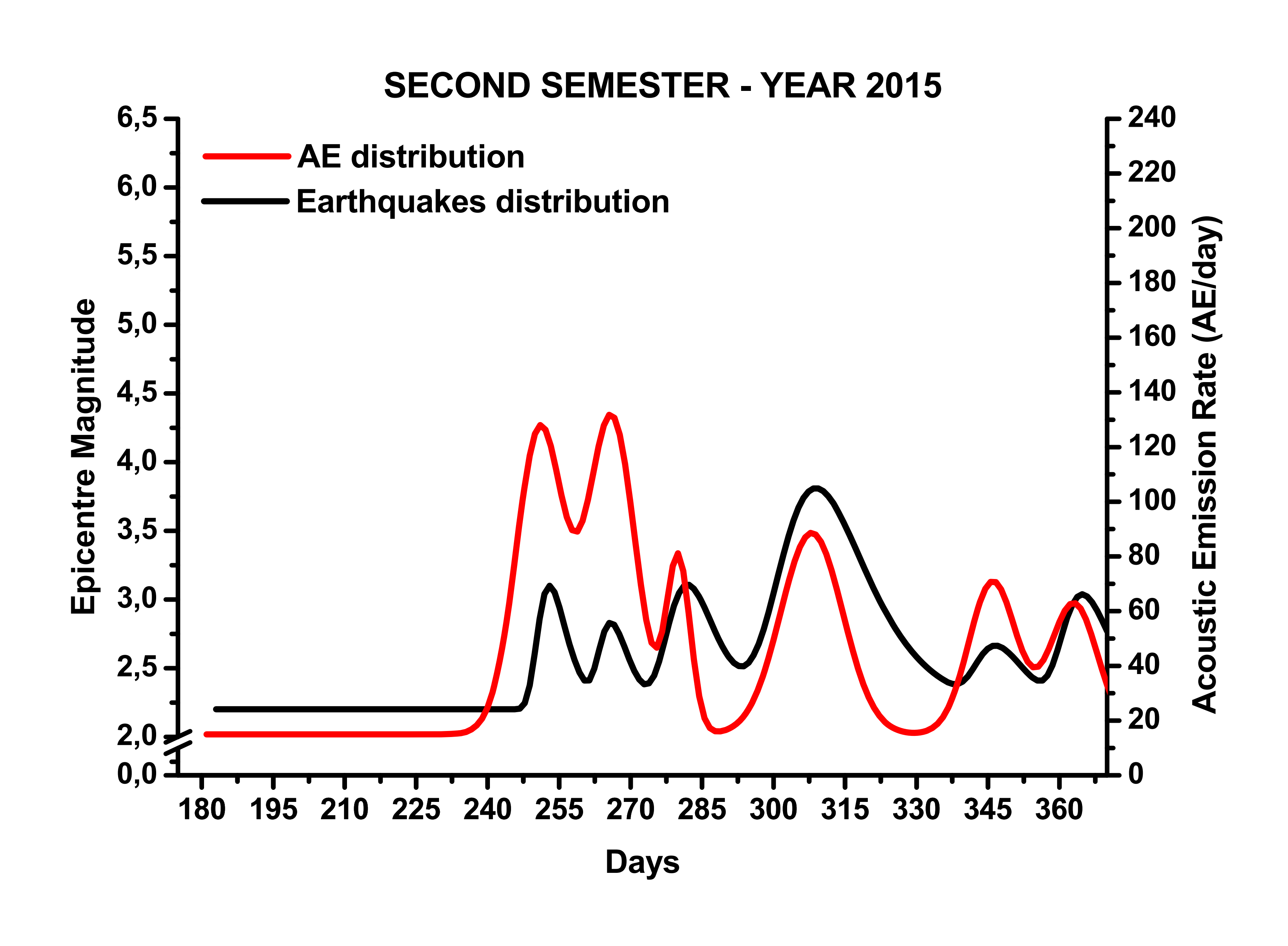

AE vs EARTHQUAKES (First Sem. 2016)

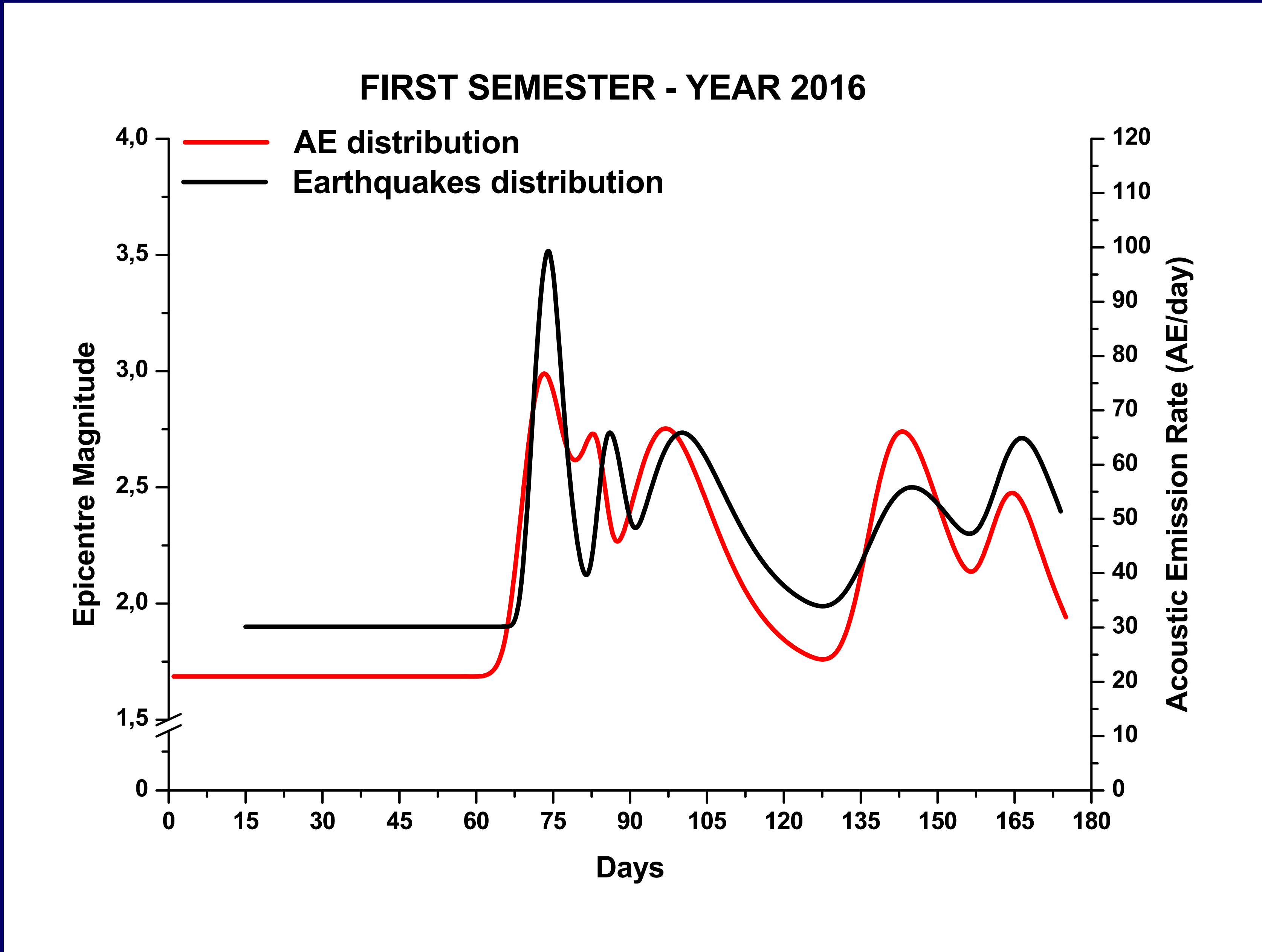

AE vs EARTHQUAKES (Second Sem. 2016)

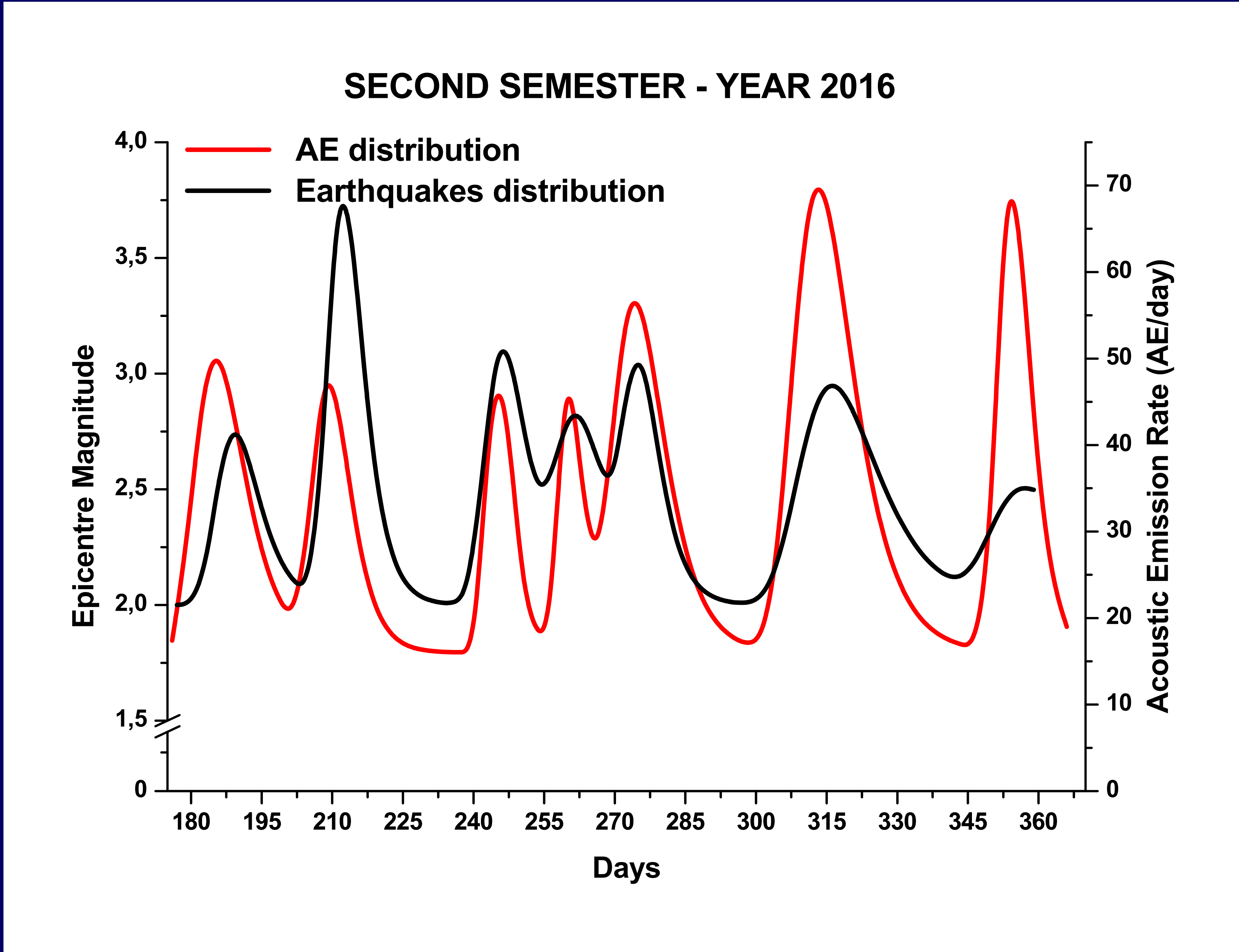

AE vs EARTHQUAKES (First Sem. 2017)

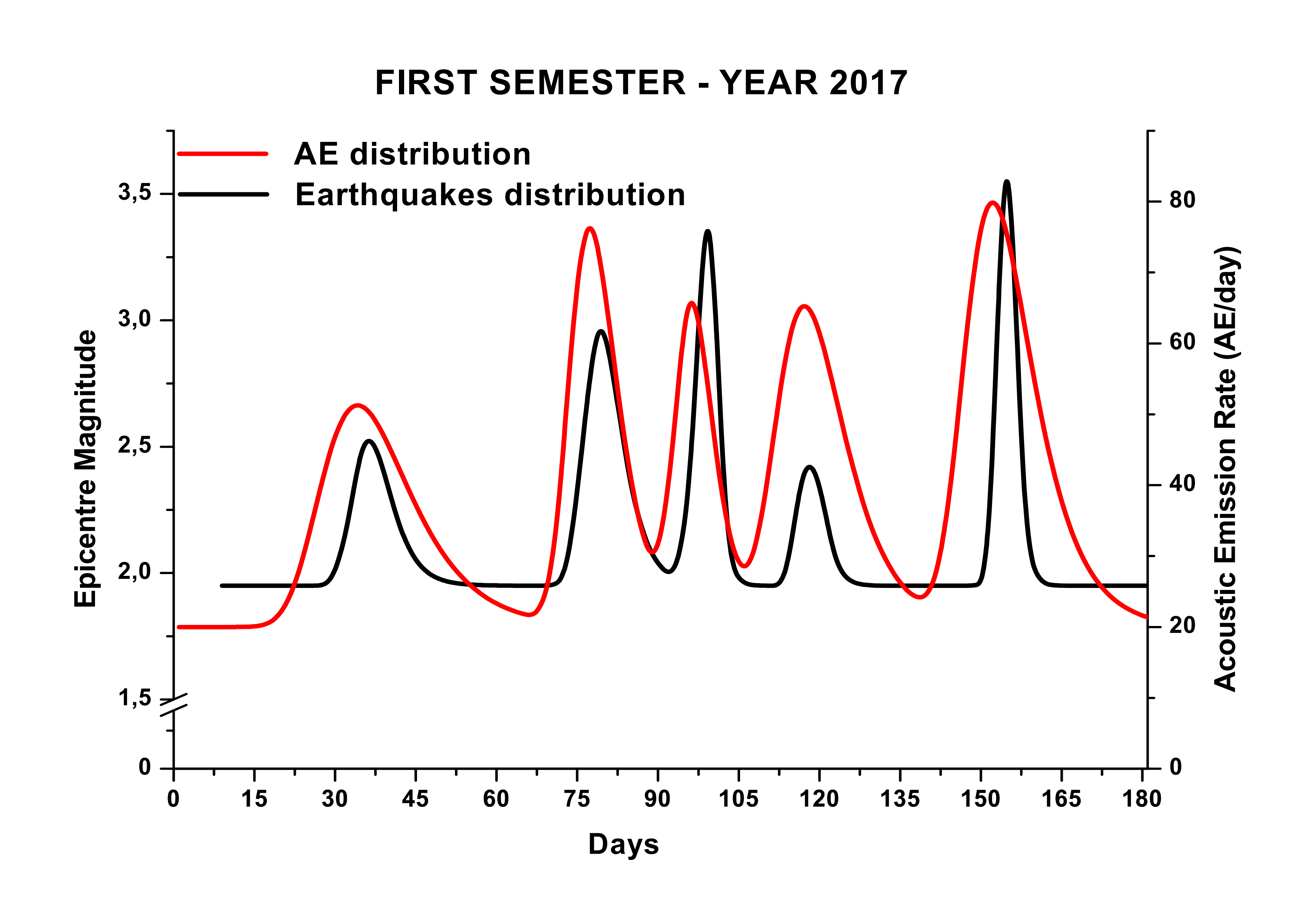

EME vs EARTHQUAKES (First Sem. 2015)

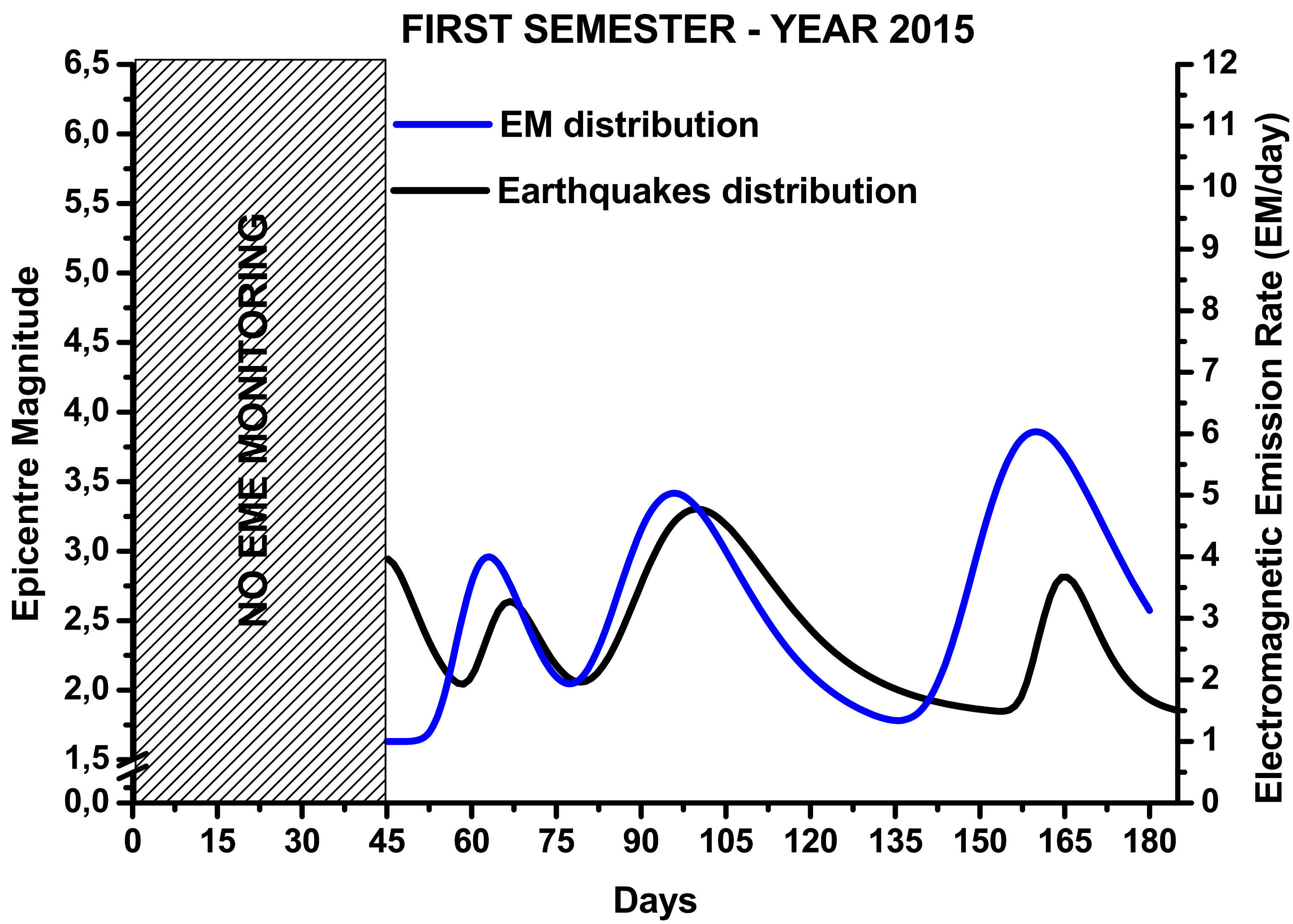

EME vs EARTHQUAKES (Second Sem. 2015)

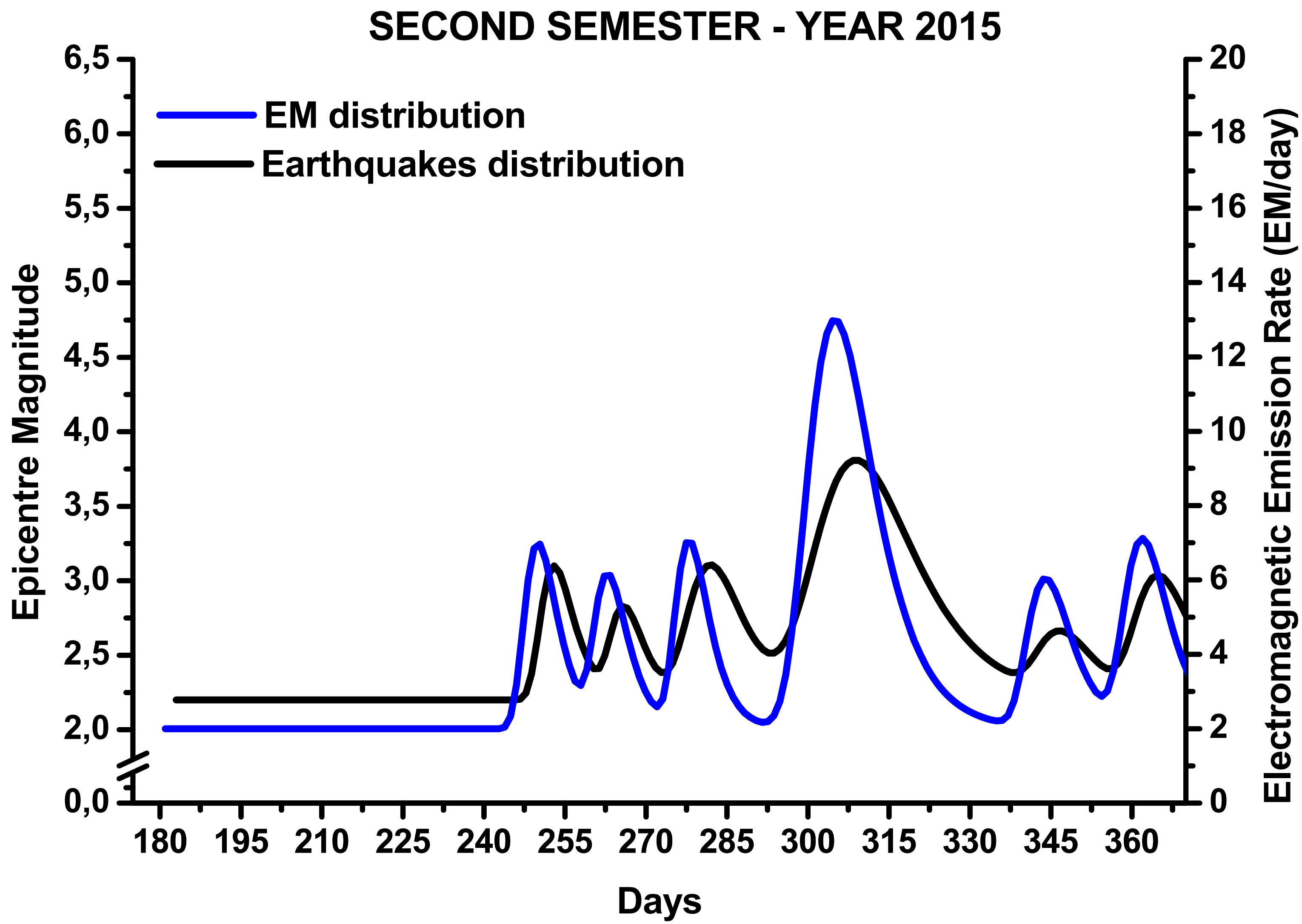

EME vs EARTHQUAKES (First Sem. 2016)

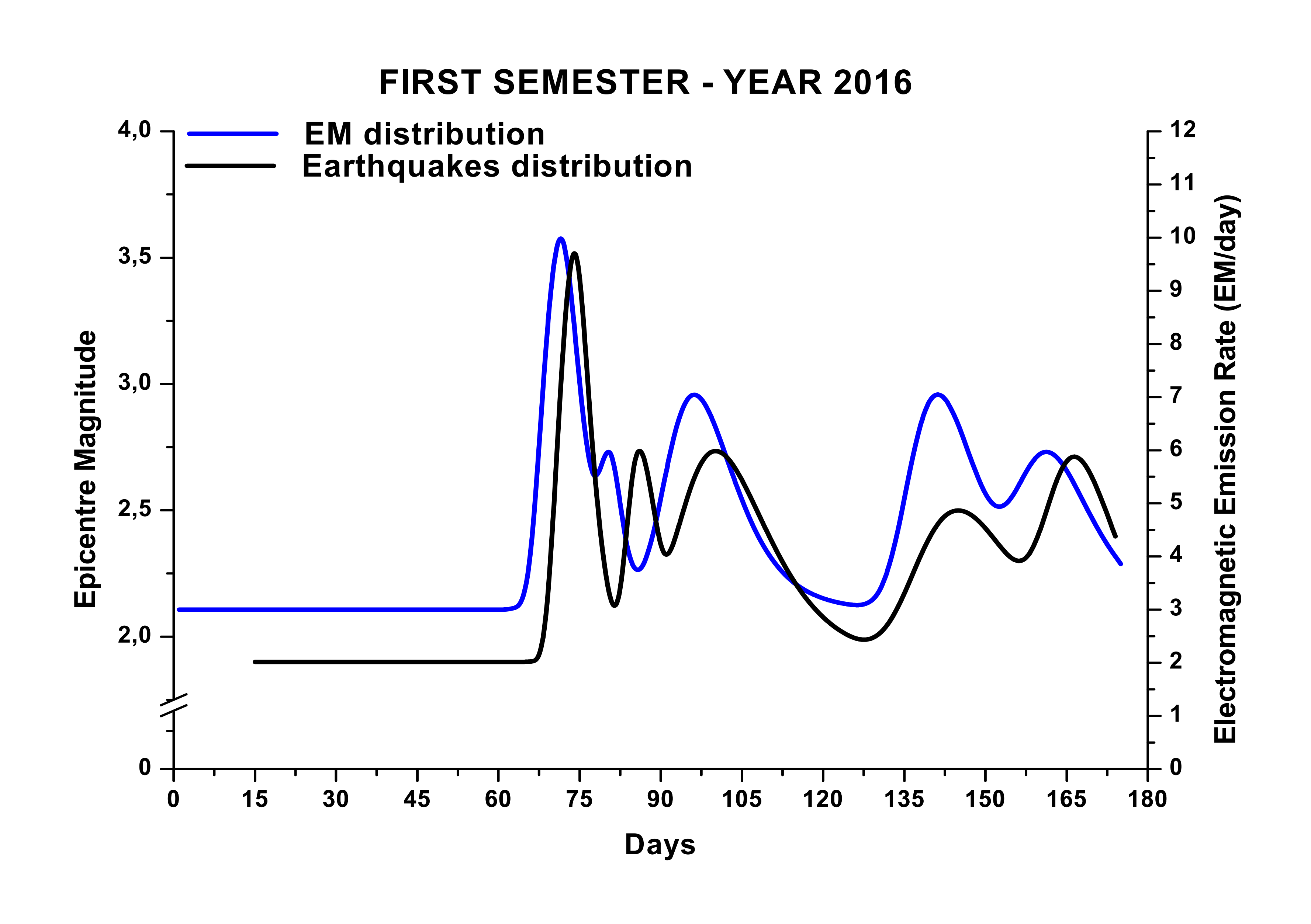

EME vs EARTHQUAKES (Second Sem. 2016)

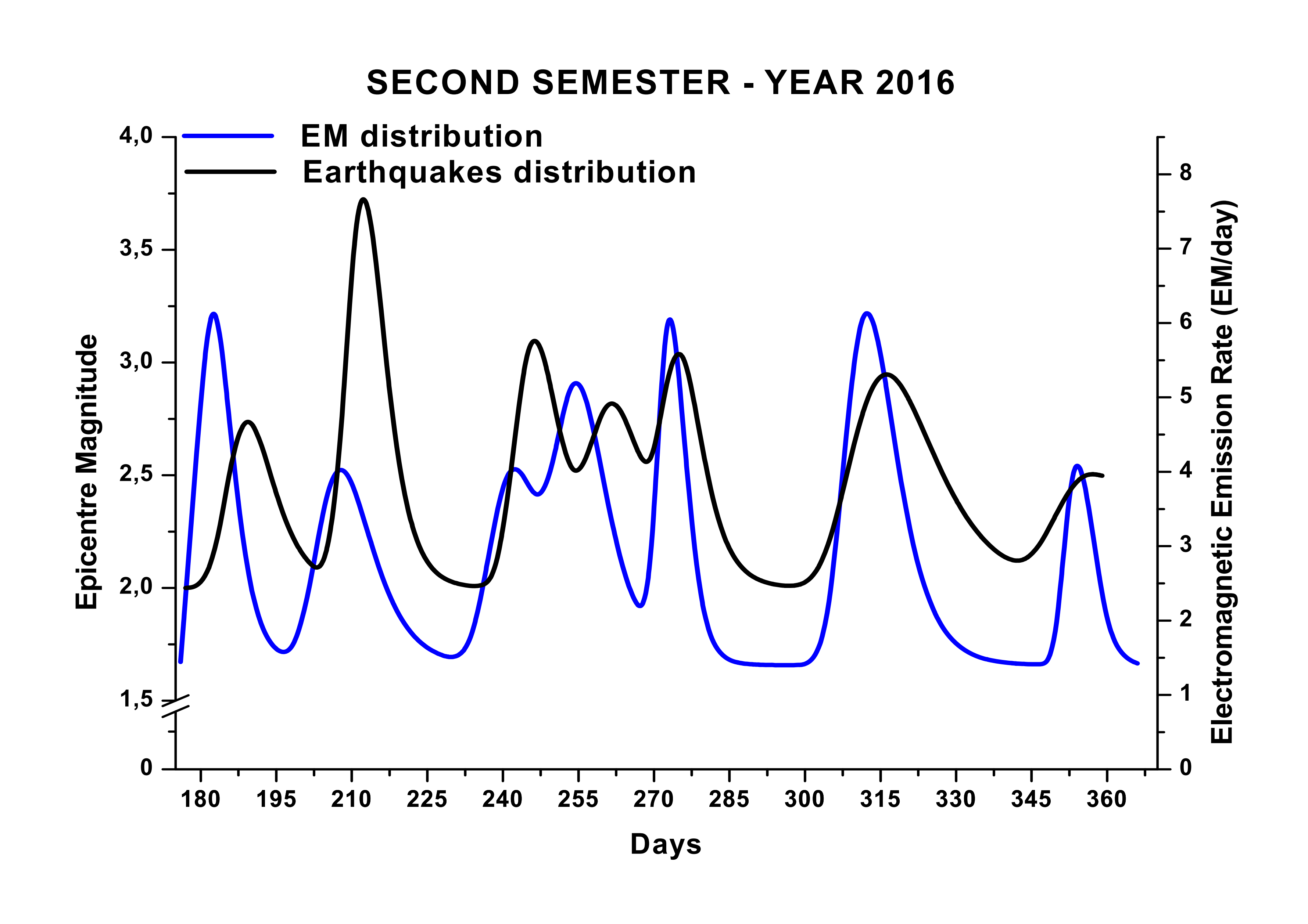

EME vs EARTHQUAKES (First Sem. 2017)

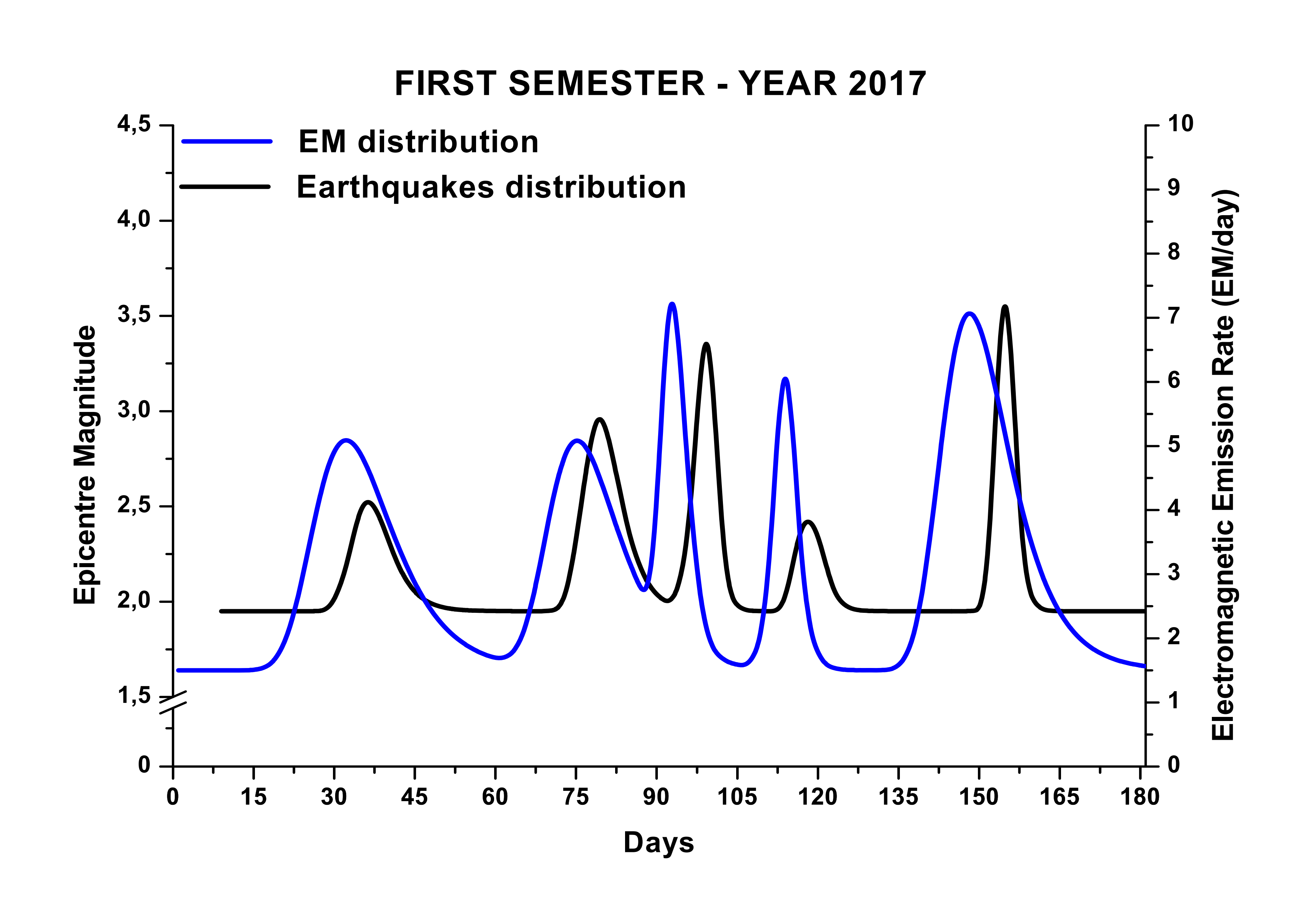

NE vs EARTHQUAKES (Second Sem. 2013)

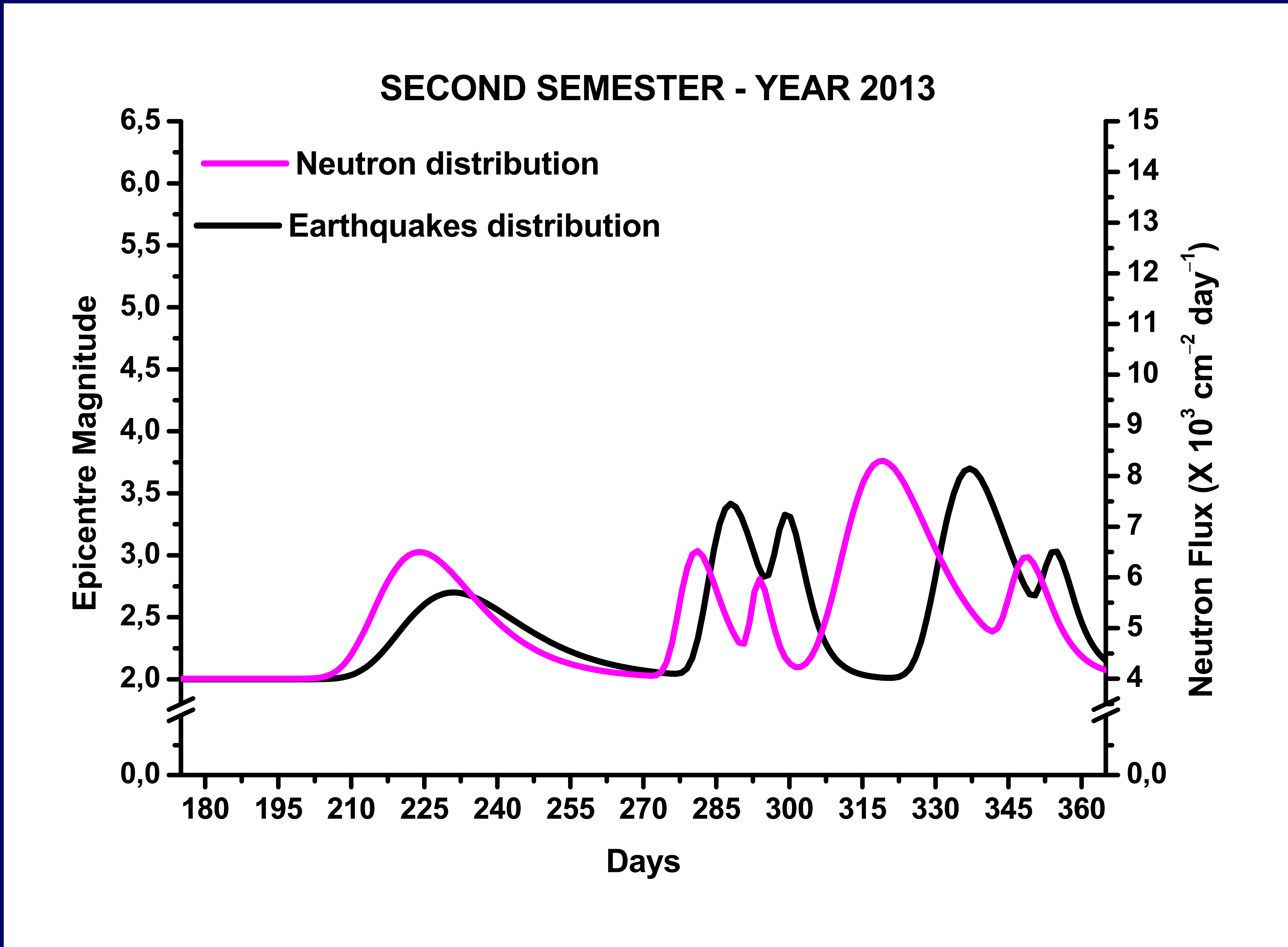

NE vs EARTHQUAKES (First Sem. 2014)

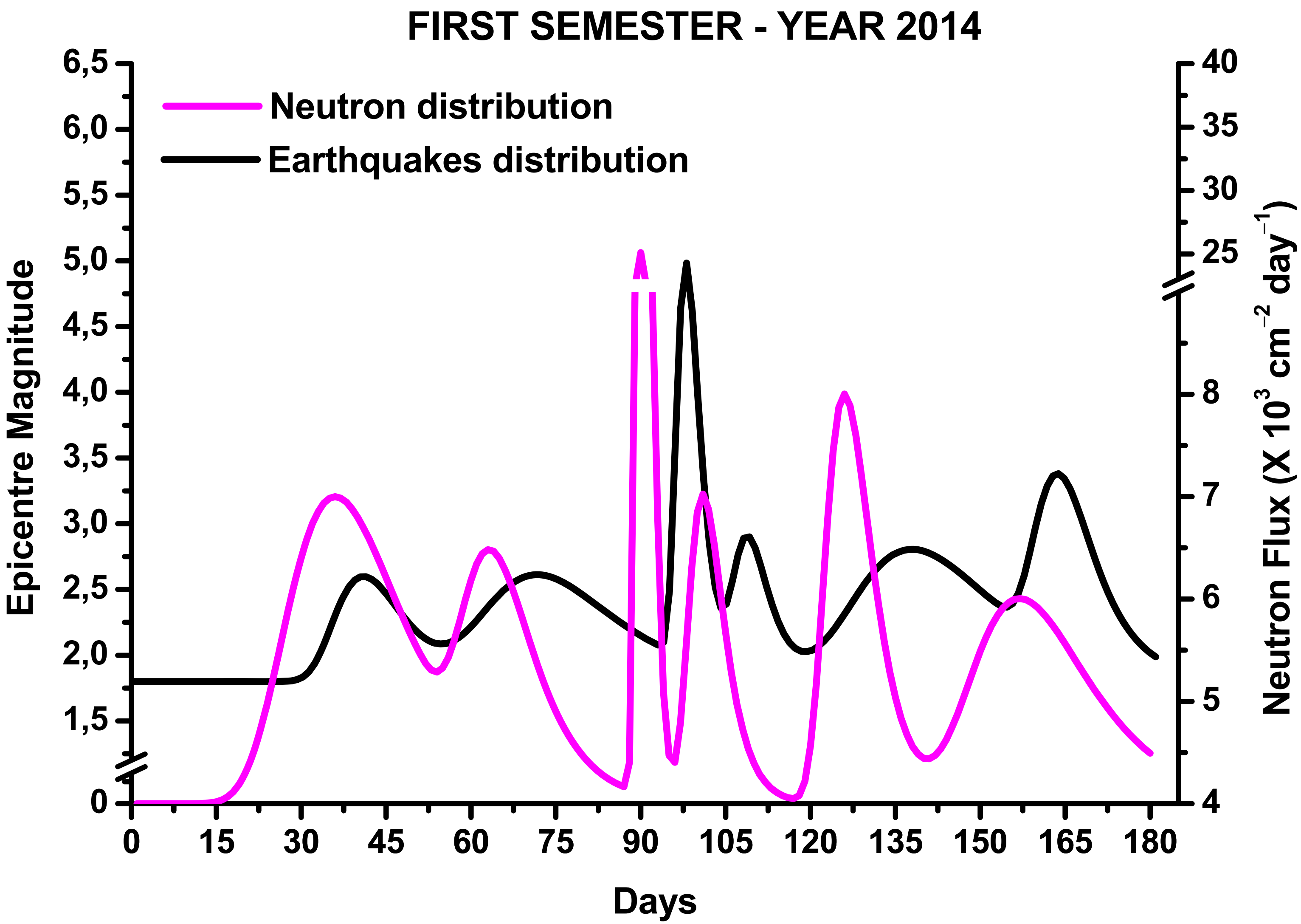

NE vs EARTHQUAKES (Second Sem. 2014)

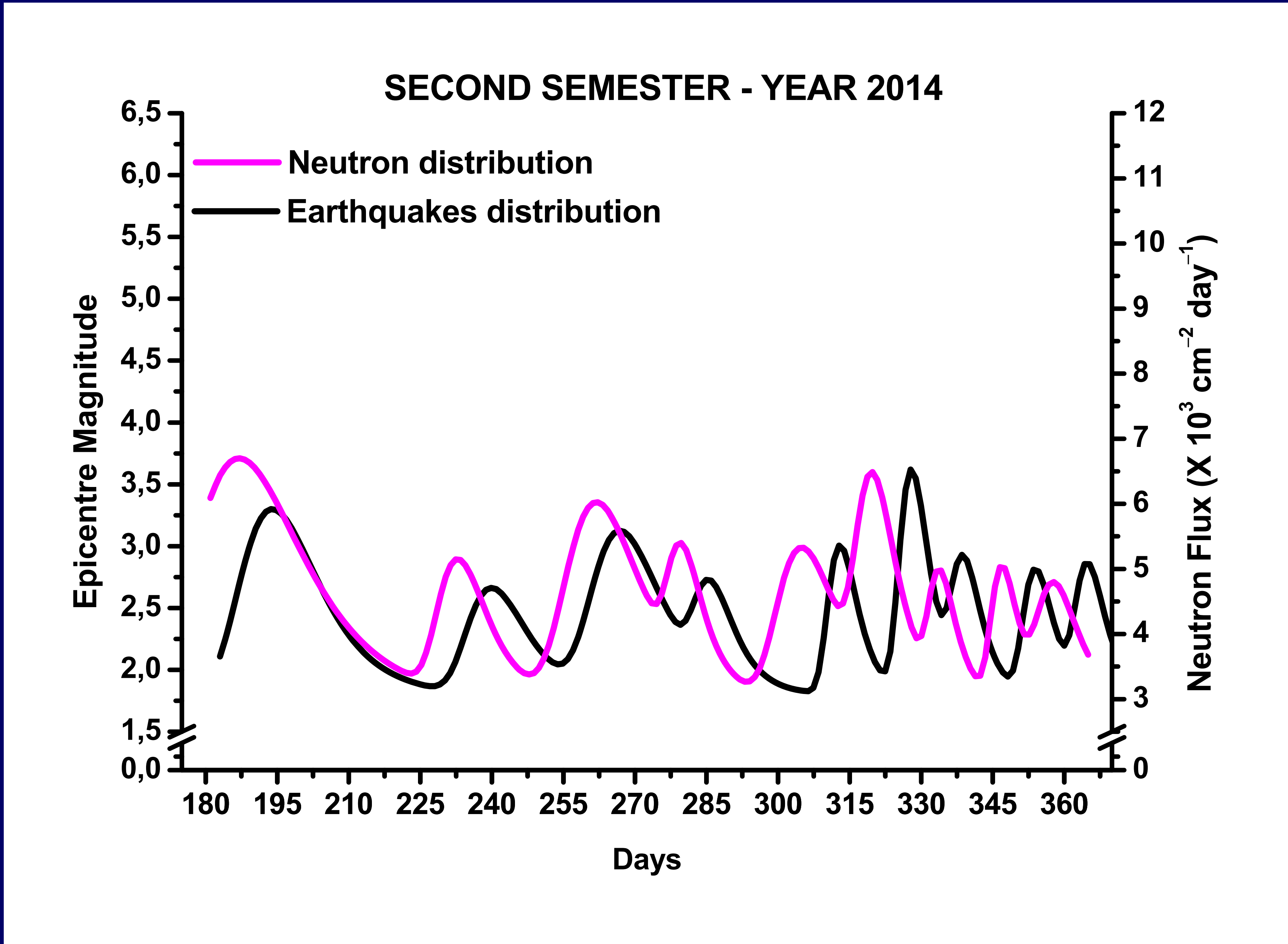

NE vs EARTHQUAKES (First Sem. 2015)

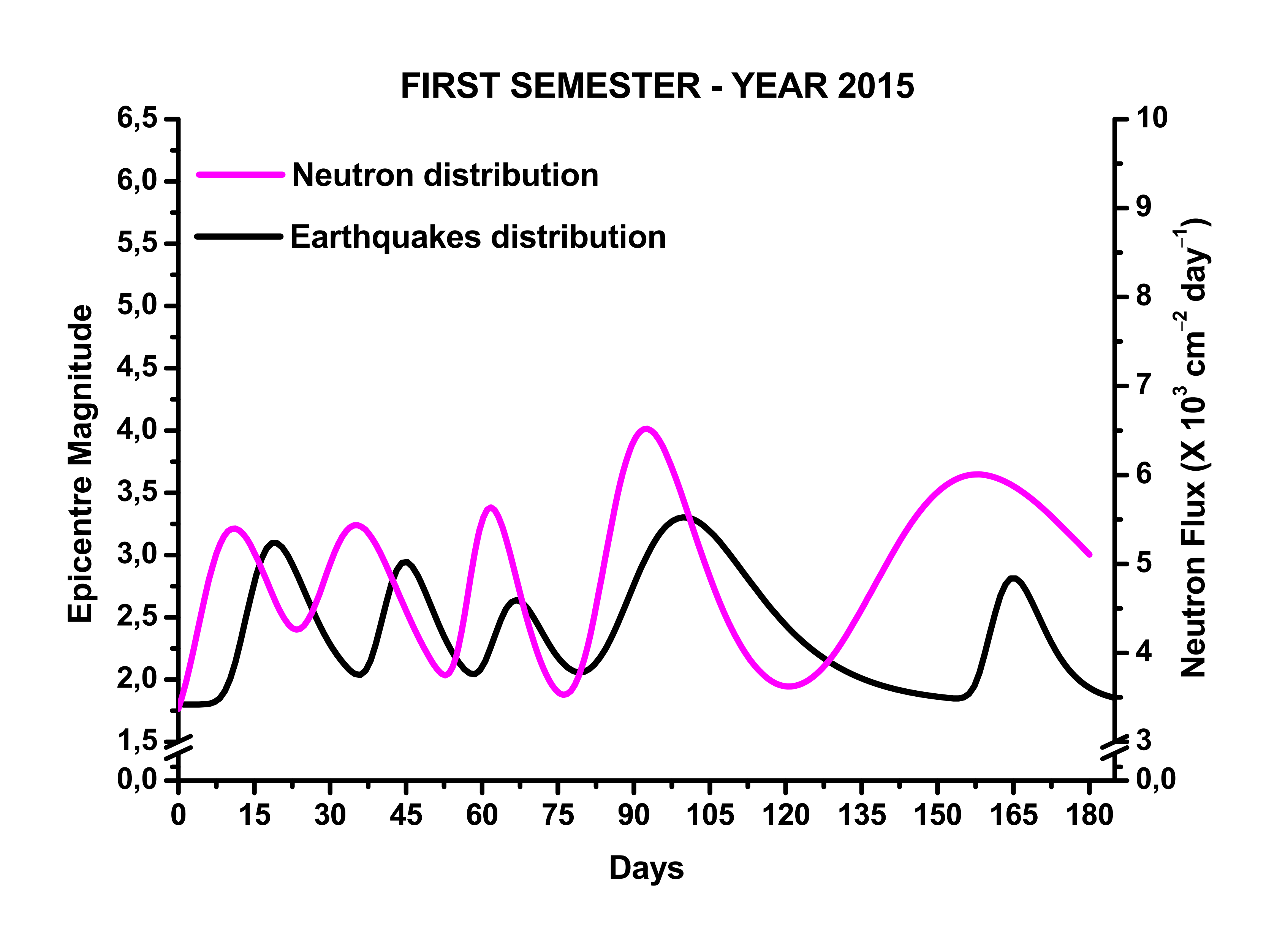

NE vs EARTHQUAKES (Second Sem. 2015)

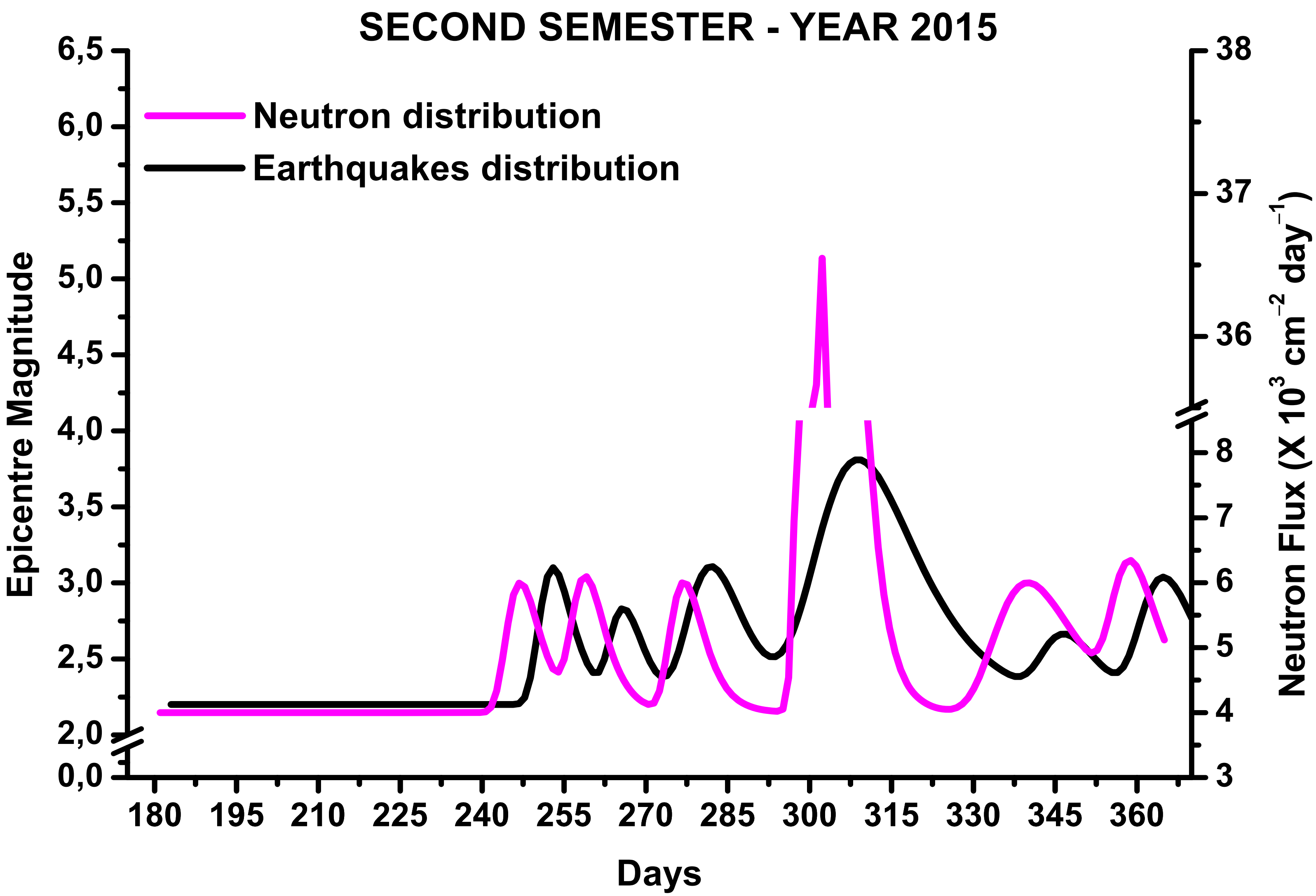

NE vs EARTHQUAKES (First Sem. 2016)

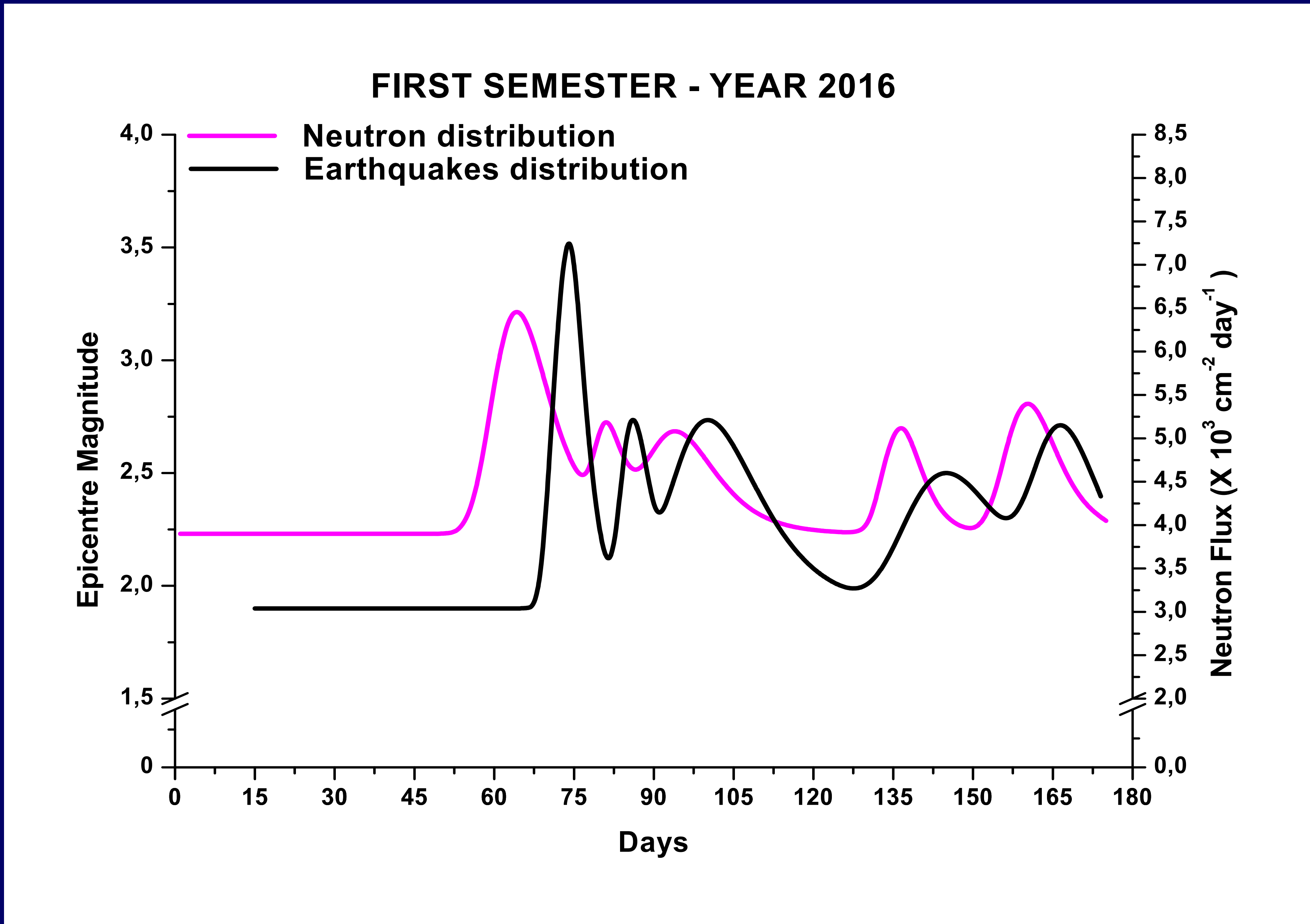

NE vs EARTHQUAKES (Second Sem. 2016)

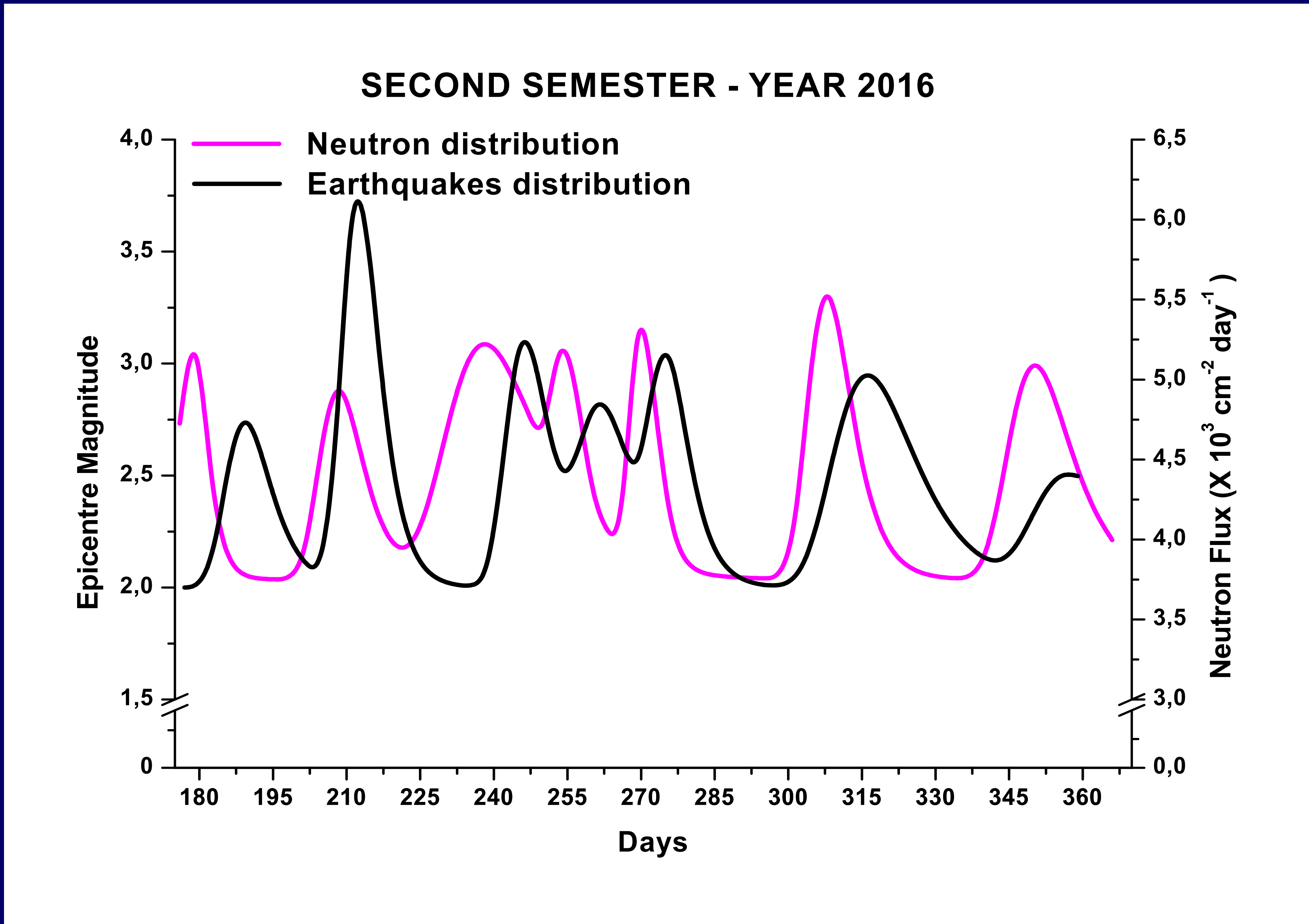

NE vs EARTHQUAKES (First Sem. 2017)

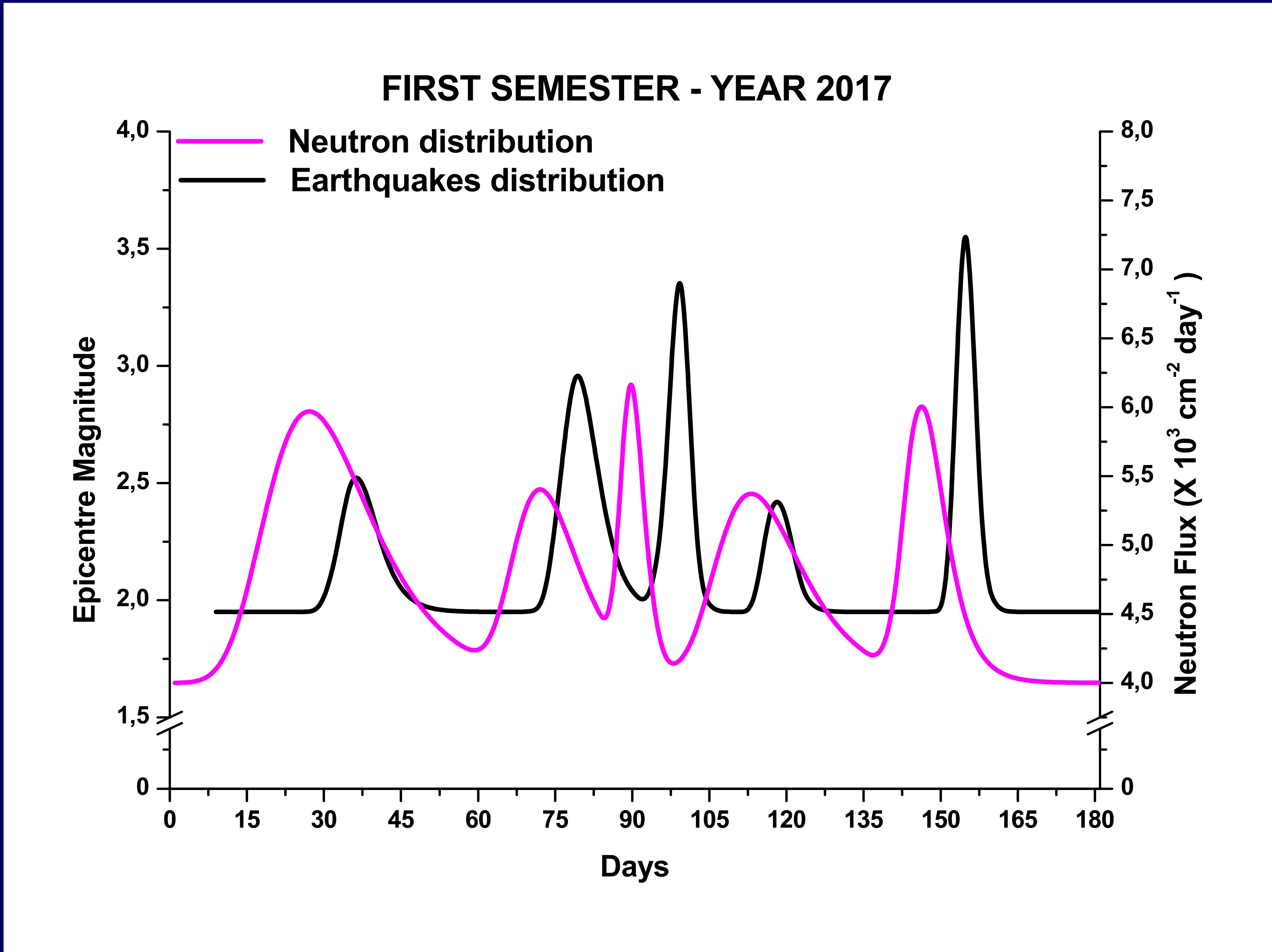

FRACTO-EMISSION CHRONOLOGICALLY ORDERED SHIFTING

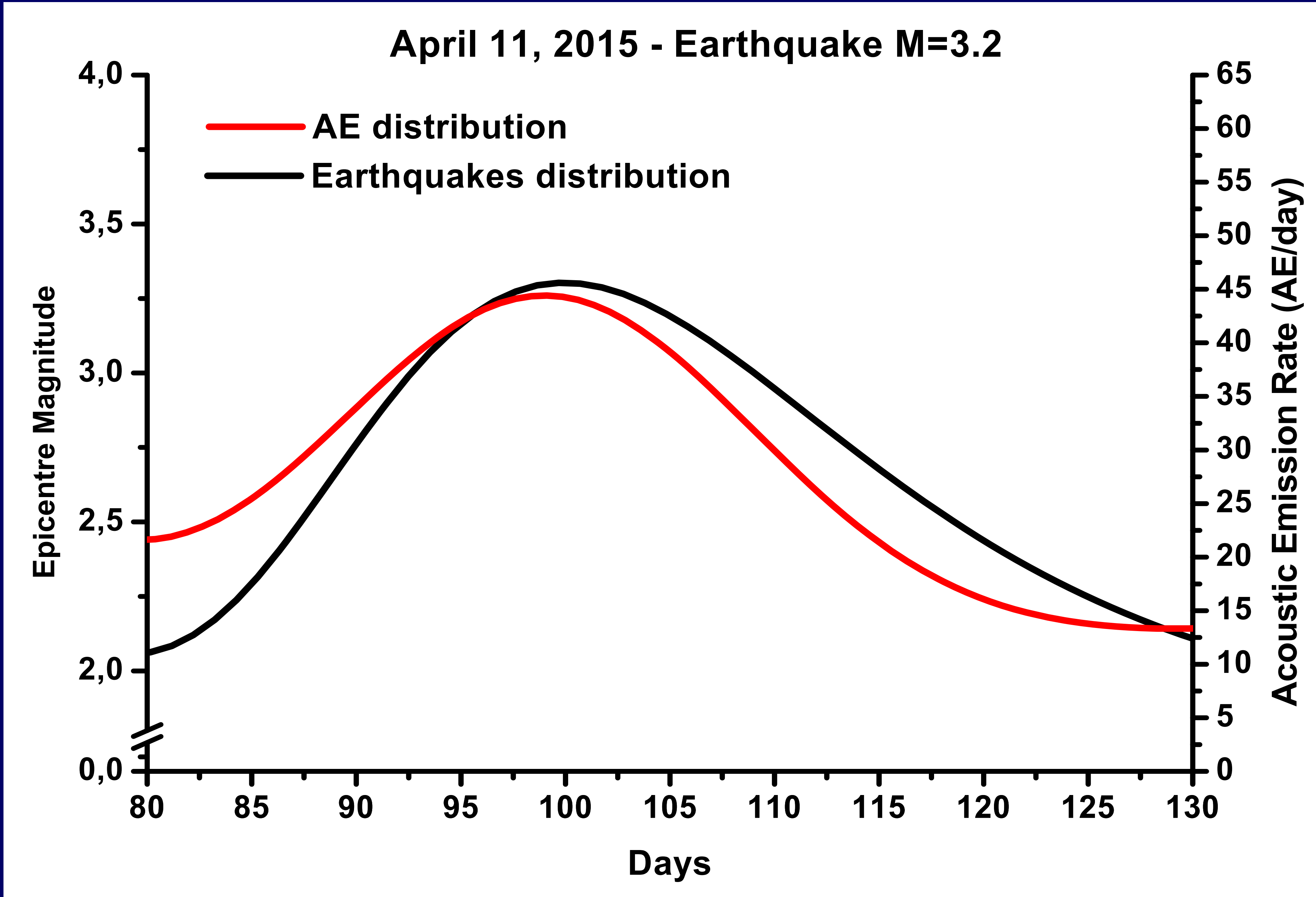

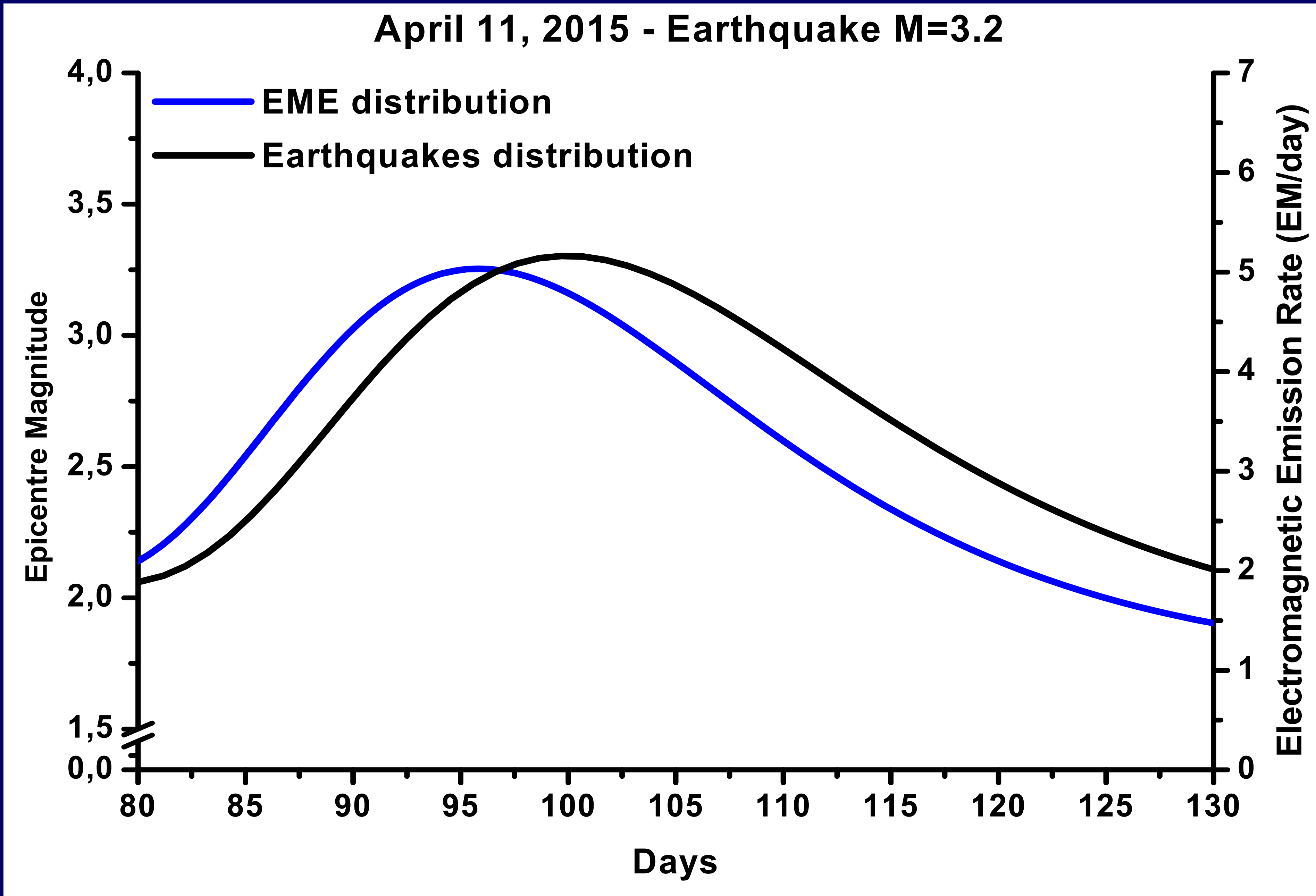

April 11, 2015 - Earthquake M=3.2
EME distribution
Earthquakes distribution
Epicentre Magnitude
Electromagnetic Emission Rate (EM/day)
Days
4,0
3,5
3,0
2,5
2,0
1,5
0,0
7
6
5
4
3
2
1
0
80
85
90
95
100
105
110
115
120
125
130

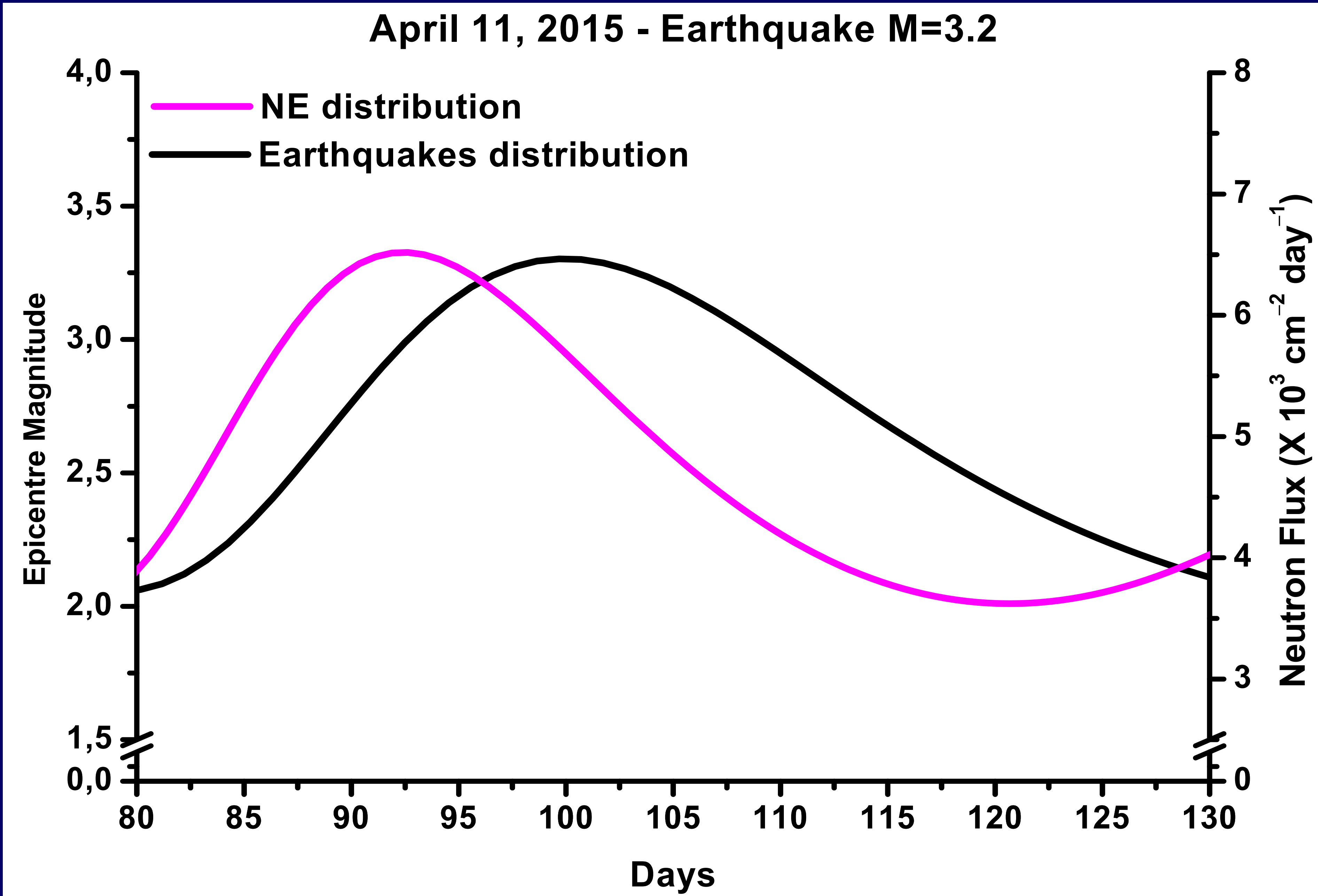

April 11, 2015 - Earthquake M=3.2
NE distribution
Earthquakes distribution
Epicentre Magnitude
4,0
3,5
3,0
2,5
2,0
1,5
0,0
Neutron Flux (X 10^3 cm^{-2} day^{-1})
8
7
6
5
4
3
0
80
85
90
95
100
105
110
115
120
125
130
Days

FRACTO-EMISSION PEAK INTENSITY vs EARTHQUAKE LOCAL MAGNITUDE

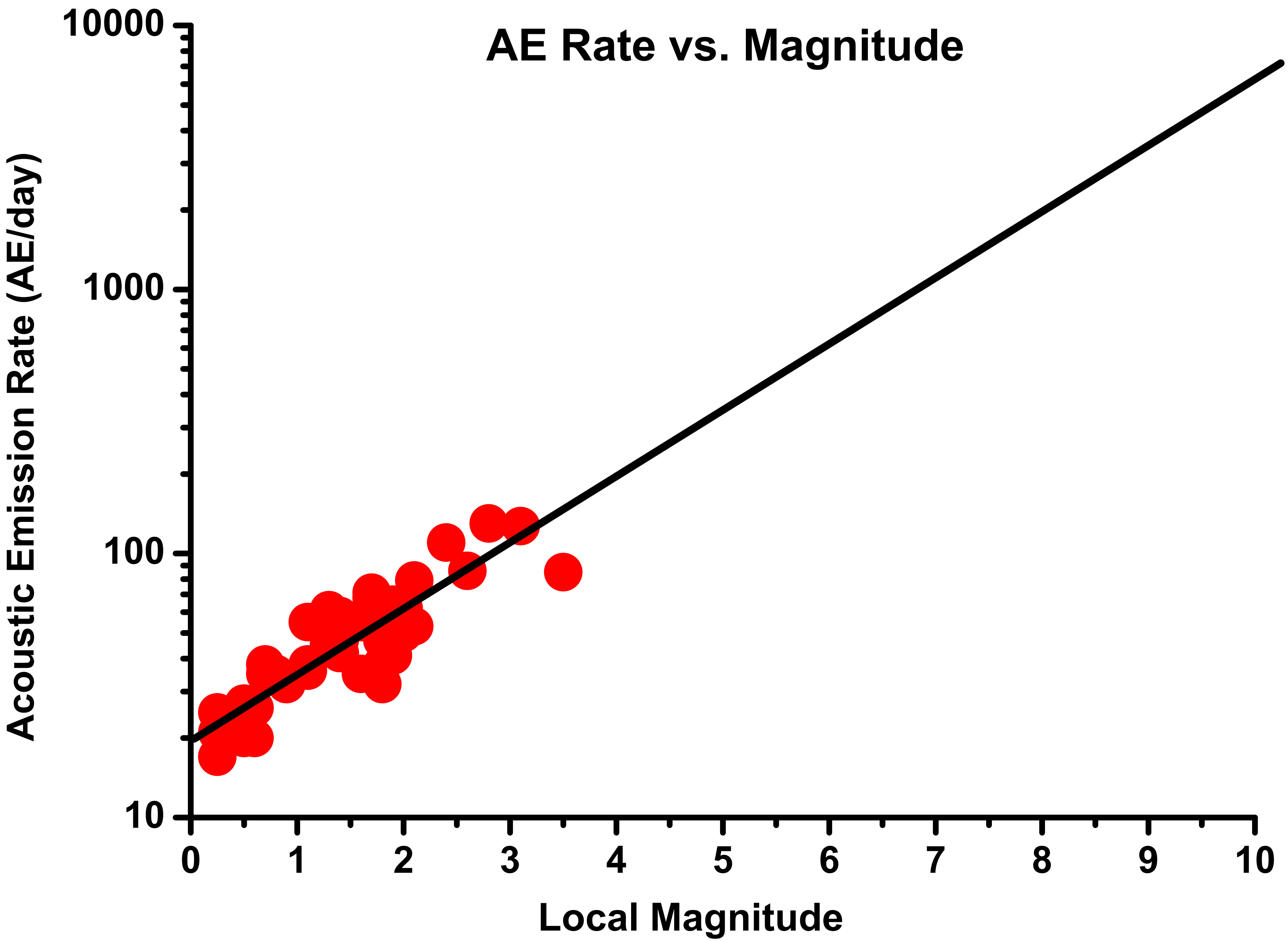

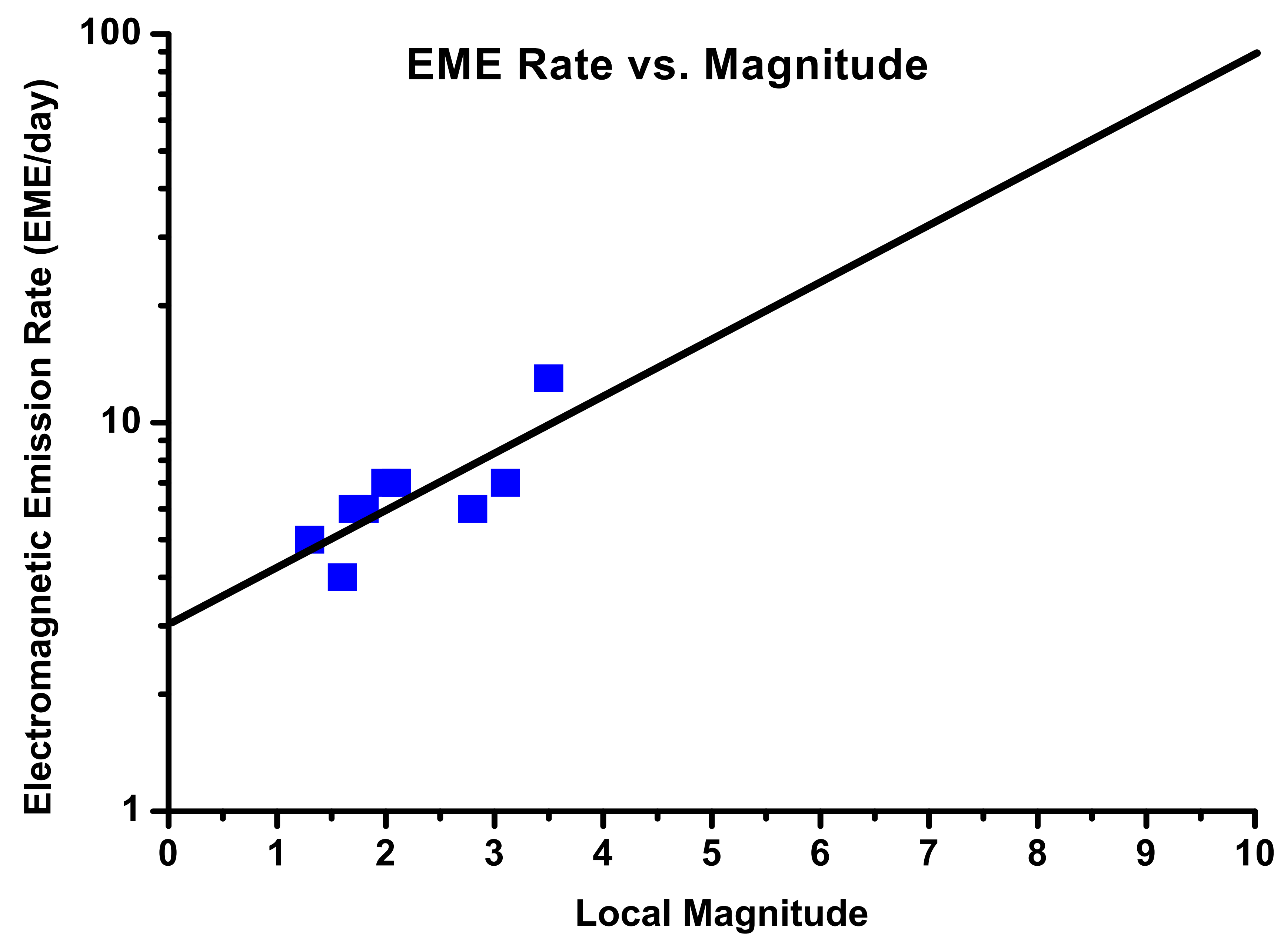

EME Rate vs. Magnitude
Electromagnetic Emission Rate (EME/day)
100
10
1
0
1
2
3
4
5
6
7
8
9
10
Local Magnitude

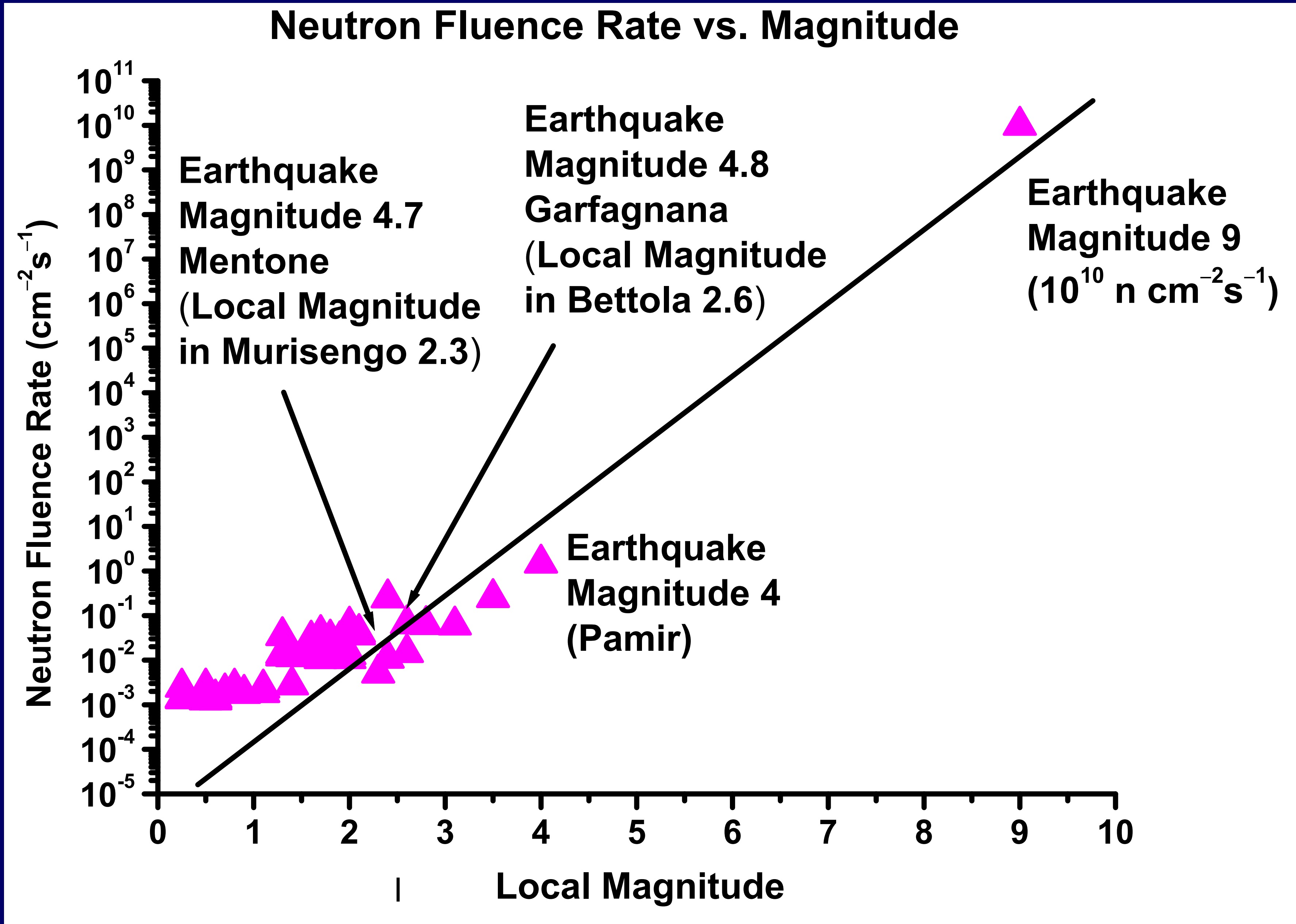

Neutron Fluence Rate vs. Magnitude
Neutron Fluence Rate (cm^{-2}s^{-1})
Local Magnitude
Earthquake Magnitude 4.7 Mentone (Local Magnitude in Murisengo 2.3)
Earthquake Magnitude 4.8 Garfagnana (Local Magnitude in Bettola 2.6)
Earthquake Magnitude 9 (10^{10} n cm^{-2}s^{-1})
Earthquake Magnitude 4 (Pamir)

Engineering Fracture Mechanics 177 (2017) 239–250

Contents lists available at ScienceDirect

Engineering Fracture Mechanics

journal homepage: www.elsevier.com/locate/engfracmech

Fracto-emissions as seismic precursors

Alberto Carpinteri *, Oscar Borla

Politecnico di Torino, Department of Structural, Geotechnical and Building Engineering, Corso Duca degli Abruzzi 24, 10129 Torino, Italy

A R T I C L E I N F O

Article history:
Received 6 December 2016
Received in revised form 6 March 2017
Accepted 7 March 2017
Available online 9 March 2017

Keywords:
Fracture
TeraHertz pressure waves
Neutron emissions
Acoustic emissions
Electromagnetic emissions
Earthquake precursors
Multi-modal statistics

A B S T R A C T

Three different forms of energy might be used as earthquake precursors for environmental protection against seismicity. At the tectonic scale, Acoustic Emission (AE) prevails, as well as Electro-Magnetic Emission (EME) at the intermediate scales, and Neutron Emission (NE) at the nano-scale. TeraHertz pressure waves are in fact produced at the last extremely small scale, and fracture experiments on natural rocks have recently demonstrated that these high-frequency waves are able to induce nuclear fission reactions with neutron and/or alpha particle emissions. Very important applications to earthquake precursors can be proposed. The authors present the results they are obtaining at a gypsum mine located in Northern Italy. In this mine, to avoid interference with human activities, the instrumental control units have been located at one hundred metres underground. The experimental results obtained from July 1st, 2013 to December 31, 2015 (five semesters) are analysed by means of a suitable multi-modal statistics. The experimental observations reveal a strong correlation between the three fracto-emission peaks (acoustic, electromagnetic, and neutron emissions) and the major earthquakes occurred in the surrounding areas.

CHEMICAL EVOLUTION AT THE PLANETARY SCALE

IRON DEPLETION vs CARBON POLLUTION

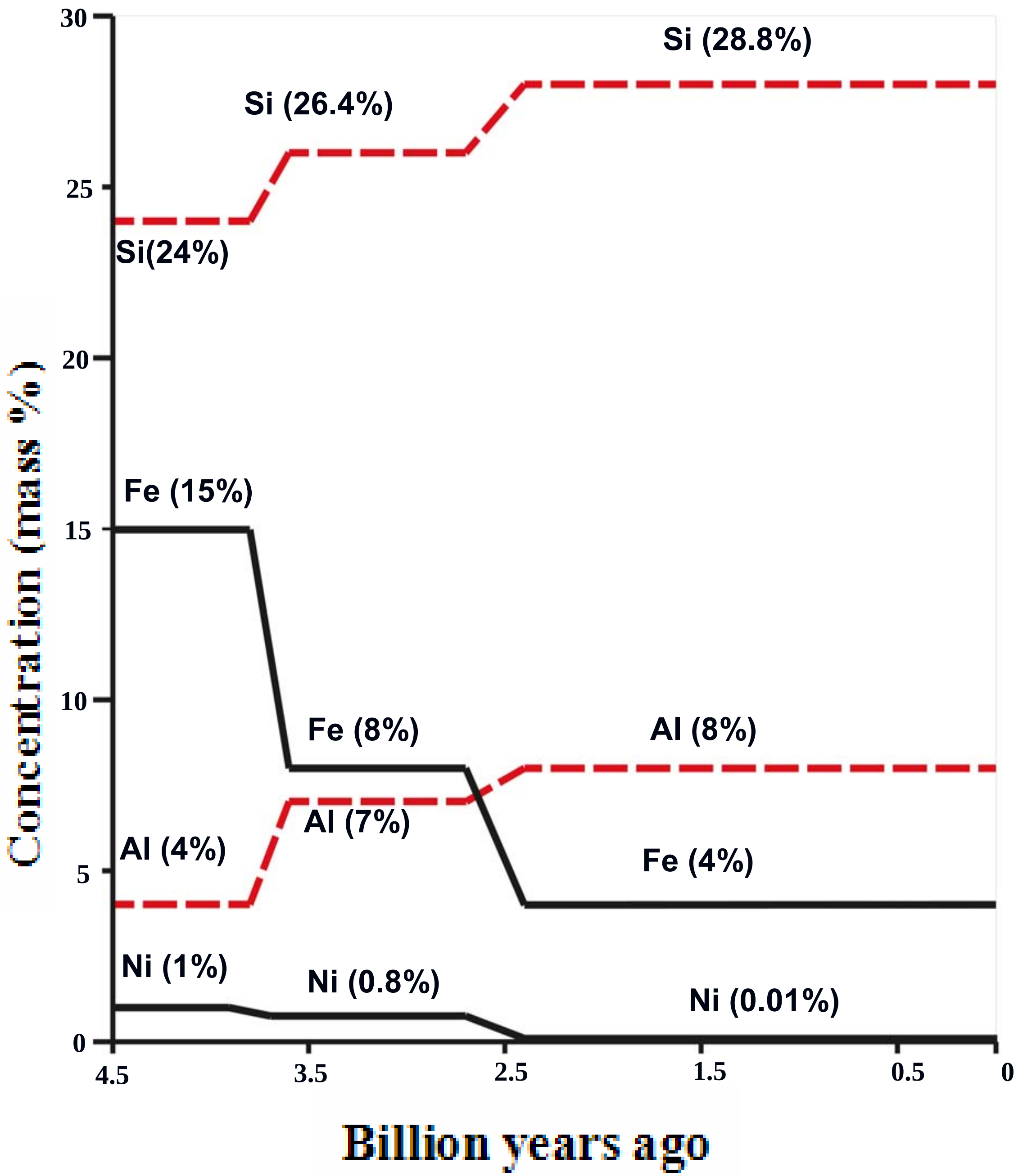

Tectonic plate formation

(3.8 Billion years ago):
Fe (–7%) + Ni (–0.2%) =
=Al (+3%) + Si (+2.4%) + C (+1.8%)

Most severe tectonic activity

(2.5 Billion years ago):
Fe (–4%) + Ni (–0.8%) =
=Al (+1%) + Si (+2.4%) + C (+1.4%)

Conjecture about ferrous elements' transformations in the Earth Crust

(1) $Fe_{26}^{56} \to 2\,Al_{13}^{27} + 2n$

(2) $Fe_{26}^{56} \to Mg_{12}^{24} + Si_{14}^{28} + 4n$

(3) $Ni_{28}^{59} \to 2\,Si_{14}^{28} + 3n$

Magnesium depletion and Carbon increment in the primordial atmosphere

The estimated Mg increase (~3.2%) is equivalent to the Carbon content in the primordial atmosphere:

$$Fe_{26}^{56} \rightarrow Mg_{12}^{24} + Si_{14}^{28} + 4n$$

$$Mg_{12}^{24} \rightarrow 2C_{6}^{12}$$

Assuming a mean density of the Earth Crust equal to 3.6 g/cm^3 and a thickness of ~60 km, the mass increase in Mg (~3.5×10^{21} kg), and therefore in C, implies a very high atmospheric pressure.

Primordial atmospheric pressure due to C increase = ~660 atm

↔

Primordial atmospheric pressure reported by other authors = ~650 atm (Liu, 2004)

Liu, L., "The inception of the oceans and CO_2-atmosphere in the early history of the Earth". *Earth Planet. Sci. Lett.*, 227, 179–184 (2004)

theguardian

Friday 8 March 2013 10.55 GMT

News | Sport | Comment | Culture | Business | Money | Life & style

Environment › Climate change

Large rise in CO2 emissions sounds climate change alarm

Hopes for 'safe' temperature increase within 2C fade as Hawaii station documents second-greatest emissions increase

"What is disturbing scientists is the acceleration of CO_2 concentrations in the atmosphere, which is occurring in spite of attempts by governments to restrain fossil fuel emissions"

Localization of iron mines

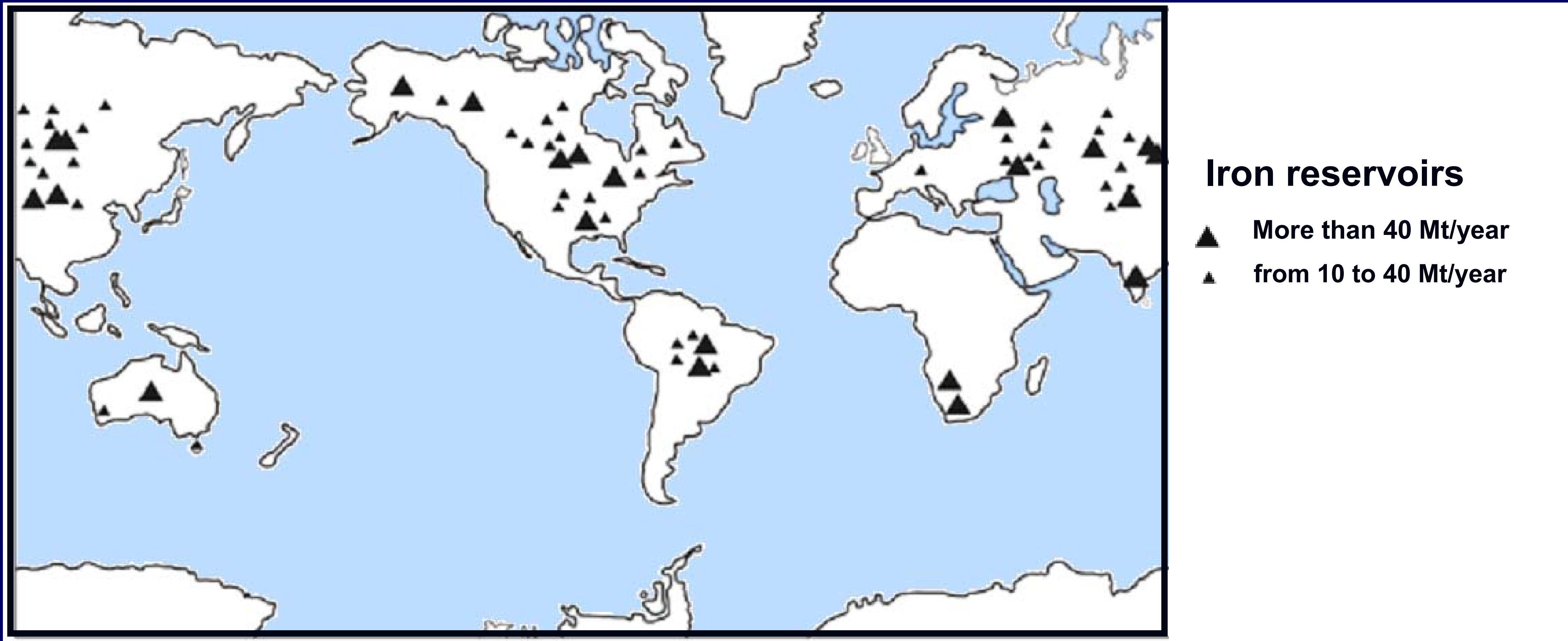

(*) World Iron Ore producers. Available at http://www.mapsofworld.com/minerals/world-iron-ore-producers.html.

(**) World Mineral Resources Map. Available at http://www.mapsofworld.com/world-mineral-map.html.

Localization of Aluminum mines

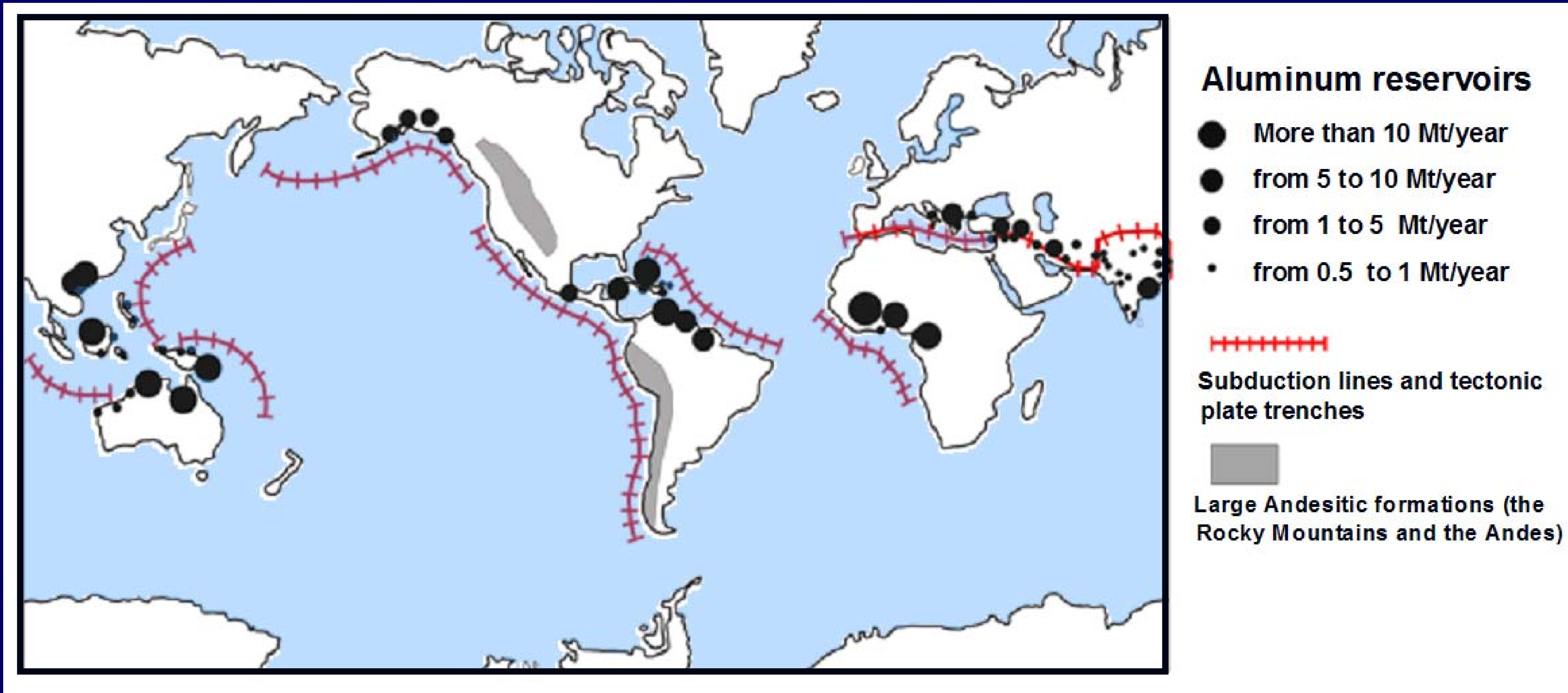

(*) World Iron Ore producers. Available at http://www.mapsofworld.com/minerals/world-iron-ore-producers.html.

(**) World Mineral Resources Map. Available at http://www.mapsofworld.com/world-mineral-map.html.

Salinity level in the Mediterranean Sea

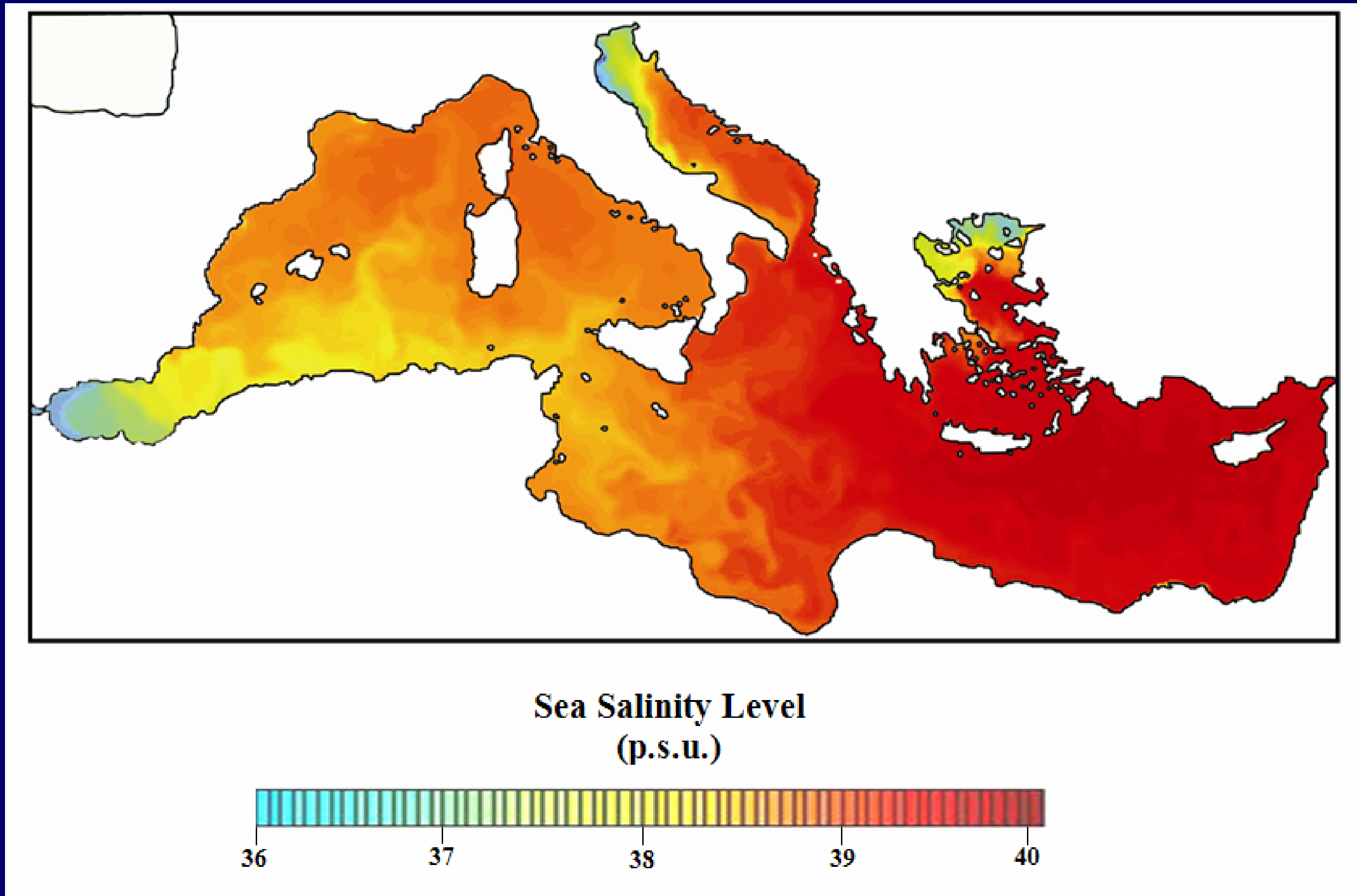

Map of the salinity level in the Mediterranean Sea expressed in p.s.u. The Mediterranean basin is characterized by the highest sea salinity level in the World.

Map of the major earthquakes in the last fifteen years

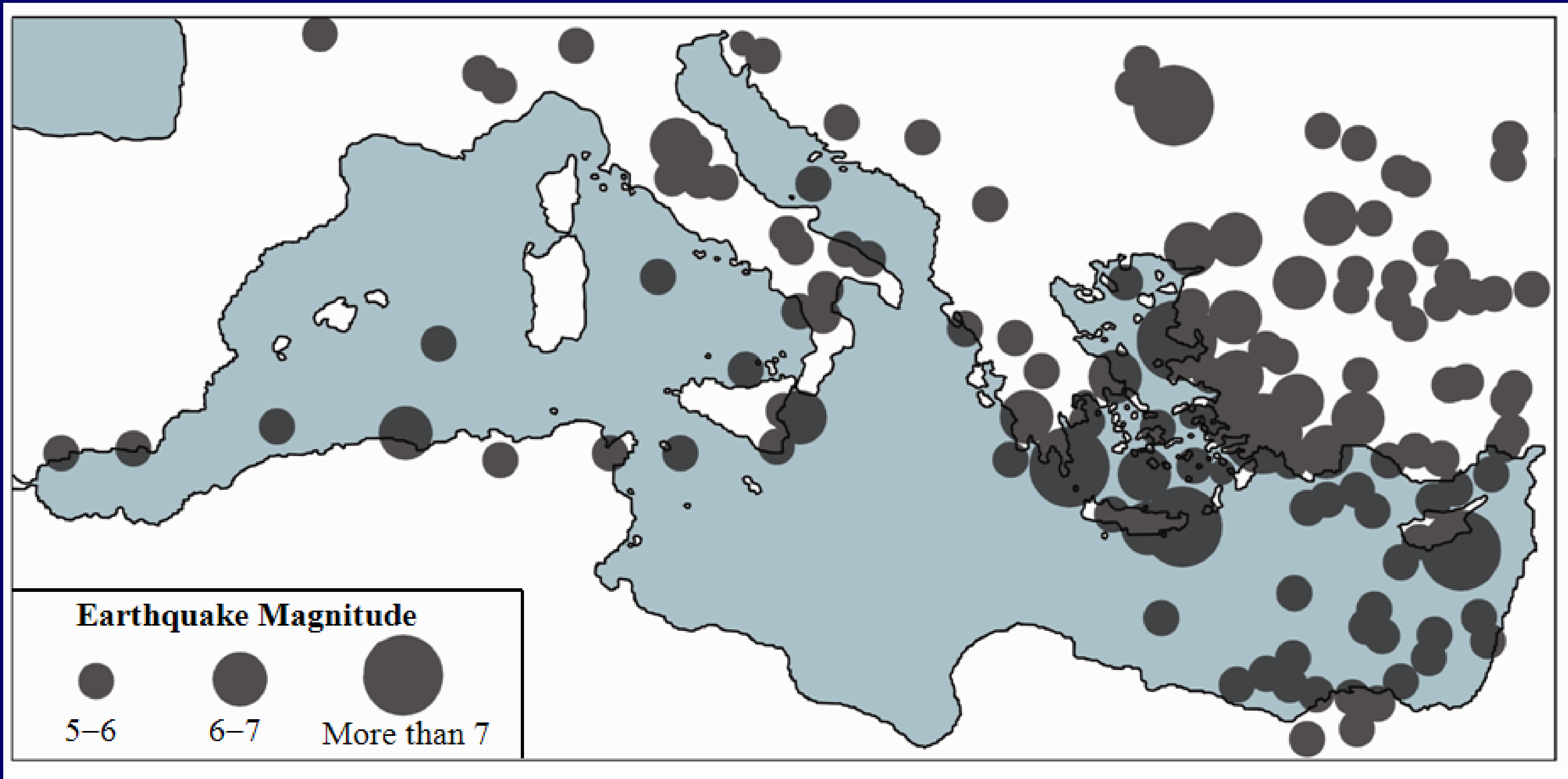

Nickel Depletion: $Ni_{28}^{59} \rightarrow Na_{11}^{23} + Cl_{17}^{35} + 1n$

HIERARCHY OF PIEZONUCLEAR FISSION REACTIONS

Two piezonuclear fission reaction jumps typical of the Earth Planet:

$$Fe_{26}, Co_{27}, Ni_{28} \qquad \text{(NI-FE)}$$

$$\downarrow$$

$$Mg_{12}, Al_{13}, Si_{14} \qquad \text{(SI-MA, SI-AL)}$$

$$\downarrow$$

$$C_{6}, N_{7}, O_{8} \qquad \text{(Atmosphere)}$$

CALCIUM DEPLETION vs OCEAN FORMATION

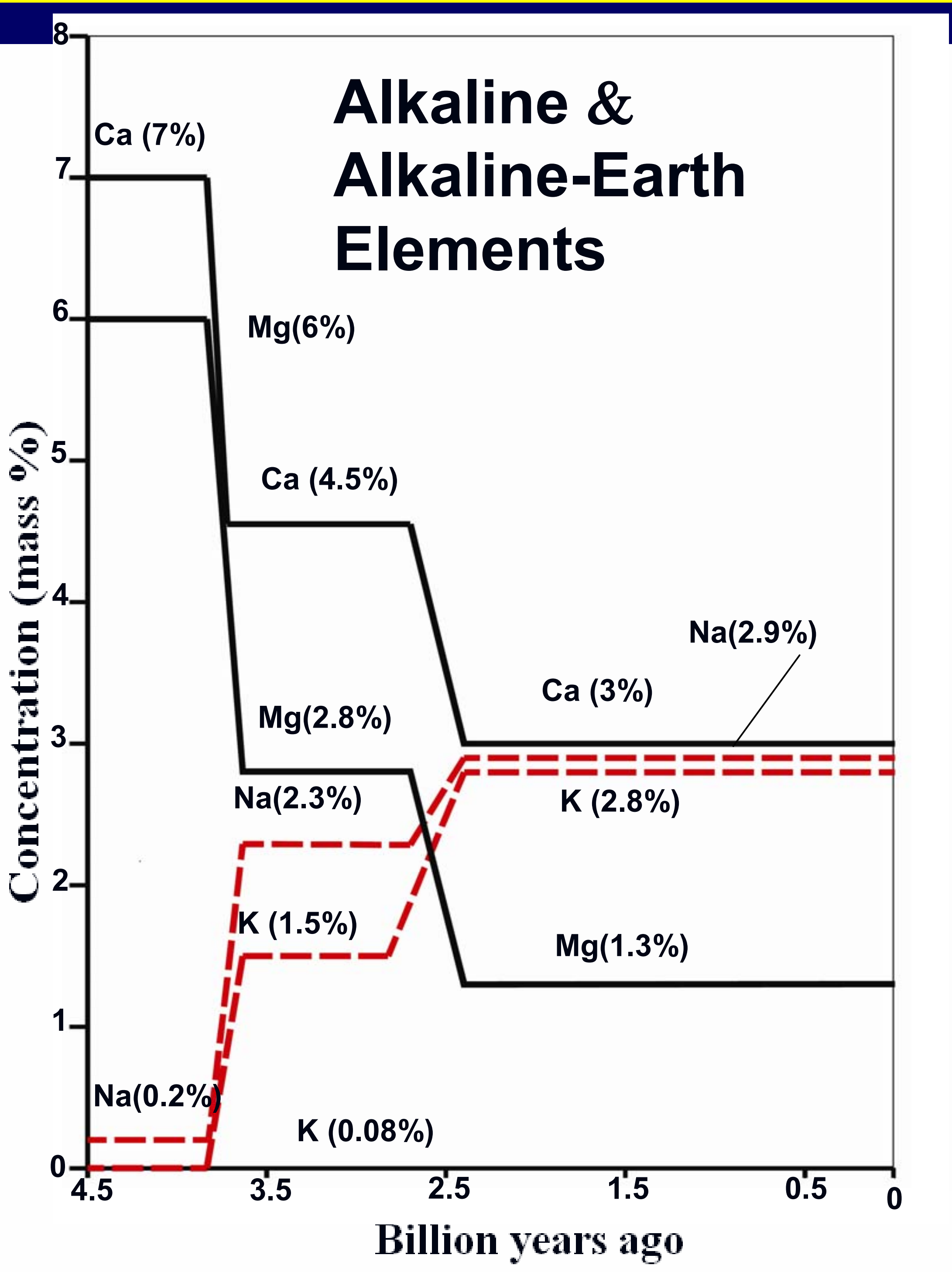

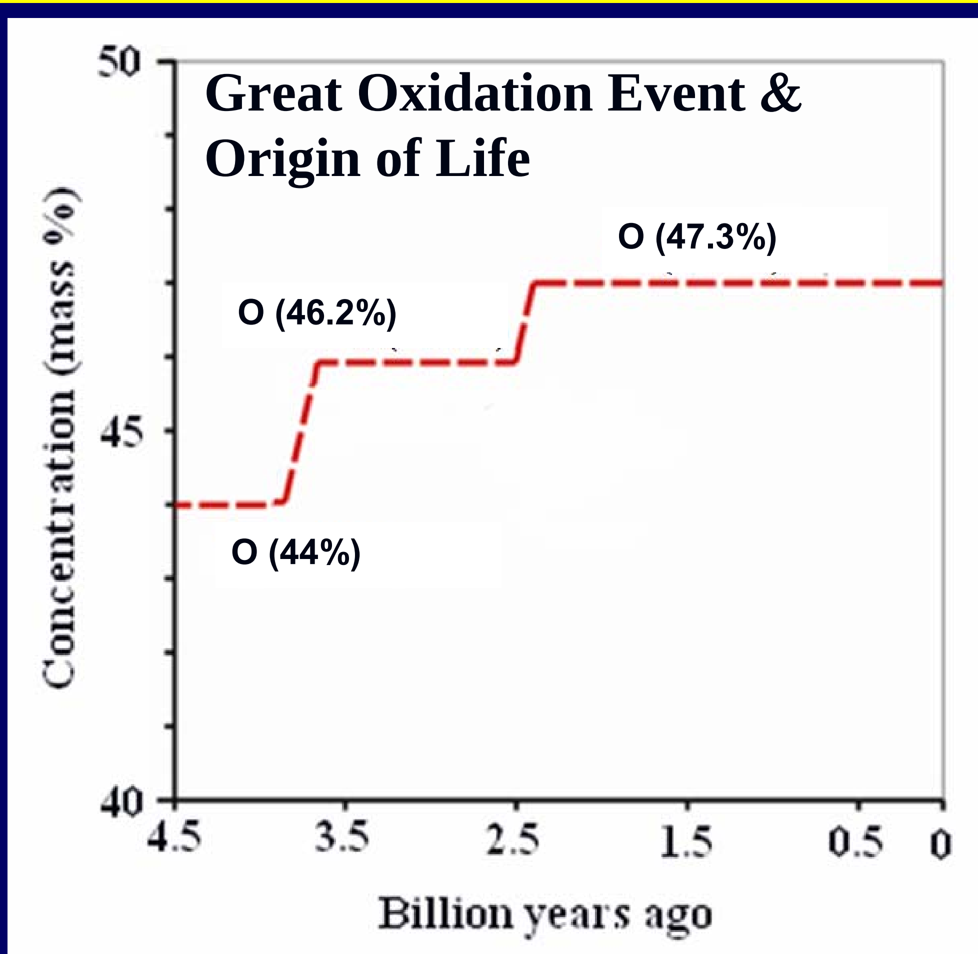

3.8 Billion years ago:
Ca (–2.5%) + Mg(–3.2%) =
= K (+1.4%) + Na (+2.1%) + O (+2.2%)

2.5 Billion years ago:
Ca (–1.5%) + Mg(–1.5%) =
=K (+1.3%) + Na (+0.6%) + O (+1.1%)

Conjecture about Alkaline-Earth elements' transformations

(1) $Mg_{12}^{24} \rightarrow Na_{11}^{23} + H_1^1$

(2) $Mg_{12}^{24} \rightarrow O_8^{16} + 2H_1^1 + He_2^4 + 2n$

(3) $Ca_{20}^{40} \rightarrow K_{19}^{39} + H_1^1$

(4) $Ca_{20}^{40} \rightarrow 2O_8^{16} + 4H_1^1 + 4n$

Conjecture about Alkaline-Earth elements' transformations

(1) $Mg_{12}^{24} \rightarrow Na_{11}^{23} + H_1^1$

(2) $Mg_{12}^{24} \rightarrow O_8^{16} + 2H_1^1 + He_2^4 + 2n$

(3) $Ca_{20}^{40} \rightarrow K_{19}^{39} + H_1^1$

(4) $Ca_{20}^{40} \rightarrow 2O_8^{16} + 4H_1^1 + 4n$

Ocean Formation

Calcium depletion and ocean formation

Global decrease in Ca (–4.0%) is counterbalanced by an increase in K (+2.7%) and in H_2O (+1.3%).

$$Ca_{20}^{40} \rightarrow K_{19}^{39} + H_1^1$$

$$Ca_{20}^{40} \rightarrow 2O_8^{16} + 4H_1^1 + 4n$$

Assuming a mean density of the Earth Crust equal to 3.6 g/cm3 and a thickness of ~60 km, the partial mass decrease in Ca due to the second reaction is about 1.40 $\times 10^{21}$ kg.

Considering a global ocean surface of 3.61 $\times 10^{14}$ m^2, and an average depth of 3950 m, we obtain a mass of water of about 1.35 $\times 10^{21}$ kg

Partial decrease in Ca 1.40 $\times 10^{21}$ kg ⟷ **Mass of H_2O in the oceans today 1.35 $\times 10^{21}$ kg**

CHEMICAL EVOLUTION IN THE PLANETS OF SOLAR SYSTEM

MARS: THREE INDEPENDENT INVESTIGATIONS

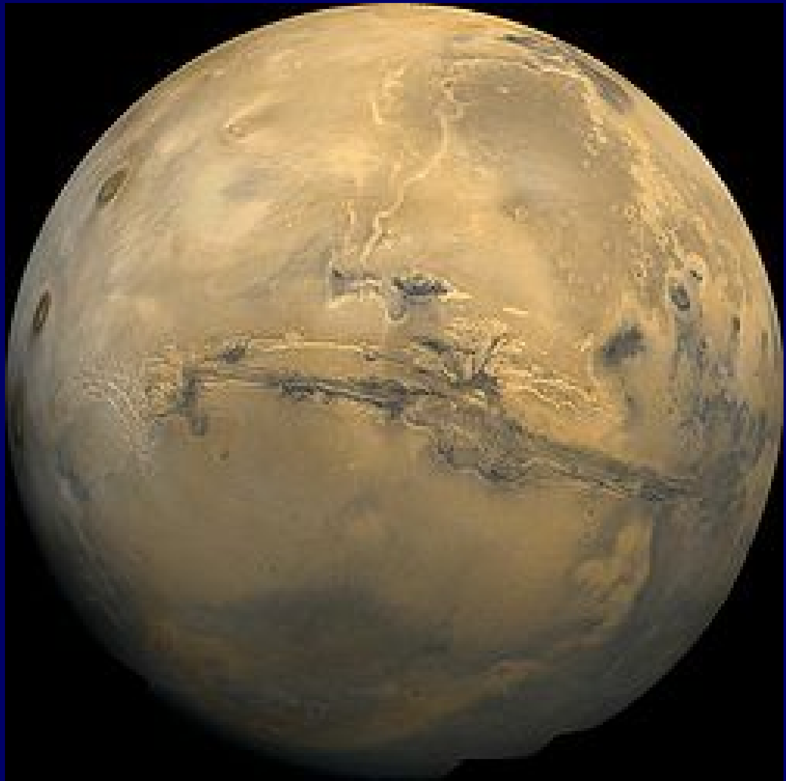

Mars Odissey, Nasa 2001
Mars Global Surveyor, Nasa 1996

- **Seismicity**
- **Neutron Emissions**
- **Elemental Abundance**

1. Knapmeyer M. et al. "Working Models for Spatial Distribution and Level of Mars Seismicity" *J. of Geophys. Res*., 111, E11006, (2006).
2. Hahn, B., McLennan, S., "Gamma-Ray Spectometer Elemental Abundance Correlation with Martian Surface Age: Implication for Martian Crustal Evolution". *Lunar and Planet. Sci.* 37,1904 (2006).
3. Mitrofanov, I. et al., "Maps of Subsurface Hydrogen from the High Energy Neutron Detector, Mars Odyssey", *Science*, 297, 78-81, (2002).

Faults

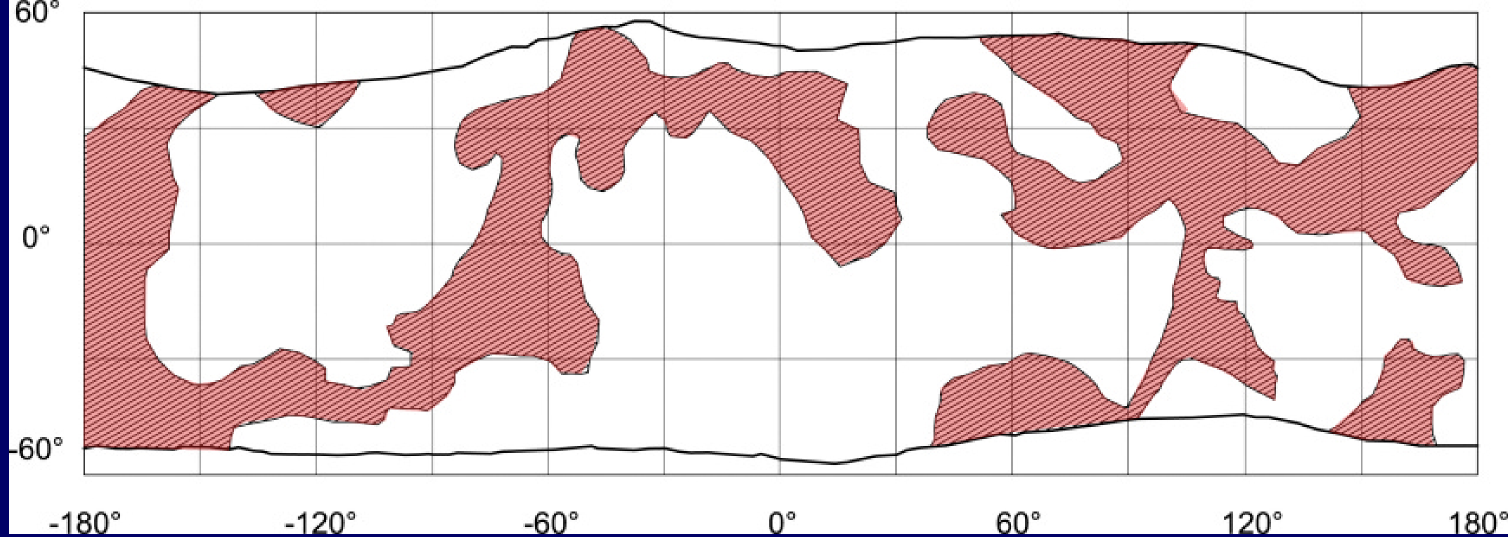

Neutrons (> 0.18 cps)

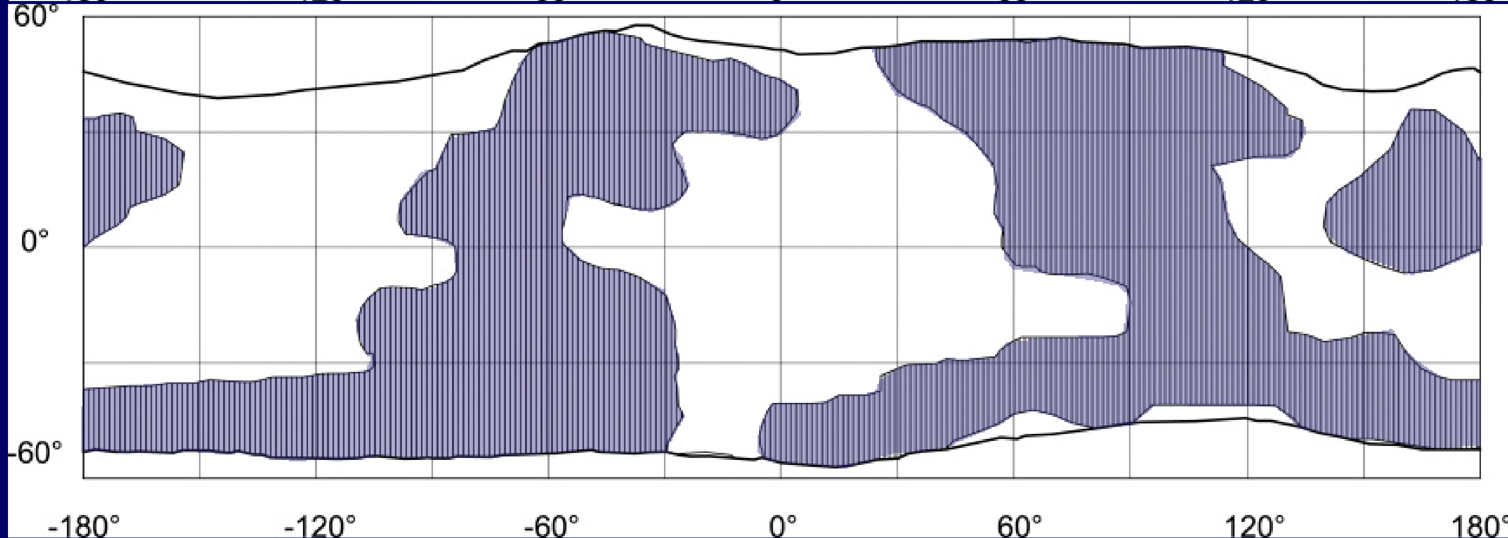

Iron (≥ 15%)

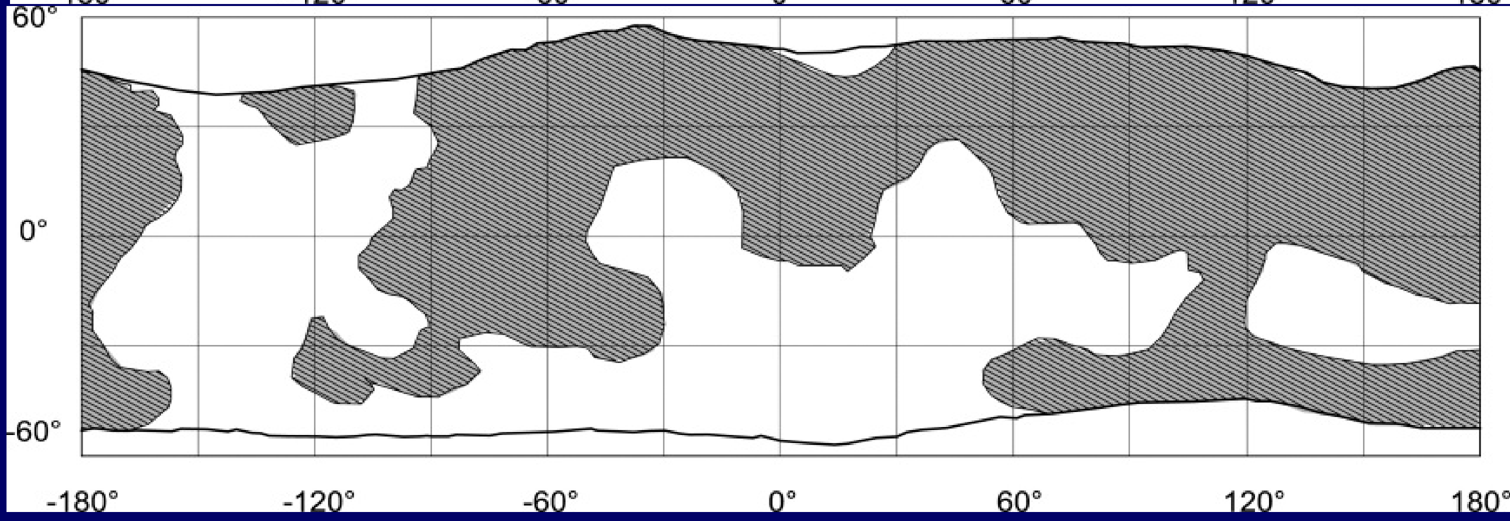

Faults vs Neutrons

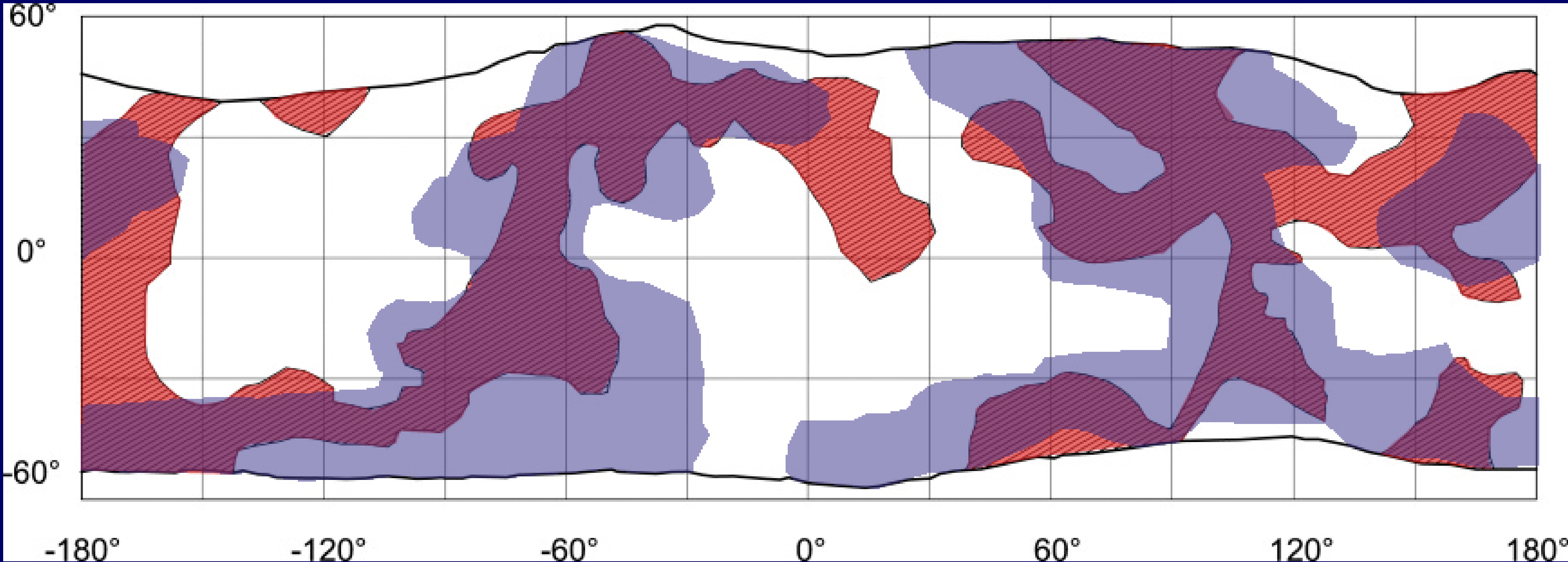

Faults

Neutrons (> 0.18 cps)

Faults vs Iron

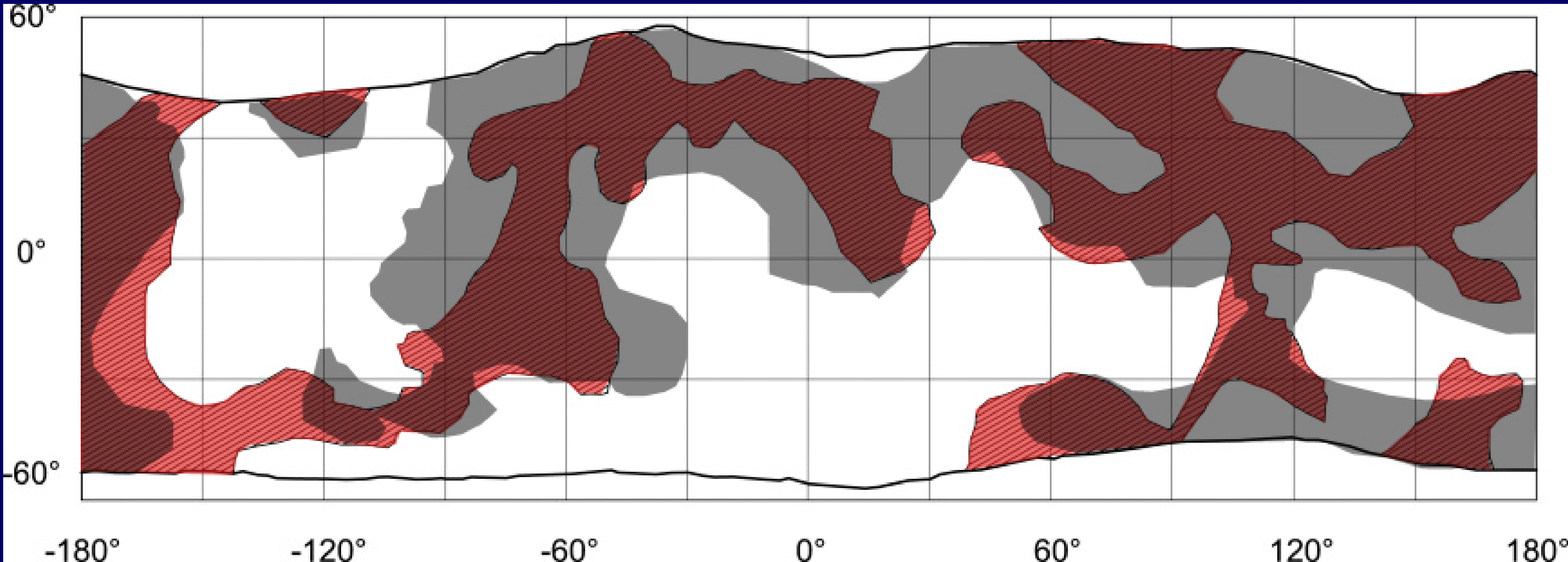

Faults

Iron (≥ 15%)

Iron vs Neutrons

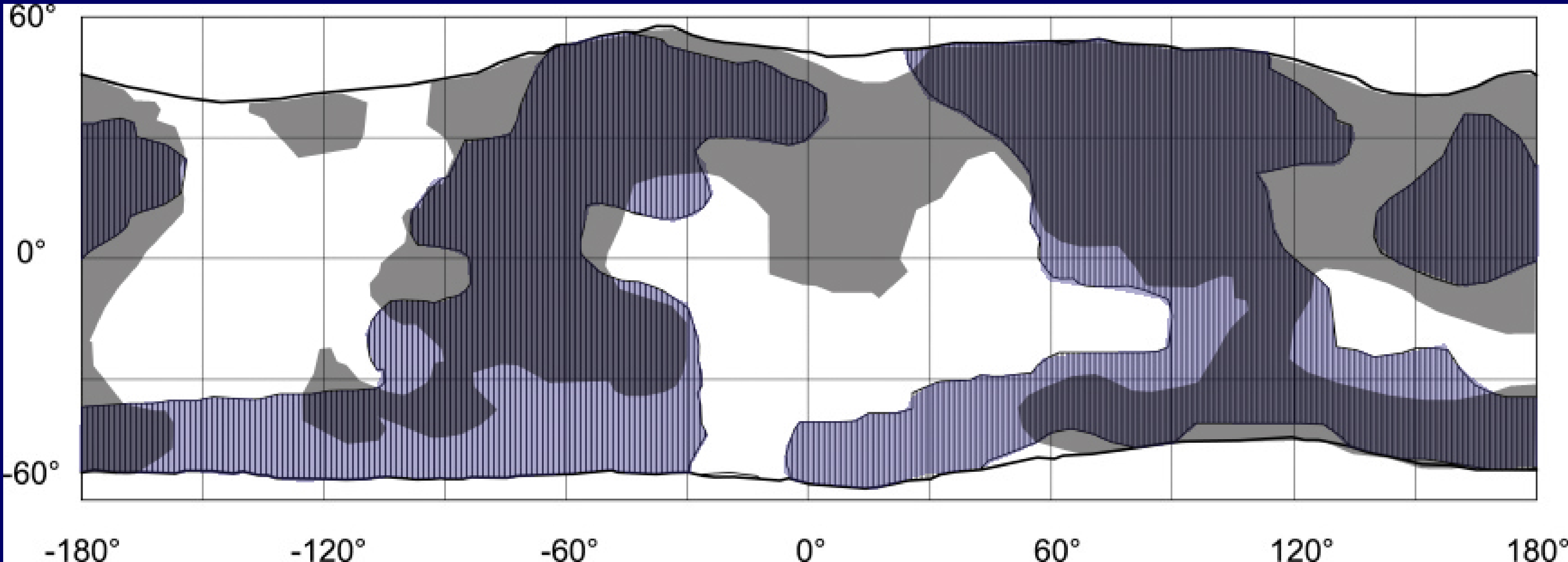

Iron (≥ 15%)

Neutrons (> 0.18 cps)

Element evolution: Ni-Fe transformation

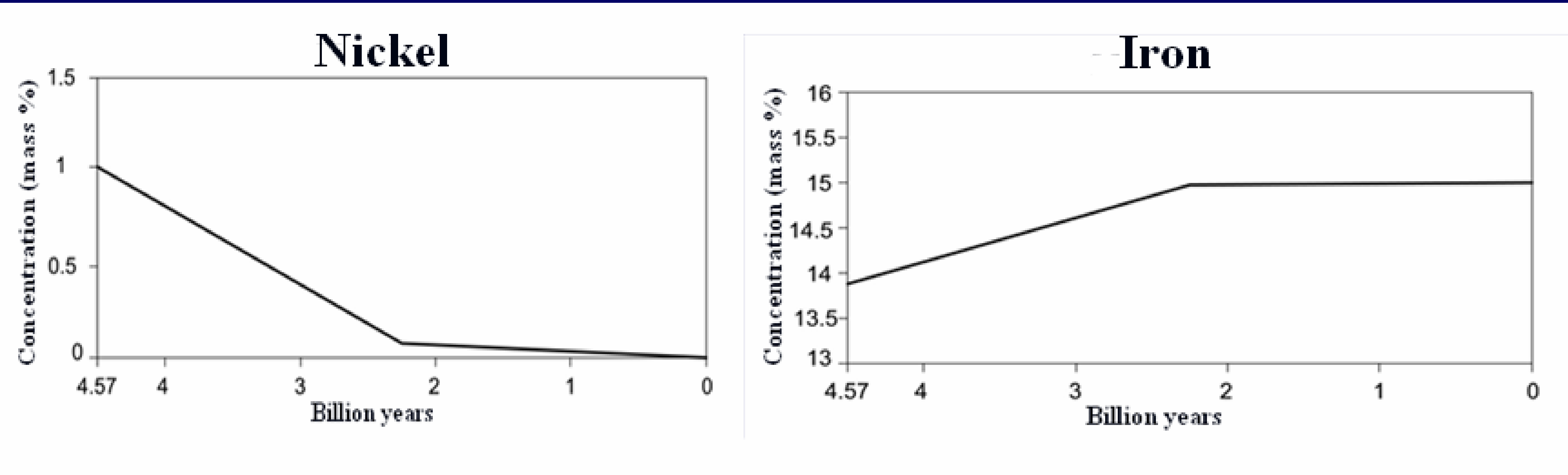

Ni decrease ~ Fe increase ~ 1.0%

$$Ni^{59}_{28} \rightarrow Fe^{56}_{26} + 2H^{1}_{1} + 1n$$

1.Hahn B. C., McLennan S. M. (2006) Gamma-Ray Spectometer Elemental Abundance Correlation with Martian Surface Age: Implication for Martian Crustal Evolution. *Lunar and Planetary Science* XXXVII.

THE SOLAR CORONA

Kelvin-Helmholtz instabilities take place in the solar corona.

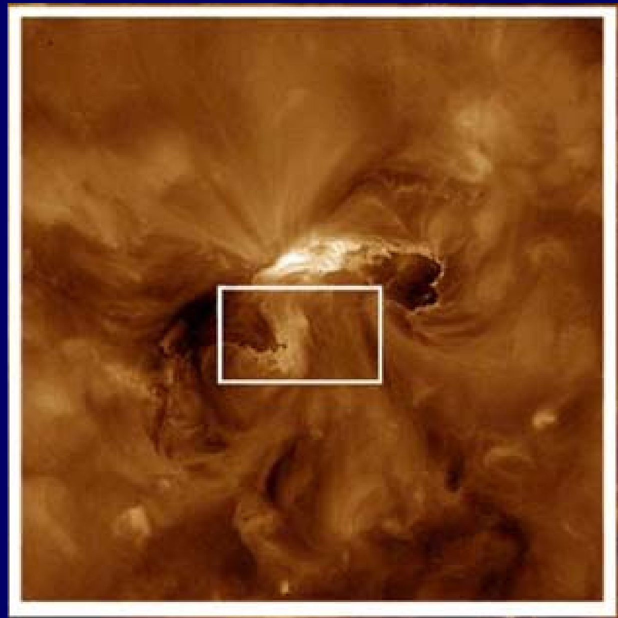

In the Sun, Li and Be are much less abundant than predicted

$$Li_3^6 \rightarrow He_2^4 + H_1^1 + 1n$$

$$Be_4^9 \rightarrow Li_3^6 + H_1^1 + 2n$$

$$Be_4^9 \rightarrow 2He_2^4 + 1n$$

Blöcker T. et al. (1998) Lithium Depletion in the Sun: A Study of Mixing Based on Hydrodynamical Simulation. Space Science Reviews, 85; 105 – 112.

Israelian G. et al. (2009) Enhanced lithium depletion in Sun-like stars with orbiting planets. Nature, 462; 189 – 191

HYDROGEN EMBRITTLEMENT, MICRO-CRACKING, AND FRACTURE IN “COLD FUSION” EXPERIMENTS

Experimental Set-up

Electrolytic Cell

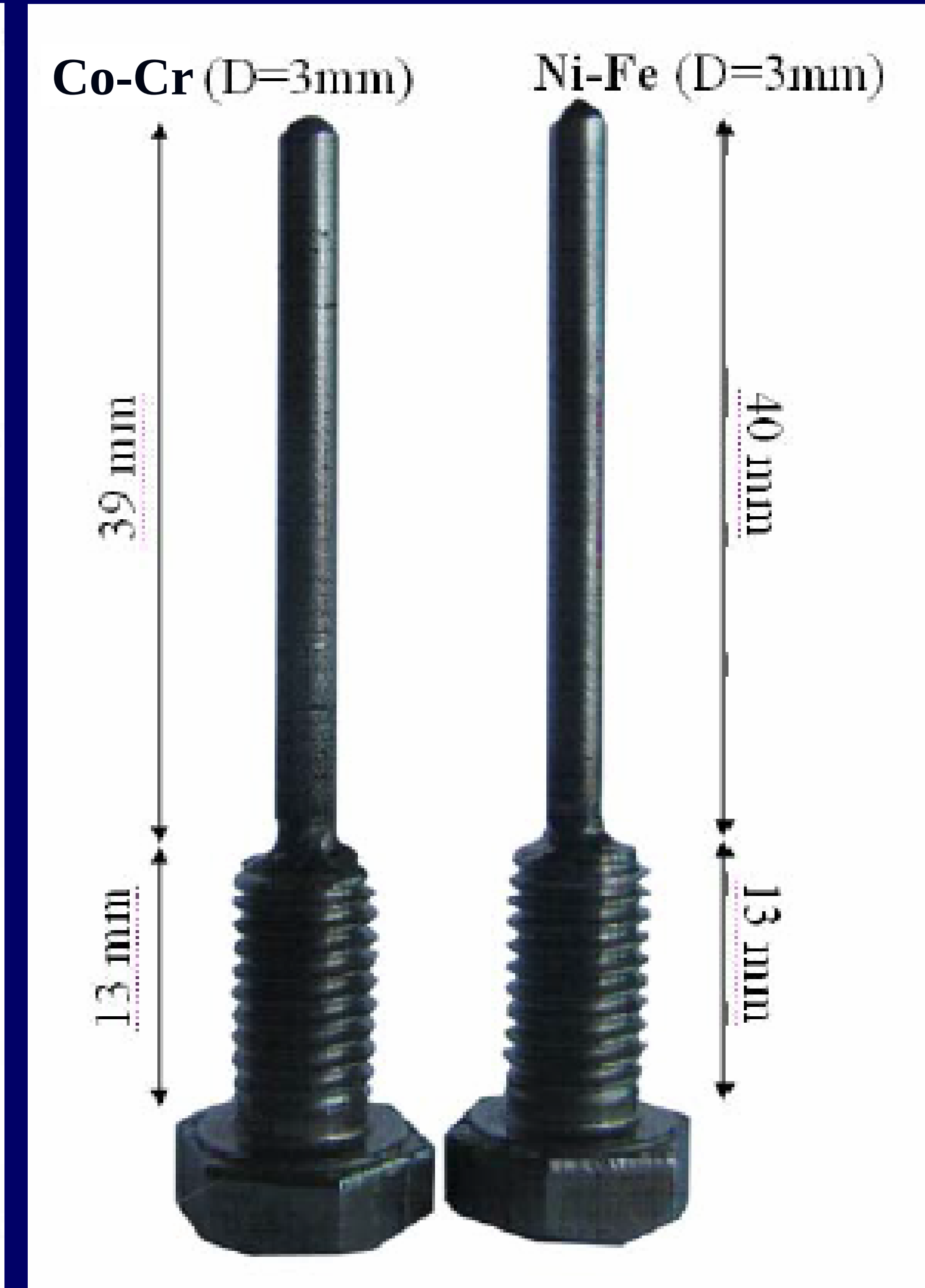

Electrodes

Cumulative Curves for Neutron Emissions

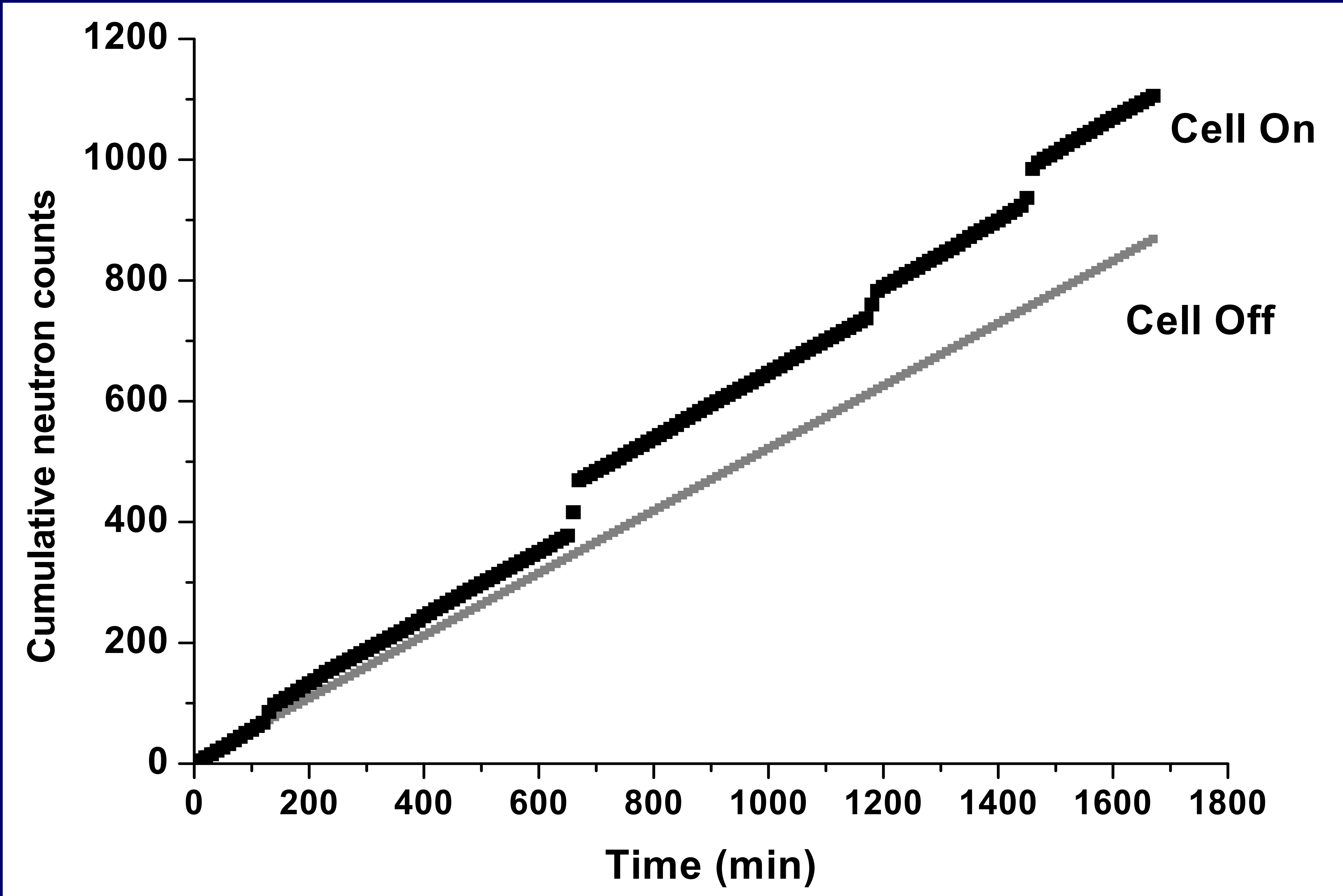

Cumulative Curves for the Alpha Emissions

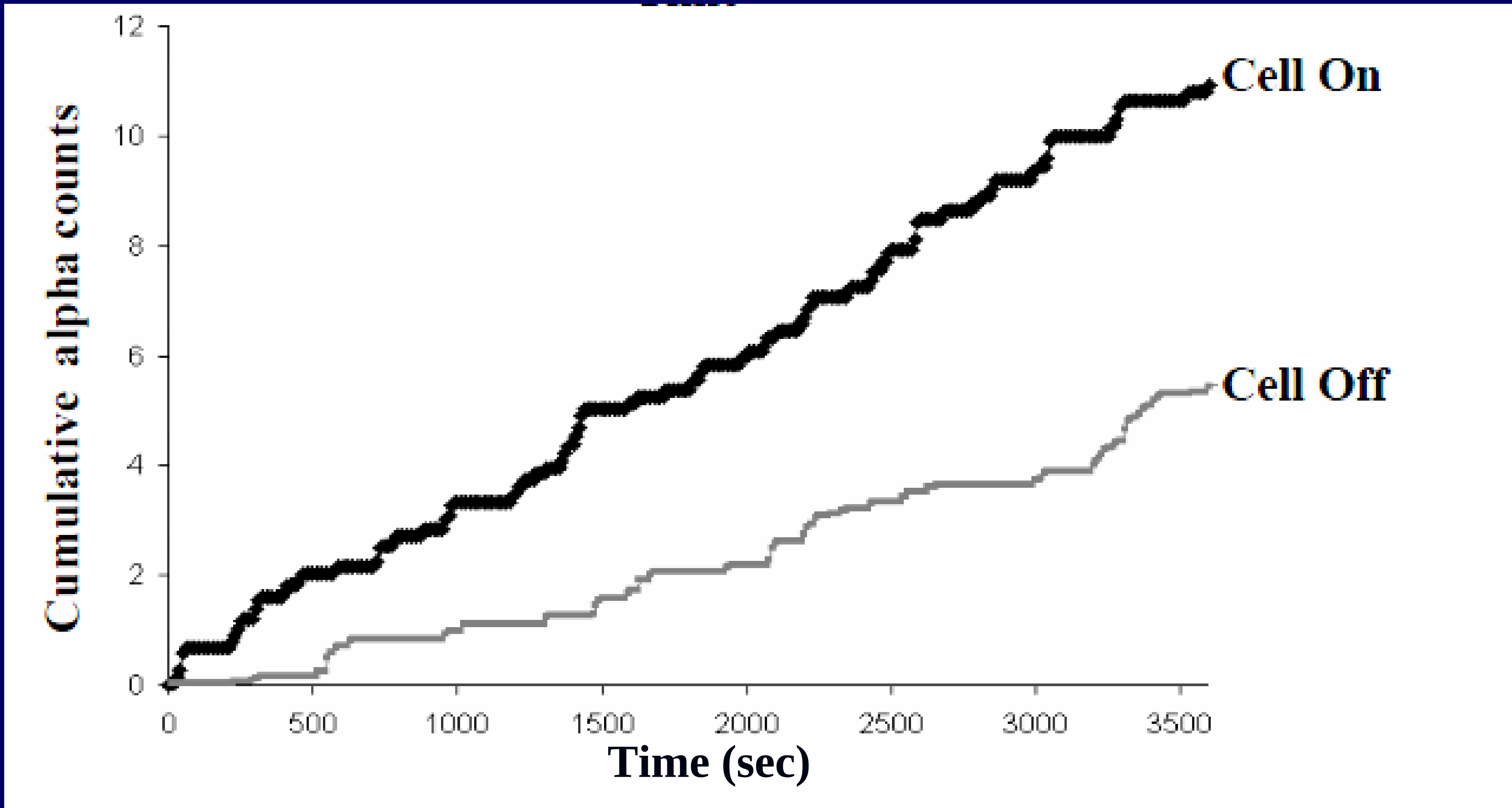

Ni-Fe Electrode : Compositional Changes

	Mean Values*				
Experiment	**Ni**	**Si**	**Mg**	**Fe**	**Cr**
After 0 h	43.9%	1.1%	0.1%	30.5%	-
After 4h	43.6%	0.5%	0.4%	30.7%	-
After 32h	35.2%	5.0%	0.2%	27.9%	-
After 38h	35.3%	1.5%	4.8%	27.3%	3.0%

Ni (–8.6%) = Si (+3.9%) +Mg (+4.7%)

$$Ni_{28}^{58} \rightarrow 2Si_{14}^{28} + 2n$$

$$Ni_{28}^{58} \rightarrow 2Mg_{12}^{24} + 2He_{2}^{4} + 2n$$

PALLADIUM ELECTRODE AFTER THE TEST

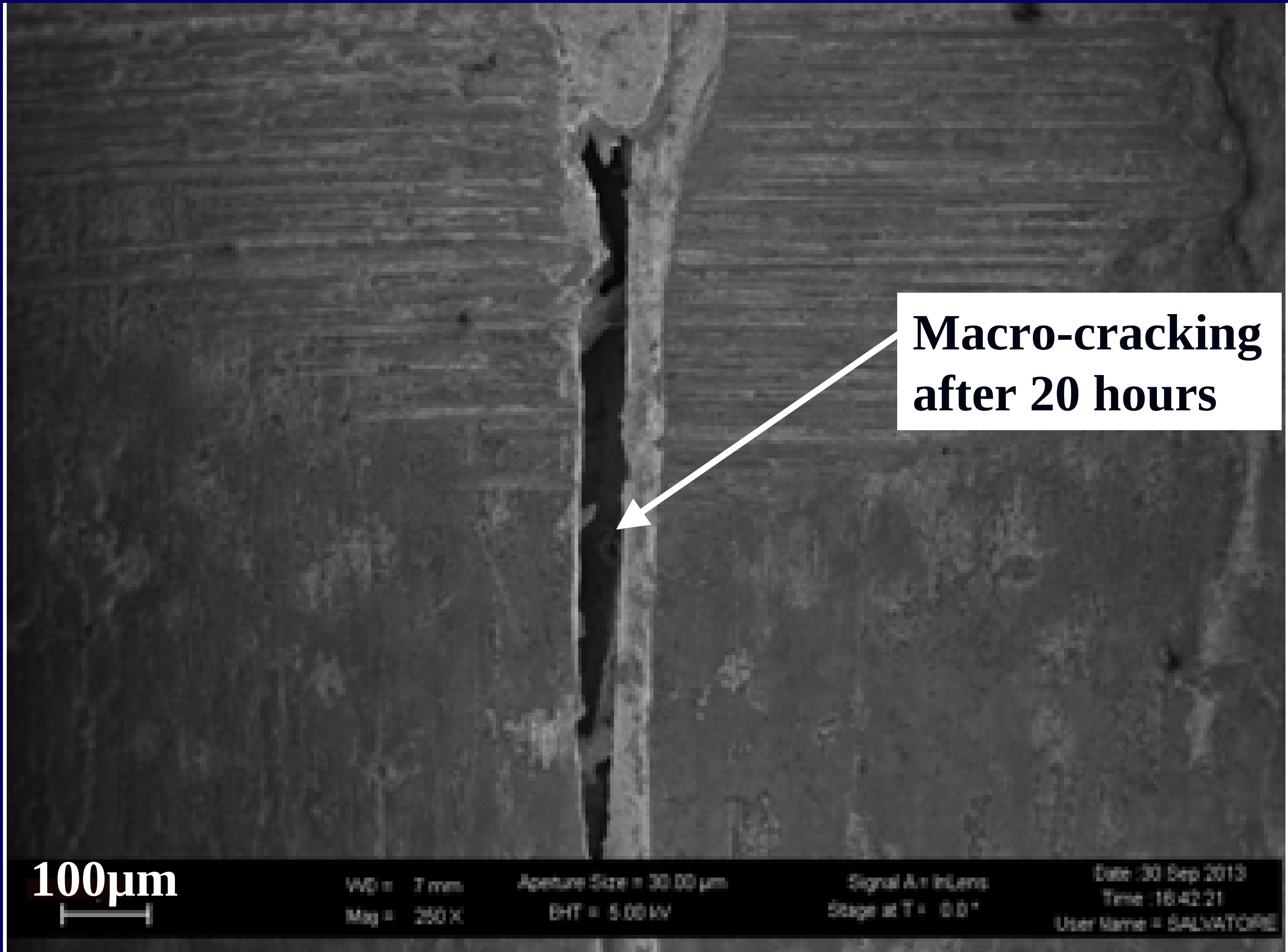

SODIUM-POTASSIUM PUMP (Na-K ATPase)

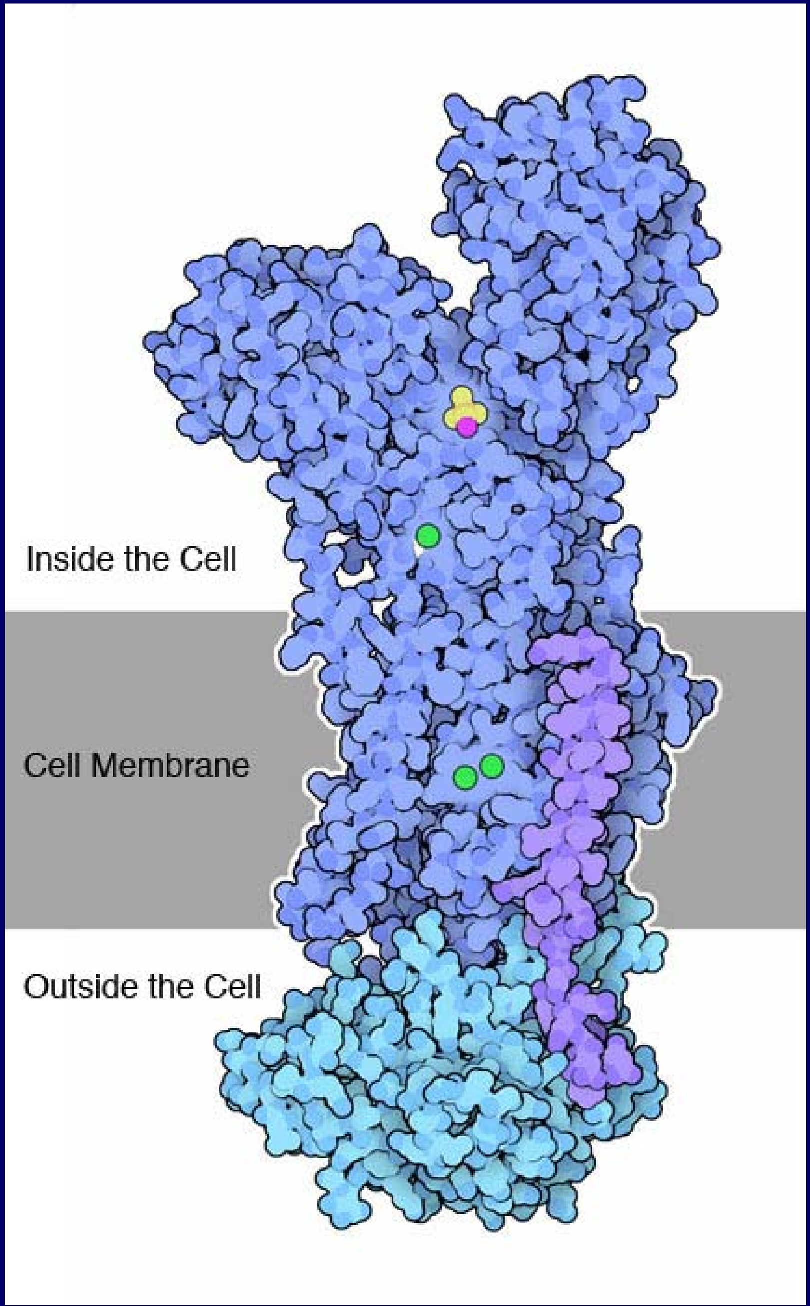

RAMAN SPECTRUM

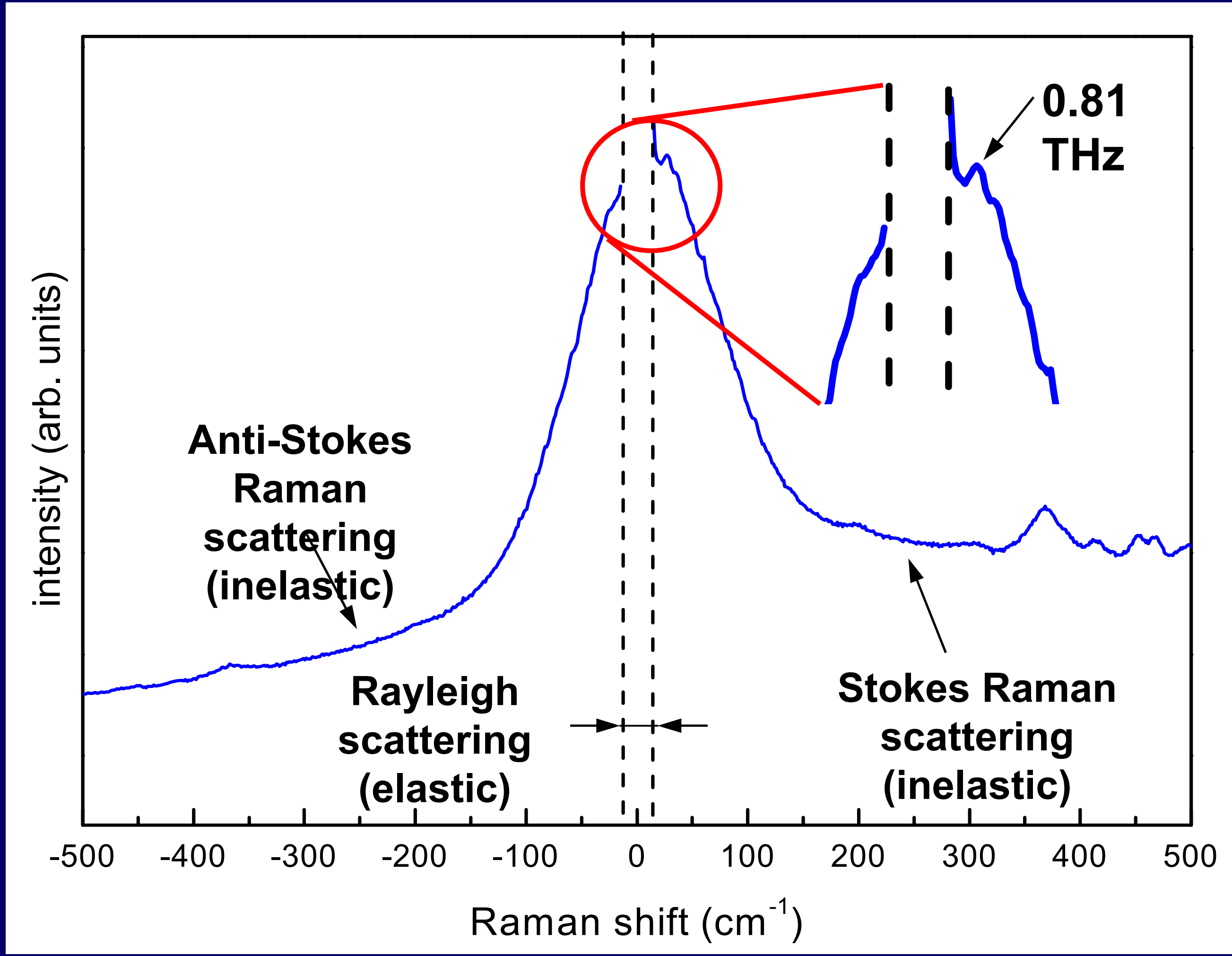

Journal of Biomolecular Structure and Dynamics, 2018
https://doi.org/10.1080/07391102.2018.1425638

Terahertz vibration modes in Na/K-ATPase

Alberto Carpinteri, Gianfranco Piana, Andrea Bassani and Giuseppe Lacidogna*

Department of Structural, Geotechnical and Building Engineering, Politecnico di Torino, Corso Duca degli Abruzzi 24, 10129, Torino, Italy

Communicated by Ramaswamy H. Sarma

(*Received 18 December 2017; accepted 4 January 2018*)

Mechanical vibration in the Terahertz range is believed to be connected with protein functions. In this paper, we present the results of a normal-mode analysis (modal analysis) of a Na/K-ATPase all-atom model, focusing the attention on low-frequency vibration modes. The numerical model helps in the interpretation of experimental results previously obtained by the authors via Raman spectroscopy of Na/K-ATPase samples, where several unassigned peaks were found in the sub-500 cm^{-1} range. In particular, vibration modes corresponding to peaks at 27, 190 and 300 cm^{-1}, found experimentally, are confirmed here numerically, together with some other modes at lower frequencies (wavenumbers) that were not possible to observe in the experimental test. All the aforementioned modes correspond to vibrations involving the protein ends, i.e. portions directly related to the operating mechanism of the sodium-potassium pump.

Keywords: sodium-potassium pump; THz vibration; all-atom simulation; modal analysis; lattice model

IS THE SHROUD OF TURIN IN RELATION TO THE OLD JERUSALEM HISTORICAL EARTHQUAKE?